(2)

AD

CONTRACTOR REPORT ARCCB-CR-90012

FINAL REPORT ON TURNING AND BORING MACHINABILITY TESTS ON TITANIUM BETA C TUBES

METCUT RESEARCH ASSOCIATES, INC.
CINCINNATI, OHIO 45242-1812

APRIL 1990

US ARMY ARMAMENT RESEARCH,
DEVELOPMENT AND ENGINEERING CENTER
CLOSE COMBAT ARMAMENTS CENTER
BENÉT LABORATORIES
WATERVLIET, N.Y. 12189-4050

APPROVED FOR PUBLIC RELEASE; DISTRIBUTION UNLIMITED

SECURITY CLASSIFICATION OF THIS PAGE (When Data Entered)

REPORT DOCUMENTATION PAGE

READ INSTRUCTIONS BEFORE COMPLETING FORM

1. REPORT NUMBER: ARCCB-CR-90012	2. GOVT ACCESSION NO.
3. RECIPIENT'S CATALOG NUMBER	
4. TITLE (and Subtitle): FINAL REPORT ON TURNING AND BORING MACHINABILITY TESTS ON TITANIUM BETA C TUBES	5. TYPE OF REPORT & PERIOD COVERED: Final Report, September 1986 - July 1988
	6. PERFORMING ORG. REPORT NUMBER
7. AUTHOR(s)	8. CONTRACT OR GRANT NUMBER(s): DAAA22-86-D-0278
9. PERFORMING ORGANIZATION NAME AND ADDRESS: Metcut Research Associates, Inc., 11240 Cornell Park Drive, Cincinnati, OH 45242-1812	10. PROGRAM ELEMENT, PROJECT, TASK AREA & WORK UNIT NUMBERS
11. CONTROLLING OFFICE NAME AND ADDRESS: U.S. Army ARDEC, Close Combat Armaments Center, Picatinny Arsenal, NJ 07806-5000	12. REPORT DATE: April 1990
	13. NUMBER OF PAGES: 144
14. MONITORING AGENCY NAME & ADDRESS(if different from Controlling Office): U.S. Army ARDEC, Benet Laboratories, SMCAR-CCB-TL, Watervliet, NY 12189-4050	15. SECURITY CLASS. (of this report): UNCLASSIFIED
	15a. DECLASSIFICATION/DOWNGRADING SCHEDULE

16. DISTRIBUTION STATEMENT (of this Report)

Approved for public release; distribution unlimited.

17. DISTRIBUTION STATEMENT (of the abstract entered in Block 20, if different from Report)

18. SUPPLEMENTARY NOTES

Joseph P. Bak - Benet Laboratories Project Engineer

19. KEY WORDS (Continue on reverse side if necessary and identify by block number)

Titanium (Beta C) Alloy
Turning
Boring
Honing
Cutting Speed
Depth of Cut
Feed
Tool Evaluation
Tool Life Model
Machinery and Tools

20. ABSTRACT (Continue on reverse side if necessary and identify by block number)

This report contains machinability data generated during turning, boring, and bore finishing tests of Beta C cylinders performed by Metcut Research Associates, Inc. Evaluations of material, tooling, cutting fluids, and machining parameters were used to establish an optimum machining and processing database for turning and deep hole finishing of hollow titanium alloy cylinders.

DD FORM 1 JAN 73 1473 EDITION OF 1 NOV 65 IS OBSOLETE

UNCLASSIFIED

SECURITY CLASSIFICATION OF THIS PAGE (When Data Entered)

DISCLAIMER

The findings in this report are not to be construed as an official Department of the Army position unless so designated by other authorized documents.

The use of trade name(s) and/or manufacturer(s) does not constitute an official indorsement or approval.

DESTRUCTION NOTICE

For classified documents, follow the procedures in DoD 5200.22-M, Industrial Security Manual, Section II-19 or DoD 5200.1-R, Information Security Program Regulation, Chapter IX.

For unclassified, limited documents, destroy by any method that will prevent disclosure of contents or reconstruction of the document.

For unclassified, unlimited documents, destroy when the report is no longer needed. Do not return it to the originator.

TABLE OF CONTENTS

INTRODUCTION

The objective of this contract was to conduct an extensive machinability study and process evaluation of a deep hole boring and finishing, and OD turning of hollow Ti-3Al-8V-6Cr-4Zr-4Mo (Beta C) cylinders. The tests were performed in a laboratory-controlled environment to develop a comprehensive database that would represent and encompass the state of the art in cutting tool material, tooling applications, and optimum process parameters. The results of this research will be part of a process planning database for the production manufacturing of nine-foot long cylinders of the same titanium alloy.

The testing procedure followed in this program was the same as that previously used in several similar contracts with the U. S. Air Force Materials Laboratory. In those test programs, like this one, the work materials were expensive and in short supply. Techniques were developed to maximize the amount of machinability data that could be obtained from a relatively small amount of available material. Abbreviated screening tests were used to determine the best cutting tool materials and the most effective cutting fluid and tool geometry combinations. Once these screening tests were completed, the cutting speed, feed rate, and tool life relationships were explored. When available material permitted, the speed-feed-tool life relationship was modeled using computer assistance to calculate the mathematical model which best described the laboratory data and provided the statistical analysis along with the descriptive equation. This technique represents the basic testing theory used in this program.

SUMMARY OF LABORATORY TESTING

CUTTING TOOL MATERIAL COMPARISON

TOOL	TYPE	PERFORMANCE	FAILURE	COMMENTS
KC910	TiC/Al_2O_3 coated carb.	best	uniform wear	more expensive
883	C-2 carbide	very good	uniform wear	cost effective
KC850	TiC/TiN coated carb.	good	cratered	more expensive
K313	micrograin carbide	fair	uniform wear	somewhat expensive
K68	C-2 carbide	fair	uniform wear	not expensive
RAMET I	micrograin carbide	fair	uniform wear	somewhat expensive
570	Al_2O_3 coated carbide	fair to poor	uniform wear	more expensive
KC950	TiC/Al_2O_3/TiN coated carb.	poor	heavy wear	more expensive
NORALIDE	Silicon Nitride	unsuitable	heavy wear	quite expensive
KYON 2000	Silicon Nit./ Al_2O_3 Cer.	unsuitable	heavy wear	quite expensive
AMBORITE	Cubic Boron Nitride	unsuitable	DOC notch	extremely expensive
WG-300	SiC whisker Al_2O_3 Cer.	unsuitable	chipped	very expensive
ISCANITE	Silicon Nitride	unsuitable	chipped	quite expensive

TOOL MATERIAL EVALUATION

The results of the tool material evaluation are shown in Figure 1. Included in this evaluation were (company and grade/name designation):

1. C-2 carbide (Carboloy 883, Kennametal K68)
2. Titanium nitride coated carbide (Kennametal KC850, KC950)
3. Aluminum oxide coated carbide (Carboloy 570, Kennametal KC910)
4. Silicon nitride or sialon inserts (Norton Noralide, Kennametal Kyon 2000, Iscar Iscanite)
5. Polycrystalline cubic boron nitride (DeBeers Amborite)
6. Aluminum oxide ceramic reinforced with silicon carbide whiskers (Greenleaf WG-300)
7. Micrograin carbide (VR Wesson Ramet I, Kennametal K313)

These tools were compared at the following machining conditions:

Cutting Speed: 200 feet/minute (fpm)

Feed: 0.005 inch/revolution (ipr)

Depth of Cut: 0.050 inch

Cutting Fluid: Dry

The following tool geometry was used in this comparison:

Back Rake (BR): -5°	End (ECEA) and Side Cutting Edge Angles (SCEA): 45°
Side Rake (SR): -5°	End & Side Clearance: 5°

The tool materials producing the longest tool life were the aluminum oxide coated carbide (22.4 minutes), the C-2 carbide (20 minutes), and the titanium nitride coated carbide (15 minutes). Most of the other tools failed rather quickly, providing relatively short tool life.

The polycrystalline cubic boron nitride (Amborite) failed by a depth of cut notch after only 1.3 minutes of cutting. The silicon carbide whisker reinforced aluminum oxide tool (WG-300) chipped after cutting for only 30 seconds. This tool was also tested at a cutting speed of 1000 ft./min. where it lasted for 10 seconds.

The Kennametal Kyon 2000 cut for 30 seconds and had 0.030 inch uniform wear as did the Norton Noralide tool after 53 seconds of cutting.

Other tools tested were two micrograin carbides (Ramet I and K313) and a cobalt high speed steel (AISI M-44). The micrograin carbide is tougher than a regular carbide insert and sometimes can perform better than high speed steel tools at cutting speeds appropriate for high speed steel tools. The results with the high speed steel tools and one of the micrograin carbides are shown in Figures 2 and 3. These data are listed in Tables I, II, and III.

In Figure 2, the test results with these two types of tools using positive back rake are shown. The high speed steel tools were tested at two different feed rates, 0.003 and 0.005 inch per revolution (ipr). At the 50 feet per minute (fpm) cutting speed and 0.005 ipr feed, the micrograin carbide tool outperformed the high speed steel by 250%, 24 minutes for the high speed steel and 84 minutes for the micrograin carbide.

These tools were also tested with a negative back rake and the results are shown in Figure 3. Included with these data, for comparison, is the tool life with the 883 carbide tool. The 883 cutting tool performed the best, producing a tool life of 216 minutes at a cutting speed of 150 fpm, with a metal removal rate of 0.45 cubic inches per minute, compared to 150 minutes tool life for the high speed steel at a metal removal rate of 0.09 cubic inches per minute. By comparison, the Ramet I provided 103 minutes at a metal removal rate of 0.45 cubic inches per minute, while the high speed steel tool cut for 9.0 minutes at a metal removal rate of 0.15 cubic inches per minute. The 883 carbide produced a 60% longer tool life at three times the metal removal rate.

The best three tools emerging from this study were the C-2 Carboloy 883, the aluminum oxide coated Kennametal KC910, and the Kennamatal K313, which was introduced later in the contract period.

More extensive tests were performed with the KC910 and 883 tools and the results are shown in Figure 4. The tool life curves of both tools are similar, with the 883 showing about 30% longer tool life at 175 fpm. Since the 883 carbide is lower in price than the coated carbide, it would be the preferred choice of these two tool materials.

Another tool which could be substituted for the Carboloy 883 tool was the Kennametal K313 tool. This tool performed very similar to the 883 tool as shown in the cutting speed versus tool life curve in Figure 5 and the feed versus tool life curve in Figure 6. Since the K313 is a micrograin carbide, it should be tougher, but less wear resistant than the 883 carbide. This relationship is verified by the slightly longer tool life of the 883 at the higher speeds in Figure 5, and the longer tool life of the K313 at the highest feed in Figure 6. The data for Figures 4, 5, and 6 are listed in Table IV.

TOOL GEOMETRY, FEED, CUTTING FLUID, AND DEPTH OF CUT

With the 883 carbide, determined to be the most practical tool material, tests were performed to determine the effect of tool geometry. It was discovered that the feed also had an important influence when the side cutting edge angle (SCEA) was varied. The tool geometries tested were 15° SCEA versus 45° SCEA. Both negative 5° back rake and positive 5° back rake were also evaluated.

The tool life curves of the 15° and 45° SCEA are shown in Figures 7 and 8. The difference in Figures 7 and 8 is in the feed rate used. In Figure 7, the feed was 0.005 ipr and in Figure 8 the rate was 0.010 ipr. The best tool life was achieved with the 45° SCEA. In Figure 7, at 0.005 ipr the 45° SCEA permitted a 21% higher cutting speed than the 15° SCEA tools. At the heavier feed of 0.010 ipr in Figure 8, the 45° SCEA produced a longer tool life at the lower cutting speeds only. The actual advantage of the higher side cutting edge angle is to reduce the chip thickness by spreading the chip over a longer length of cut. This advantage is reduced, as shown in Figures 7 and 8, at the higher feed rate which increases (makes thicker) the other dimension of the chip cross section.

The effect of the back rake angle, positive versus negative, is shown in Figure 9. For a tool life level of 30 minutes, the negative back rake tool permitted a 19% higher cutting speed than the positive rake tool. The effect of the feed rate is demonstrated in Figures 10 and 11. With both tool geometries, 15° and 45° side cutting edge angles, increasing the feed from 0.005 ipr to 0.010 ipr resulted in a major decrease in both tool life and cutting speed. Table V lists the supporting data for Figures 7, 8, 9, 10, and 11.

CUTTING FLUIDS

An additional task was to evaluate the effect of various cutting fluids. Three different cutting fluid systems were investigated, dry (no coolant), Trim Sol (an emulsifiable heavy duty chlorinated soluble oil), and Mobilmet 235 (a semi-synthetic). The tool life curves produced with each fluid are shown in Figure 12. These data, listed in Table VI, show that the best tool life was obtained with the Trim Sol cutting fluid. At the constant cutting speed of 200 fpm, the results were as follows:

Cutting Fluid	Tool Life minutes	Percent Decrease in Tool Life
Trim Sol	30	-
Mobilmet 235	23	23%
Dry	20	33%

DEPTH OF CUT

The results of the depth-of-cut study are shown in Figures 13 and 14 and listed in Table VII. The two depths of cut examined were 0.050 inch and 0.150 inch. Since the titanium material available for laboratory testing was very expensive and therefore in relatively short supply, only a small amount of data was collected at the heavier depth of cut. The metal removal rate (cubic inches consumed per minute of tool life) is usually much higher at higher depths of cut, limiting the amount of tool life testing. At 0.150 inch depth of cut, two different feed rates were tested, 0.0025 and 0.005 ipr. The tool life curves at these two feed rates are presented in Figure 13. At 0.150 inch depth of cut and 0.0025 ipr, the tool life reached a peak of 180 minutes at 150 fpm, and then dropped off to 60.0 and 68.2 minutes at both higher and lower speeds of 175 and 100 fpm, respectively. When the feed rate was increased to 0.005 ipr, the tool life was comparatively poor, 47.0 minutes at 75 fpm and 60.0 minutes at 100 fpm.

In Figure 14, the effect of the two depths of cut at the feed of 0.005 ipr is shown. Increasing the depth of cut from 0.050 inch to 0.150 inch resulted in a significant decrease in tool life at cutting speeds below 150 fpm. However, this is a normal practice for rough-machining conditions, decreasing the cutting speed to permit increases in feed and/or depth of cut.

CHIP CONTROL

The subject of chip control (the breaking of the chips) was explored using a mechanical, barrier-type, adjustable carbide chip breaker, over an SNG-432 insert. Two tool holders were used, one with a 15° SCEA and the other with a 45° SCEA. At the low cutting speed of 75 fpm, the chips would not break at a 0.050 inch depth of cut. Increasing the depth of cut to 0.075 inch produced chip control. By adjusting the chip breaker closer to the cutting edge of the insert, chip control could be achieved at 0.050 inch depth of cut. However, at 150 fpm, the suitable cutting speed for machining this titanium alloy, the conditions were reversed, in that chip control was obtained at 0.050 inch depth of cut, but not at 0.075 inch depth of cut. When the depth of cut was increased to 0.150 inch, the chip control was satisfactory over a range of cutting speed from 75 to 250 fpm. Chip control is usually easier to obtain when the cross section of the chip is increased by either increased feed or depth of cut. The tool holder with the 45° SCEA was tried at 150 fpm, 0.050 inch depth of cut, and 0.005 ipr, using the same barrier-type of adjustable chip breaker. At these conditions, satisfactory chip control was obtained. In summary, if the machining conditions are light, then the barrier must be set close to the cutting edge. For heavier conditions of feed and depth of cut, the barrier can be adjusted farther from the cutting edge. Inserts with molded chip control grooves (see Figure 60) work in essentially the same manner, in that different cutting conditions (feed and depth of cut) require grooves of varying width and depth.

TOOL LIFE MODEL

The tool life model conditions were constructed from the information developed in the preliminary tests. The best combination of tool material and tool geometry was the C-2 carbide with a 45° side cutting edge angle and negative 5° back rake, using Trim Sol cutting fluid mixed 1:20. In order to conserve material, the tool life model was developed at 0.050 inch depth of cut. The tool life model values were fitted with a first order plus interaction logarithmic equation. The turning test data resulted in the following equation:

$$\text{Ln}(Y1) = -79.09 + 13.30\ \text{Ln}(X1) - 20.39\ \text{Ln}(X2) + 3.41\ \text{Ln}(X1)\ \text{Ln}(X2)$$

where:

Y1 = tool life (minutes)

X1 = cutting speed (fpm)

X2 = feed rate (ipr)

The analysis of variance table is shown below:

Source	Sum of Square	d.f.	Mean Square	f-ratio
residual	0.8526	5	0.1705	
regression	133.1988	4	33.2997	195.2832
regression (cfm)	12.4763	3	4.1588	24.3888
mean	120.7224	1		
total	134.0514	9		
total (cfm)	13.3289	8		

R-squared = 0.99364

R-squared (cfm) = 0.93603

variance = 0.17052

number of tests = 9

A graph of the model is shown in Figure 16. The raw data are presented in Table VIII. This tool life model shows the interrelationship between tool life, cutting speed, and feed. The cutting speed is plotted versus the feed with lines of constant tool life value. This tool life model permits selection of either the machining parameters (cutting speed or feed) or the tool life. When any two selections are made, the third value can easily be found in Figure 16. For example, if the required tool life is 180 minutes and the cutting speed is 190 fpm, the resulting feed would be 0.003 ipr.

If the surface finish requirements limit the allowable feed, then several selections of cutting speed would be available, depending on the required tool life. For roughing conditions, where surface finish is not a factor, heavier feed rates can be selected for maximum metal removal rates, while still operating at a known tool life level.

CUTTING FORCE TESTING

The cutting force tests were performed with a Kistler three-axis lathe dynamometer. All the force measurements were made on the outside diameter of the titanium Beta C tubes. The effect of the use of cutting fluid on the cutting forces is presented in a series of bar charts shown in Figures 17, 18, and 19. These data are recorded in Table IX. Three cutting tool materials were used in this evaluation: KC850, K313, and 883. The tests were conducted with and without (dry) cutting fluid, and also in the sharp and dull condition. The dull tool condition consisted of tools with either 0.015 inch uniform wear or 0.030 inch localized wear. Figure 17 shows the radial force data, while the tangential forces are shown in Figure 18 and the axial forces in Figure 19. The effect of the presence or absence of the cutting fluid on the axial and radial forces was minor, except with the KC850, where the forces were higher with the cutting fluid. The tangential forces were always lower with the cutting fluid, even though the difference was no greater than 20%. The dull cutting force data were added for reference only. It is difficult to make accurate or reliable comparisons with dull tool data since the wearland on the dull tool varies from one tool to another.

The modeled force data are shown in Figures 20, 21, and 22 and listed in Table X. This model is of forces taken at the same cutting speeds and feeds as the tool life model in Figure 16 and Table VIII. The tangential force model is shown in Figure 20, the axial force model in Figure 21, and the radial force model in Figure 22. In the tangential force model in Figure 20, the cutting speed has little effect on force. Both the axial and radial force models, in Figures 21 and 22, show the effects of speed on forces, particularly at the lower cutting speeds. In all three models, the feed shows the consistent expected effect on force, namely, that higher feeds generate higher cutting forces.

The effect of cutting speed on the cutting forces at different depths of cut is shown in Figures 23, 24, and 25. At all four depths of cut, 0.050, 0.100, 0.150, and 0.200 inch, the cutting speed had little effect on the tangential cutting force as shown in Figure 23. Both the axial and radial forces increased the heavier depth of cut as the cutting speed increased. In general, heavier depths of cut produced higher forces, as expected.

The effect of feed on the cutting forces is shown in Figures 26, 27, and 28. These figures show that increasing the feed, at all four depths of cut, caused an increase in the cutting forces, particularly the radial and tangential forces.

The percent increases in cutting force associated with an increase in feed from 0.005 to 0.010 ipr at a cutting speed of 150 fpm are shown below for four depths of cut:

Depth of Cut inch	Axial Force	Radial Force	Tangential Force
0.050	45%	32%	347%
0.100	75%	72%	113%
0.150	88%	92%	68%
0.200	94%	104%	48%

The effect of depth of cut at different cutting speeds, 150, 200, and 250 fpm, and different feeds, 0.005, 0.007 and 0.010 ipr, is presented in Figures 29 through 34. As expected, the depth of cut has a significant effect on the cutting forces, heavier depths producing higher force levels. Table X also provides the background data for Figures 23 through 34.

Increasing the depth of cut from 0.050 inch to 0.200 inch at the following feeds and speeds causes increases in the cutting forces by the following amounts:

Feed: 0.005 ipr (Figures 29, 31, 33)

Cutting Speed-fpm	Axial Force	Radial Force	Tangential Force
150	352%	178%	332%
200	1000%	289%	302%
250	6000%	664%	273%

Cutting speed: 150 fpm (Figures 30, 32, 34)

Feed-ipr	Axial Force	Radial Force	Tangential Force
0.005	215%	156%	617%
0.007	267%	223%	258%
0.010	320%	299%	138%

WEAR PHOTOGRAPHS

Photographs were taken of the worn carbide inserts to show typical wear patterns. Wear photographs were taken of several Carboloy 883 tools which were tested at 0.150 inch depth of cut. Figure 35 shows a photograph of a tool tested at 200 fpm, 0.0025 ipr, with 38.8 minutes of cutting time. This shows a good example of the wear pattern called depth-of-cut notch, frequently occurring when turning materials which exhibit work hardening from machining. The uniform wear is very light, 0.004 inch, but the length of the notch is 0.032 inch.

The photograph of the tool used to machine the titanium at 100 fpm, 0.005 ipr, and 0.150 inch depth for 60 minutes of cutting time shows a badly chipped cutting edge in Figure 36. Figure 37 shows the wear on a tool tested at the same cutting speed and for the same cutting time, but at a lower feed, 0.0025 ipr. Figure 37 shows good uniform wear with no chipping.

A different 883 carbide tool was photographed at 90 minutes, Figure 38, at 120 minutes, Figure 39, and again at 180 minutes in Figure 40. This tool continued to develop uniform wear up to 180 minutes, at which point the cutting edge, weakened from cratering, collapsed, leaving the appearance of a chipped tool.

Figure 41 shows the wear photographs of a tool used in a boring test for 428 minutes. The pattern shows uniform wear, along with the typical ragged edge of a tool that has cut for this long. This tool machined the titanium at 150 fpm, 0.0025 ipr, 0.050 inch depth of cut for 428.3 minutes.

SURFACE INTEGRITY

Eight surface integrity test cuts were prepared on the outer surface of one of the cylinders which had been thoroughly used to generate turning data. A "used" cylinder was selected since it would be sectioned (sawed into small pieces) to obtain the metallographic samples necessary for this examination. The following machining conditions were used for this study:

Cutting speed: 150 feet/minute (fpm)

Feed: 0.005 inch/revolution (ipr)

Cutting Fluid: Trim Sol (1:20)

The variables in the eight tests were sharp and dull tools, and four levels of depth of cut, 0.050, 0.100, 0.150, and 0.200 inch. Sharp tools were defined as having no more than 0.004 inch wear, while a dull tool was one with 0.015 inch wear.

Radial sections were metallurgically prepared and viewed in the unetched and in the etched condition (using hydrofluoric acid, nitric acid, and water) at magnifications ranging from 100X to 1000X. Low magnification photomicrographs (30X for mount #31229 and 10X and 50X for mount #31230) were obtained to show the severe microstructural segregation or banding which was typical of all eight samples examined. Although the entire shoulder profile was viewed, photomicrographs were taken only on the turned surface rather than on the shoulder area.

The major difference in surface alteration as a result of machining conditions appears to be dependent on the tool wear. The depth of the plastically deformed layer or zone, an indication of surface integrity damage, was nominally less than 0.0002 inch for the sharp tool condition, and as much as 0.0[illegible] inch for the dull tools.

Figure 42 shows the surface machined at 0.050 inch depth of cut with a sharp tool. The photomicrograph at 30X clearly identifies the banding type of segregation typical in all the samples. The machined surface is generally smooth, with very isolated laps extending inward less than 0.0002 inch. There was no additional evidence of plastic deformation or other microstructural alterations.

The surface machined at 0.050 inch depth of cut with a dull tool is shown in Figure 43. The machined surface is generally smooth with repeating standing scallops or feed lines, associated with a continuous plastically deformed layer. Light etching areas were generally located at the crest of a standing scallop. The maximum depth was less than 0.001 inch. The metallographic examinations of the surfaces machined at 0.100, 0.150, and 0.200 inch depths of cut exhibit essentially the same characteristics as the surfaces machined at 0.050 inch depth of cut, indicating that this parameter does not influence the amount of surface integrity damage.

The following list describes the conditions under which the remaining depicted surfaces were produced:

Figure 44	0.100" depth of cut; sharp tool
Figure 45	0.100" depth of cut; dull tool
Figure 46	0.150" depth of cut; sharp tool
Figure 47	0.150" depth of cut; dull tool
Figure 48	0.200" depth of cut; sharp tool
Figure 49	0.200" depth of cut; dull tool

SCANNING ELECTRON MICROSCOPE ENERGY DISPERSIVE SPECTROSCOPY

Eight groups of chips, which were generated by machining with and without cutting fluid, with two different cutting speeds, and with two different tool materials (883 and KC910), were submitted for SEM-EDS analysis. The purpose of the study was to ascertain whether any metal transfer of the cutting tool material had taken place on the surfaces of the chips generated during the machining operations.

Samples of chips from each group were examined on a Cambridge StereoScan 600 Scanning Electron Microscope (SEM) equipped with an EDAX X-ray Spectrometer. SEM examination and X-ray analysis of the samples were conducted at magnifications ranging from 200X to 5000X. No reference was obtained on the KC910 insert. The results of the analysis were as follows. In all eight groups, the same elements in approximately the same proportion were detected on the surfaces of the chips. These elements were identified as titanium, aluminum, zirconium, molybdenum, vanadium, and chromium. These elements are identified on the X-ray energy spectra in Figures 50 through 53. No tungsten or cobalt was detected on the surfaces of the chips that were generated with the KC910 tool. Moreover, the slight disparity in intensity could have resulted from surface texture or contour. At high magnifications (2000X to 5000X), no significant rise in the aluminum intensity was observed. As a reference, a typical X-ray energy spectrum was obtained from an 883 carbide insert (tungsten carbide in a cobalt matrix) in Figure 54.

Figure 55 is an SEM image typifying the surface of the chips in a region containing metal "build-up."

Summary

The energy dispersive X-ray analysis showed no evidence to indicate that transfer of cutting tool material onto the chips, generated in cutting, had occurred during machining. It should be noted, however, that this analysis is not capable of detecting the transfer of minute quantities of material, that is, in the order of angstroms or atom layers thick. Such a surface determination would require the use of more sophisticated techniques such as Auger Electron Spectroscopy (AES) and/or Ion Scattering Spectrometry (ISS).

PRODUCTION PROCESS PARAMETERS

Introduction

The laboratory tests were structured to produce machining conditions which would sustain tool life sufficient for a nine-foot long cut in the inside diameter of tubes having the same (or close) dimensions as the samples submitted to us for testing. These goals were met, at the 0.050 inch depth of cut as explained below.

Tool life or cutting time, in minutes, had to be sufficient to make a cut of 9 feet or 108 inches. At the conditions of 150 fpm, 0.050 ipr, and 0.050 inch depth of cut, the tool life obtained in the laboratory was 216 minutes. This length of cutting time was sufficient to make a 9-foot long I.D. cut in tube with the same dimensions as our test samples, as illustrated by the following calculation example:

If: V = the cutting speed, 150 fpm; f = the feed, 0.005 ipr; D = the I.D., 5.25 inches, of the sample tube; N = the rpm.

Then: $$N = \frac{12 \times V}{\times D} = \frac{12 \times 150}{\times 5.25} = 109 \text{ rpm}$$

The tool life, TL, required for a 108-inch or a 9-foot cut would be:

$$\frac{\text{rev (rpm)}}{\text{min}} \times \frac{\text{in (feed)}}{\text{rev}} = \frac{\text{in}}{\text{min}} = \frac{108''}{TL}$$

Solving for TL, the tool life:

$$TL = \frac{108''}{109 \text{ rpm} \times 0.005 \text{ ipr feed}} = 198 \text{ minutes}$$

This calculation shows that 198 minutes of cutting time are required to complete one 9-foot long pass in the 5.25 inch I.D. at 150 fpm, 0.005 ipr, and 0.050 inch depth of cut, using a single-tooth boring head. The 216 minutes of tool life obtained in the laboratory tests is slightly (9%) more than adequate for this need. If a 2-tooth boring head, which is common, is used, then only 101 minutes are required for one 9-foot pass, and the tool wear should be relatively light.

Using the data shown in Figure 13 or Table VII for tool life values obtained at 0.150 inch depth of cut, and repeating the calculation as above (rpm = 109, feed = 0.0025 ipr, and TL from Fig. 13 = 180 min.), indicated that only half of the 9-foot length could be bored at this depth of cut before the one Carboloy 883 insert would be dull and need replacing or indexing. However, if the boring head contains 2 inserts, then the tool life would be barely adequate for one 9-foot pass. The data in Figure 13 are for one insert or "tooth" and the 0.0025 ipr is really the chip load for one tool. If 2 teeth are used, the chip load is still 0.0025 inch per tooth, but the feed rate is now 0.00 ipr. At double the advance per revolution, the time required per pass is then reduced to half.

A vital key to obtaining the predicted tool life is to machine through a surface which is not severely work hardened. The as-received I.D. and O.D. surfaces were removed with skin cuts before the tool life tests were conducted.

Cutting through a work-hardened surface produces tool wear in the form of "depth-of-cut notch" as shown in Figure 35. This type of wear can seriously weaken the tool and cause a catastrophic breakage of the inserts long before the uniform wear would cause the tool to need changing. The notching effect of wear can be alleviated to some extent by increasing the lead angle or side cutting edge angle (SCEA). Conventional boring heads do not often offer this tool geometry as standard and, therefore, are not usually suitable for machining this type of titanium alloy. Another possible source for problems in obtaining the predicted tool life is the C-2 grade of tungsten carbide. All manufacturers' grades do not perform alike because they do not have the same wear resistance when machining this alloy.

Process Development for Manufacturing

This contract required three pieces of the titanium Beta C to be machined to a print that was supplied. The purpose of this part of the contract was to develop a workable machining process which could be transferred to a manufacturing environment for production machining of 9-foot long tubes rather than 3-foot parts. The three parts to be machined had no real function in and of themselves, but were merely the vehicle to develop the process. The potential success of the process would be verified by the final quality of the three parts defined by their conformance to the print.

The first attempt at machining the parts did not succeed in making acceptable parts, but was a valuable learning experience. A local subcontract machining service, which makes a considerable amount of titanium parts, was selected for this task. This effort was performed on a large MAZAK CNC turret lathe using a test piece rather than one of the designated tubes to be finish-machined. The tooling for this exercise, from KOMET R B, was an ABS type, 2-tooth indexable insert boring head which could be attached to a series of extensions for various bore depths. This head had moveable cartridges with radial adjustment to vary the diameter being cut. Successive passes at a constant depth of cut could be made on the same test piece. Replaceable carbide wear (guide) pads were added to the boring head for stability, along with an adapter for through-the-tool coolant flow. Two problems emerged which prevented this system from working successfully. The first problem was dynamic instability of the cantilevered boring bar. To completely reach through the 3-foot long tube, the total length of the bar had to exceed 3 feet. Several initial tests were performed with only a 19-inch extension to reach half the length of the piece. These tests usually resulted in tool failure. The boring head on the 36-inch long, cantilevered extension could not enter the tube at the required depth of cut (0.050 inch) without severe chatter. To offset this problem, a counter bore was cut into the entrance end of the tube using a short extension on the boring bar for maximum rigidity. Once the counterbore was made, the boring cut was resumed and the second problem was encountered.

This problem was simply carbide tool wear or breakdown. The KOMET engineers monitoring the test insisted (in spite of data to the contrary) on using excessively high cutting speeds which resulted in short tool life and premature tool failure. When the carbide inserts started to wear and cut the I.D. under-size, the carbide wear or guide pads seized in the titanium material, resulting in their breakage. The problem was incorrectly diagnosed as lack of lubrication because a water-base cutting fluid (Trim Sol 1:20) was used. The tests were suspended since the compounded problems were considered insurmountable for the short term. The results of these tests emphasized the need for a deep hole boring (gun drilling or trepanning) machine.

The American Heller Company, which manufactures BTA deep hole boring heads, provided Metcut with the name of a subcontract machining service which had a long bed, large diameter, deep hole boring machine. This company, Hanard Machine Co., located in Salem, Oregon, was contacted and arrangements were made to have the three parts machined there. A custom diameter boring head, which would fit the Boehringer Trepanning Machine, was ordered from American Heller and machine time was scheduled at Hanard to perform the machining analysis.

I.D. BORING OPERATION

Machine Tool

The boring operation was conducted on a 40 horsepower Boehringer Model No. V 800 Trepanning/Skiving Machine. This machine had the following capacities: 72 inches length of work; diameter: 6 inches for trepanning, 11 inches for skiving; spindle torque: 3300 ft.lbs.; feed thrust: 28,000 N; spindle speed: 35 to 1800 rpm; feed rate: 0.8 to 157 in./min. The oil flow capacity was 170 gallons per minute (gpm).

Any rigid gun drilling or trepanning machine of adequate-size capacity will also have proportionately adequate power and oil flow rate. The maximum power used in our machining tests was approximately 15 hp. For steady-state machining, before the inserts became dull, the required power was 10 to 13 hp. Since the tool life in machining this particular titanium alloy was somewhat sensitive to the cutting speed and the feed, the amount of depth of cut will have an important influence on the metal removal rate and the proportionate horsepower required.

Boring Head

The unique feature of the boring head manufactured by American Heller was the use fiber (micarta type) guide pads instead of carbide pads. See Figure 56. This modification is very important for machining titanium alloys. Titanium alloys have a strong tendency to weld to or seize against tungsten carbide at normal machining temperatures (1000°F to 1200°F).

I.D. BORING OPERATION (continued)

By replacing the normal carbide pads with the nonmetallic fiber materials the possibility of welding to the pads is eliminated. However, the boring head used in our tests did not use the geometry of a high lead (SCEA) angle to thin the chip and reduce the depth-of-cut notch wear. The design provided by American Heller was one they had successfully used before in boring titanium alloys. Because of the heavy depth of cut, 0.275 inch on a side, the chip gullet in the original design, Figure 56, was inadequate to flush the chips back through the boring bar. Consequently, severe chip jamming at the face of the cutter occurred, resulting in breakage of the inserts and stopping the test. This opening, which was originally about 3/8 inch in diameter, was ultimately opened to about 1-1/4 inch in diameter, as illustrated in Figure 57, to permit free flow of chips flushing through the cutter. Even with the oil flow rate of 170 gpm the chips could not be flushed through the smaller opening fast enough to prevent jamming. Figure 58 shows actual photographs of the boring head before and after the chip gullet was modified. Even though the photographs are not close-up for fine details, the general concept is evident and shows how the enlargement extends in the axial direction as well as the radial direction of the cutter face.

Tool Materials

The tool material used in the deep hole boring tests was Newcomer C2 carbide grade N22. The performance of this carbide compared to the Carboloy 883 is shown in Figure 15. The tool life of the N22 was about one-third the tool life of the 883, as seen in Table XI.

I.D. BORING OPERATION (continued)

The N22 carbide was the stock material at Heller and the schedule would not permit the delivery delay (8 to 10 weeks) to obtain 883 carbide from Carboloy. The test data in Figure 15 were developed with the Caria-T oil since this oil was used in the Boehringer machine at Hanard.

The fact that the N22 carbide would not last as long as desired created another problem, lack of chip control. The inserts were ground with a barrier-type chip breaker which worked effectively until the wear on the cutting edge effectively removed the correct angle and spacing between the cutting edge and the barrier. Without chip control, the continuous snarl of chips can cause severe problems. If the chips get entangled around the insert, and are "recut", the result usually is tool breakage. Often the tangled chips will scratch or scar the machined surface and either ruin the finish or increase the amount of secondary operations to reach the desired size and finish. The subject of chip control is addressed more thoroughly in the turning section which follows and also in Appendix A.

Machining Conditions

Test cuts were made at 124 fpm (90 rpm), 155 fpm (112 rpm), and 249 fpm (180 rpm). The rpm was adjusted with a gear box change. There was no variable speed feature to set the rpm at an exact level. The feed rate, which was variable, was maintained between 0.002 and 0.003 inch per tooth, for the 2-tooth cutter.

I.D. BORING OPERATION (continued)

The variable feed adjustment was somewhat approximate and could not be accurately set without trial and error attempts. The cutting fluid was a sulfo-chlorinated oil identified as Garia-T. This oil was distributed by National Chemical Corp. in Detroit, Michigan.

I.D. HONING OPERATION

Honing tests were performed on several cylinders to determine the correct process variables for this finishing operation. This work was conducted at Precision Diameters Inc., located in Centerville, Ohio, a suburb of Dayton, Ohio. These data are listed in Table XII.

Machine Tool

The honing operation was performed on a Sunnen Model CHV machine equipped with a Model CHV-1000 Remote Feed Honing Tool. See Table XIII.

Honing Oil

The honing oil used in this operation was Sunnen MAN-863 Oil, undiluted.

Honing Stones

A choice of stone sets to be used for rough honing consisted of either Sunnen WW51-A45 or WW51-NR51. The WW51-A45 is a 150 grit aluminum oxide stone. The WW51-NR51 is a resinoid bonded 220 grit cubic boron nitride (CBN) stone. The stock removal rate is essentially the same for both the aluminum oxide and the CBN. The advantage in using the CBN stones is a significantly slower wear rate on the stones, since the CBN is much harder than the aluminum oxide.

I.D. HONING OPERATION (continued)

For bores up to 9-feet long, the CBN stones may be more practical, even though they are more expensive than the aluminum oxide, to complete the entire bore length without having to stop and change the stones. The WW51-J95 stones were used for finish-honing the bores. The J95 designation is for a 500 grit silicon carbide stone.

Honing Parameters

Speed

The optimum rotational honing speed was expressed as 1200 rpm divided by the I.D., measured in inches or: $N = \frac{1200}{D}$

Where: N = spindle rpm and D = the bore diameter in inches

Feed

The optimum honing stroke rate was 480 inches per minute

Stock Removal Rate

The stock removal rate, R was expressed as: $R = \frac{0.159}{D \times L \times 6}$

Where: R = the stock removal in 0.0010 incl. of diameter change per minute

D = the inside diameter in inches

L = the length of the bore in inches

0.159 is a processing constant and 6 is a material (machinability) related constant

I.D. HONING OPERATION (continued)

This relationship applies to the "cleanup" phase of the honing operation where the peaks of various heights and shapes are reduced to primarily base metal. Tests were performed on different bores with the surface finish varying from 32 to 164 microinches. The variation in surface finish did not affect the stock removal rate. When honing the as-machined surface, 0.004 inch was removed from the I.D. to obtain an 80% cleanup and leave a finish of approximately 10 microinches. However, if the finish needs to be better than 10 microinches, the stock removal rate, R, drops to 0.0002 inch change in diameter per minute for the same parameters.

O.D. TAPER TURNING OPERATION

Machine Tool

The turning tests were performed on a Cincinnati Milacron Model 12-U CNC Lathe. This 30 hp. machine would swing 25" over the ways, chuck a 12-inch diameter piece up to 84 in. long. Any rigid CNC lathe of adequate-size capacity should have the proportionate power to machine this alloy and maintain the required dimensional accuracy and surface finish. See Table XIV.

Tool Materials

Carboloy 883, the preferred grade of carbide, was used to turn the O.D. surfaces of the three process pieces. The indexable inserts used were CNMG 643, clamped in a standard tool holder, which provided a 15° side cutting edge angle (SCEA). See Figure 59 for the tool geometry details.

O.D. TAPER TURNING OPERATION (continued)

The preferred SCEA of 45° was not available and could not be quickly procured. Depth-of-cut notching (see Fig. 35 for illustration) was a more troublesome problem in removing the surface layer since the tool holder with the lower SCEA (15°) was used. Once the surface layer was removed, no major difficulties were encountered in turning the three parts to the desired size and accuracy.

Chip Control

A minor problem encountered in the O.D. turning operation was chip control. The CNMG 643 insert has an effective rake angle of -5° and provides "general-purpose" chip control for steels at a feed rate as low as 0.010 ipr. However, the Beta C titanium alloy at 415 BHN hardness is a relatively high strength material and the chips which are produced in turning are strong and do not break easily. To compound the problem, the recommended feed rate for turning this titanium alloy is 0.005 ipr, definitely below the effective range of the CNMG-643 chip control design. The recommended chip control design for a lighter feed of 0.005 ipr would be a CNMG-K 643 (a Kennametal designation) insert (see sketch, Figure 60). This light feed chip control configuration is not offered by all carbide insert manufacturers, since their major emphasis is on heavy feed applications for high metal removal rate situations. Using a high feed on this titanium alloy will reduce the tool life drastically and is not practical. Increasing the depth of cut also improves chip control, as does increasing the feed. As shown in Figure 14, heavy increases in the depth of cut (0.050 to 0.150 inch), of a 3:1 magnitude, also decreases the tool life drastically, 216 minutes to 33 minutes.

O.D.TAPER TURNING OPERATION (continued)

An excellent technical paper describing the theoretical approach to chip control configurations in inserts, "CHIP CONTROL IN TURNING" by Nakamura, Christopher, and Wuebbling is enclosed in Appendix A. Also, Kennametal, Carboloy, and other carbide insert manufacturers have very good technical sections in their general catalogs discussing the practical applications and limitations of various chip control shapes in indexable inserts.

Machining Conditions

Cutting Speed: 100 fpm on scale

150 fpm under scale

Feed: 0.005 ipr

Depth of Cut: 0.090 inch on scale, 0.095 inch under scale, 0.080 inch taper cuts, 0.060 inch finish cut (See Appendix B)

Cutting Fluid: Water Soluble Synthetic 1:20

SUMMARY OF FINISH-MACHINED PARTS

Sketches of the cylinders in the finish-machined and in the honed condition, along with the target dimensions to be met, are shown in Appendix B, Figures A through G. The target dimensions and surface finish requirements were met in the three parts used to develop a successful machining process for the titanium Beta C alloy. A major influence on the process used to bore 9-foot long cylinders will depend on the number of passes and the depth of cut on each pass. Both the laboratory data and "production" data conclusively prove the severe reduction in tool life resulting from heavy depths of cut.

TABLE I

TOOL EVALUATION AND MACHININC PARAMETERS

Tool: SNG-432 insert
BR:-5° ECEA and SCEA: 45°
SR:-5° CLEARANCE: 5°
Cutting speed: 200 fpm
Feed: 0.005 ipr
Depth of cut: 0.050 inch
Tool life end point: 0.015 inch uniform wear
Cutting fluid: dry

Tool Material	Tool Life-minutes
Kennamatal KC910	22.4
Carboloy 883	20.0
Kennametal KC850	15.0
Kennametal K313	10.0
Kennametal K68	10.0
V R Wesson RAMET I	9.0
Carboloy 570	7.7
Kennametal KC950	5.0
Norton Noralide	0.9
Kennametal Kyon 2000	0.5
DeBeers Amborite	1.3
Greenleaf WG-300	0.5
Iscar Iscanite	0.2

TABLE II

TOOL EVALUATION OF POSITIVE RAKE TOOLS

Braecut	Ramet I
BR: 0° SCEA: 15°	BR:+5° SCEA: 15°
SR:+5° ECEA: 5°	SR: 0° ECEA: 15°
CLEARANCE: 5°	CLEARANCE: 5°

Cutting Fluid: Trim Sol (1:20)
Depth of cut: 0.050 inch
Tool life end point: 0.015 inch uniform wear
0.030 inch localized wear

Tool Material	Cutting Speed fpm	Feed ipr	Tool Life minutes
Braecut M44 HSS	30	0.003	420.0
Braecut M44 HSS	30	0.005	180.0
Braecut M44 HSS	50	0.003	28.0
Braecut M44 HSS	50	0.005	24.0
Ramet I Carbide	50	0.005	180.0
Ramet I Carbide	150	0.005	10.0
Ramet I Carbide	200	0.005	2.0

TABLE III

TOOL EVALUATION NEGATIVE RAKE TOOLS

Carbide Tools	High Speed Steel
BR:-5° SCEA: 45°	BR:-5° SCEA: 15°
SR:-5° ECEA: 45°	SR:-5° ECEA: 5°
CLEARANCE: 5°	CLEARANCE: 5°

Feed: 0.005 ipr
Depth of cut: 0.050 inch
Cutting fluid: Trim Sol (1:20)
Tool life end point: 0.015 inch uniform wear
0.030 inch localized wear

Tool Material	Cutting Speed fpm	Tool Life minutes
883	150	216
Braecut M44 HSS	30	150
Ramet I	150	103
Braecut M44 HSS	50	9

TABLE IV

TOOL EVALUATION OF CARBOLOY 883, KENNAMETAL KC910 AND K313

Tool: SNG-432 inserts
BR: -5° SCEA: 45°
SR: -5° ECEA: 45°
CLEARANCE: 5°
Depth of cut: 0.050 inch
Tool life end point: 0.015 inch uniform wear
0.030 inch localized wear

Cutting Speed fpm	Feed ipr	Tool Life minutes		Cutting Fluid
		883	KC910	
175	0.005	40.0	30.0	dry
200	0.005	20.0	22.4	dry
225	0.005	-	9.3	dry
250	0.005	9.3	5.0	dry
275	0.005	7.5	-	dry
		883	K313	
150	0.003	-	300.0	Trim Sol (1:20)
150	0.005	216.0	213.0	Trim Sol (1:20)
150	0.007	90.0	120.0	Trim Sol (1:20)
200	0.005	30.0	20.0	Trim Sol (1:20)
250	0.005	15.0	5.8	Trim Sol (1:20)
275	0.005	9.0	1.0	Trim Sol (1:20)

TABLE V

TOOL GEOMETRY EVALUATION

Tool: Carboloy 883 SNG-432
Depth of cut: 0.050 inch
Cutting fluid: dry
Tool life end point: 0.015 inch uniform wear
0.030 inch localized wear

Tool Geometry	Cutting Speed fpm	Feed ipr	Tool Life minutes
BR: -5°	100	0.010	18.0
SR: -5°	125	0.010	8.1
SCEA: 15°	150	0.005	38.3
ECEA: 15°	150	0.010	7.7
CLEAR: 5°	175	0.005	15.0
	175	0.010	5.0
	200	0.005	6.5
BR: -5°	100	0.010	30.0
SR: -5°	135	0.010	10.0
SCEA: 45°	150	0.010	7.8
ECEA: 45°	175	0.005	40.0
CLEAR: 5°	200	0.005	20.0
	250	0.005	9.3
	275	0.005	7.5
BR: +5°	150	0.005	32.0
SR: 0°	175	0.005	22.1
SCEA: 45°	250	0.005	4.0
ECEA: 45°	275	0.005	2.2
CLEAR: 5°			

TABLE VI

EFFECT OF CUTTING FLUID

Tool: Carboloy 883 SNG-432
BR: -5° SCEA: 45°
SR: -5° ECEA: 45°
CLEARANCE: 5°
Feed: 0.005 ipr
Depth of cut: 0.050 inch
Tool life End Point: 0.015 inch uniform wear
0.030 inch localized wear

Cutting Speed fpm	Tool Life minutes		
	Dry	Trim Sol (1:20)	Mobilmet 235 (1:20)
150	40.0	216.0	-
200	20.0	30.0	23.0
250	9.3	15.0	13.5
275	7.5	9.0	8.0

TABLE VII

EFFECT OF DEPTH OF CUT

Tool: Carboloy 883 SNG-432
BR: -5° SCEA: 45°
SR: -5° ECEA: 45°
CLEARANCE: 5°
Cutting Fluid: Trim Sol (1:20)
Tool Life End Point: 0.015 inch uniform wear
0.030 inch localized wear

Cutting Speed fpm	Feed ipr	Tool Life minutes	
		0.050" depth	0.150" depth
75	0.005	-	47.0
100	0.0025	-	60.0
100	0.005	-	60.0
150	0.0025	-	180.0
150	0.005	216.0	33.0
175	0.0025	-	68.3
175	0.005	-	19.4
200	0.0025	30.0	38.7
200	0.005	-	10.0
250	0.005	15.0	5.0
275	0.005	9.0	-

TABLE VIII

TOOL LIFE MODEL

Tool: Carboloy 883 SNG-432
BR: -5° SCEA: 45°
SR: -5° ECEA: 45°
CLEARANCE: 5°
Depth of Cut: 0.050 inch
Cutting Fluid: Trim Sol (1:20)
Tool Life End Point: 0.015 inch uniform wear
0.030 inch localized wear

Cutting Speed fpm	Feed ipr	Tool Life minutes	Cutting Forces pounds					
			sharp			dull		
			Fa	Fr	Ft	Fa	Fr	Ft
100	0.007	150.0	78	123	147	149	322	180
100	0.015	-	90	175	236	-	-	-
100	0.020	-	104	209	321	-	-	-
150	0.005	216.0	57	112	103	131	175	125
150	0.007	90.0	72	111	127	114	222	164
150	0.010	20.0	77	140	195	153	325	234
200	0.003	125.6	40	69	70	87	137	84
200	0.005	30.0	39	72	97	80	148	112
200	0.009	7.0	59	119	176	102	230	188
200	0.015	-	144	230	222	-	-	-
250	0.005	15.0	51	95	101	173	310	117
275	0.005	9.0	43	79	90	209	400	129
300	0.015	-	131	313	230	-	-	-

TABLE IX

EFFECT OF CUTTING FLUID AND TOOL CONDITION ON CUTTING FORCE

Tool: Carboloy 883 SNG-432
BR: -5° SCEA: 45°
SR: -5° ECEA: 45°
CLEARANCE: 5°
Cutting Speed: 150 fpm
Feed: 0.005 ipr
Depth of Cut: 0.050 inch
Cutting Fluid: Trim Sol (1:20)
Tool Life End Point: 0.015 inch uniform wear
0.030 inch localized wear

Cutting Force direction	Cutting Force pounds					
	sharp tool					
	883		K313		KC850	
	wet	dry	wet	dry	wet	dry
axial force	57	51	51	58	66	71
radial force	111	106	93	94	107	112
tangential force	103	112	98	118	84	101
	dull tool					
axial force	131	117	284	269	413	338
radial force	175	188	420	415	809	659
tangential force	125	137	127	144	151	166

TABLE X

EFFECT OF DEPTH OF CUT ON CUTTING FORCE

Tool: Carboloy 883 SNG-432
BR: -5° SCEA: 45°
SR: -5° ECEA: 45°
CLEARANCE: 5°
Cutting Fluid: Trim Sol (1:20)

Cutting Speed fpm	Feed ipr	Depth inch	Cutting Force-pounds		
			axial	radial	tangential
150	0.005	0.050	57	112	103
150	0.005	0.100	80	130	186
150	0.005	0.150	165	243	284
150	0.005	0.200	174	260	355
150	0.007	0.050	72	111	164
150	0.007	0.100	188	263	275
150	0.007	0.150	197	283	398
150	0.007	0.200	289	405	516
150	0.010	0.050	77	140	195
150	0.010	0.100	214	309	370
150	0.010	0.150	231	352	511
150	0.010	0.200	390	594	683
200	0.005	0.050	39	72	97
200	0.005	0.100	80	133	189
200	0.005	0.150	202	278	289
200	0.005	0.200	359	521	405
250	0.005	0.050	51	95	101
250	0.005	0.100	83	135	194
250	0.005	0.150	200	287	287
250	0.005	0.200	380	538	420

TABLE XI

COMPARISON OF CARBOLOY 883 AND NEWCOMER N22

Carboloy 883		Newcomer N22	
BR: -5°	SCEA: 45°	BR: 0°	SCEA: 5°
SR: -5°	ECEA: 45°	SR: 0°	ECEA: 5°
CLEARANCE: 5°		CLEARANCE: 5°	

Feed: 0.050 ipr
Depth of Cut: 0.050 inch
Cutting Fluid: 883, Trim Sol (1:20)
N22, Garia-T (Oil)

Cutting Speed-fpm	Tool Life-min.	
	Carboloy 883	Newcomer N22
150	216	76
175		33
200	30	9
250	15	
275	9	

TABLE XII

DEEP HOLE BORING OPERATION

Machine Tool: A 40 horsepower Boehringer Model V 800 Trepanning Machine with the following capacity: Workpiece Size: 6 inches dia. - trepanning, 11 inches - skiving, 72 inches long
Cutting Speed: 155 fpm
Feed: 0.0033 ipr
Depth of Cut: 0.275 inch
Cutting Fluid: Garia-T Oil @ 170 gpm
Boring Head: American Heller BTA with 2 Newcomer N22 indexable inserts
BR:+5° SR:+5° CLEAR:+5°
Equipped with 4 fiber wear pads and modified to provide extra chip gullet space

TABLE XIII

HONING THE INSIDE DIAMETERS OF TITANIUM BETA C CYLINDERS

Machine Tool: Sunnen Model CHV with a Model CHV-1000 Remote Feed Tool

Honing Fluid: Sunnen MAN-863 Oil

Honing Stones: Rough Honing: Sunnen WW51-A45 or WW51-NR51
Finish Honing: Sunnen WW51-J95

Honing Speed: 1200 rpm/I.D.; 226 rpm for a 5.3-inch I.D.
Honing Feed: Stroke Rate: 480 inches per minute

Stock Removal Rate-Rough Honing:	0.159/6 D L; 0.000139 inches per minute I.D. change for a 5.3-inch I.D., 36 inches long, removing 0.004 inch from the I.D. for an 80% cleanup to 10-12 microinches
Stock Removal Rate-Finish Honing:	0.0002 inch per minute for finish below 10 microinches

TABLE XIV

O.D. TAPER TURNING OF TITANIUM BETA C

Machine Tool: Cincinnati Milacron Model 12 U 30-horsepower CNC Lathe
Tool Material: Carboloy 883 CNMG 643 inserts
BR:-5° SCEA: 15°
SR:-5° ECEA: 15°
CLEARANCE: 5°
Cutting Speed: 100 fpm - scale, 150 fpm - under scale
Feed: 0.005 ipr
Depth of Cut: 0.090 inch - scale, 0.095 inch - under scale, 0.080 inch - taper cuts, 0.060 inch - finish (see Appendix B)
Cutting Fluid: Water Soluble Synthetic 1:20

TURNING TITANIUM BETA C, 415 BHN
CUTTING TOOL MATERIAL EVALUATION

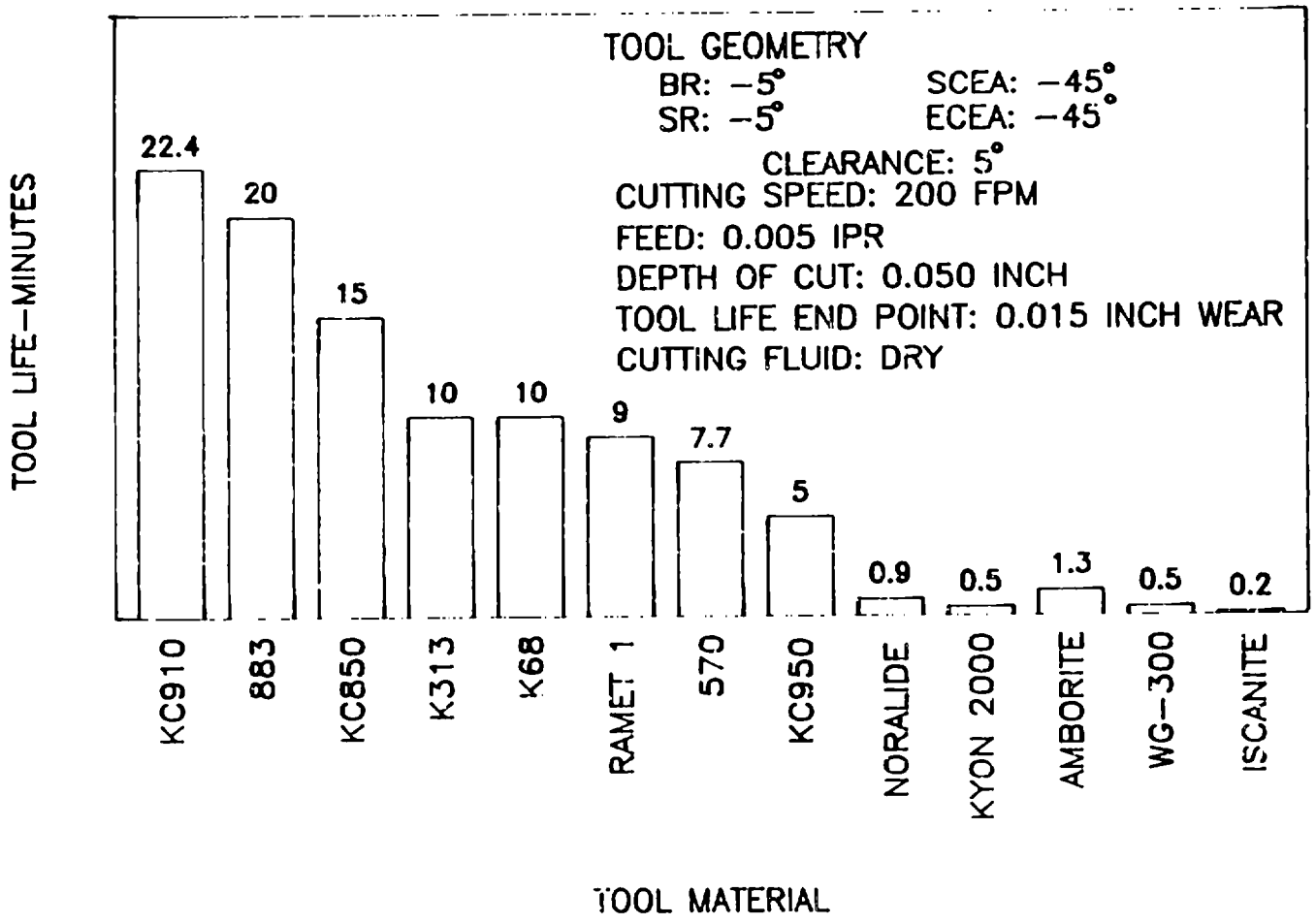

FIGURE 1

TURNING TITANIUM BETA C, 415 BHN
TOOL EVALUATION POSITIVE RAKE TOOLS

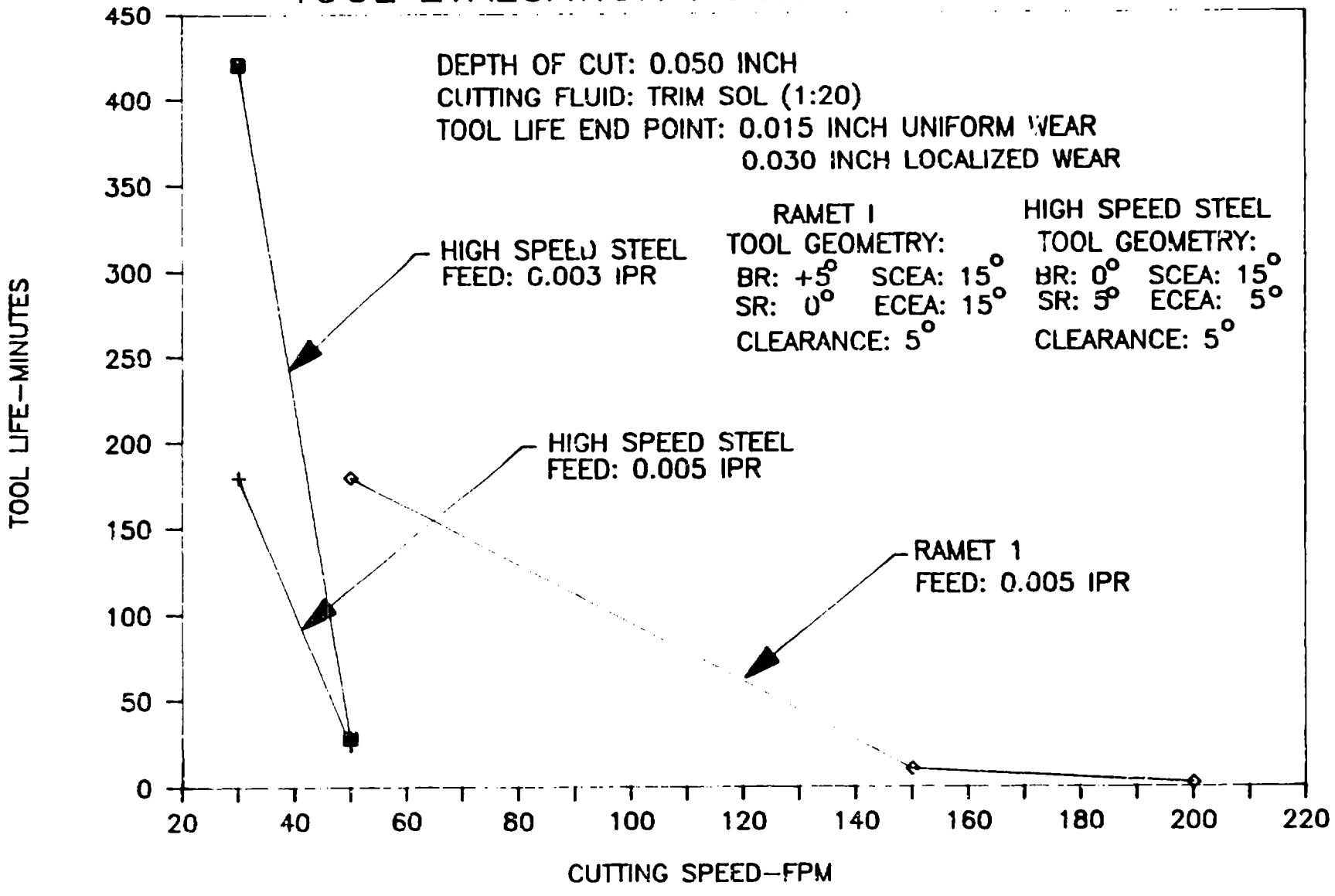

FIGURE 2

TURNING TITANIUM BETA C, 415,BHN
CUTTING TOOL MATERIAL EVALUATION
NEGATIVE RAKE CUTTING TOOLS

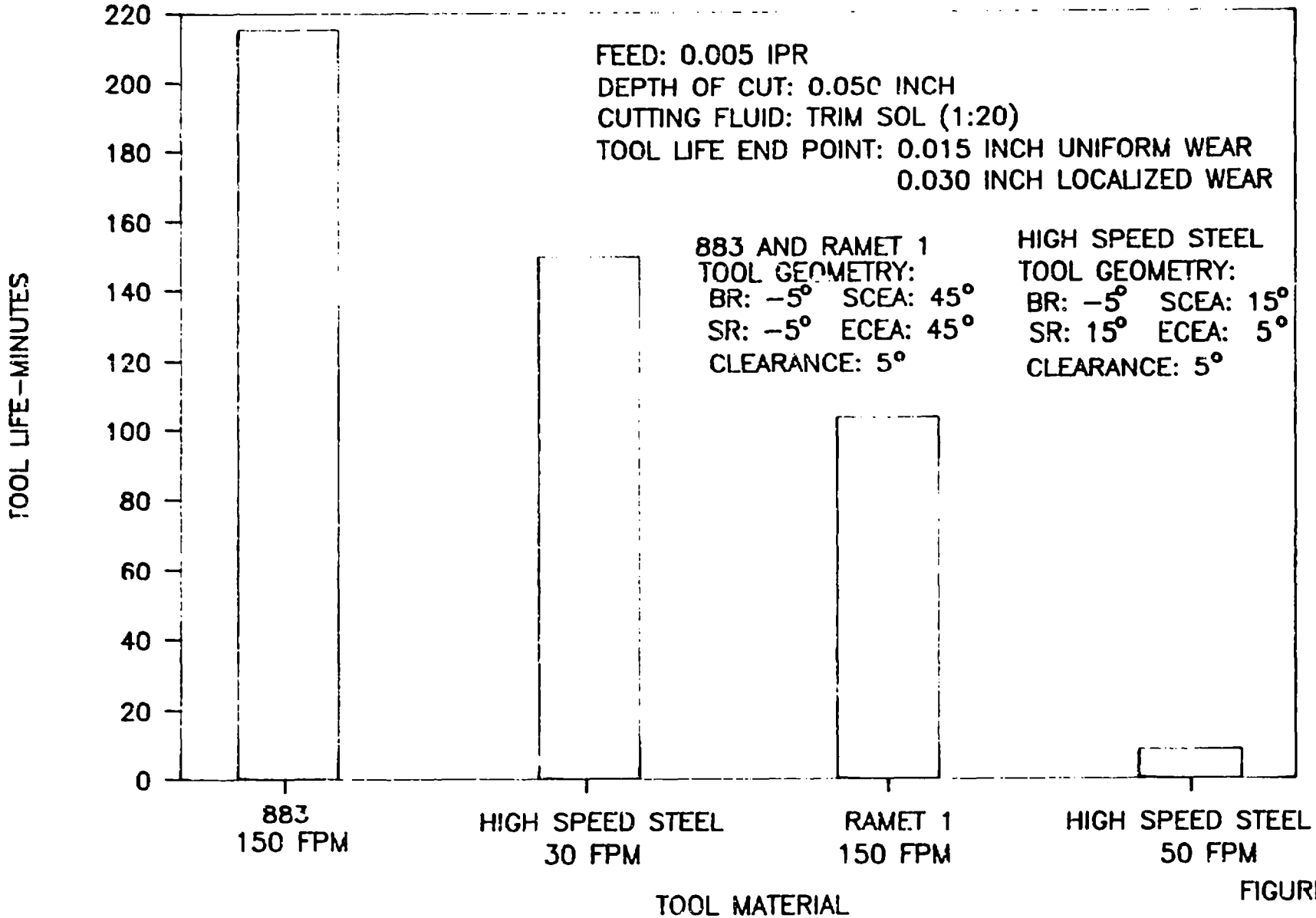

FIGURE 3

TURNING TITANIUM BETA C, 415 BHN
COMPARISON OF 883 AND KC910 CARBIDE INSERTS

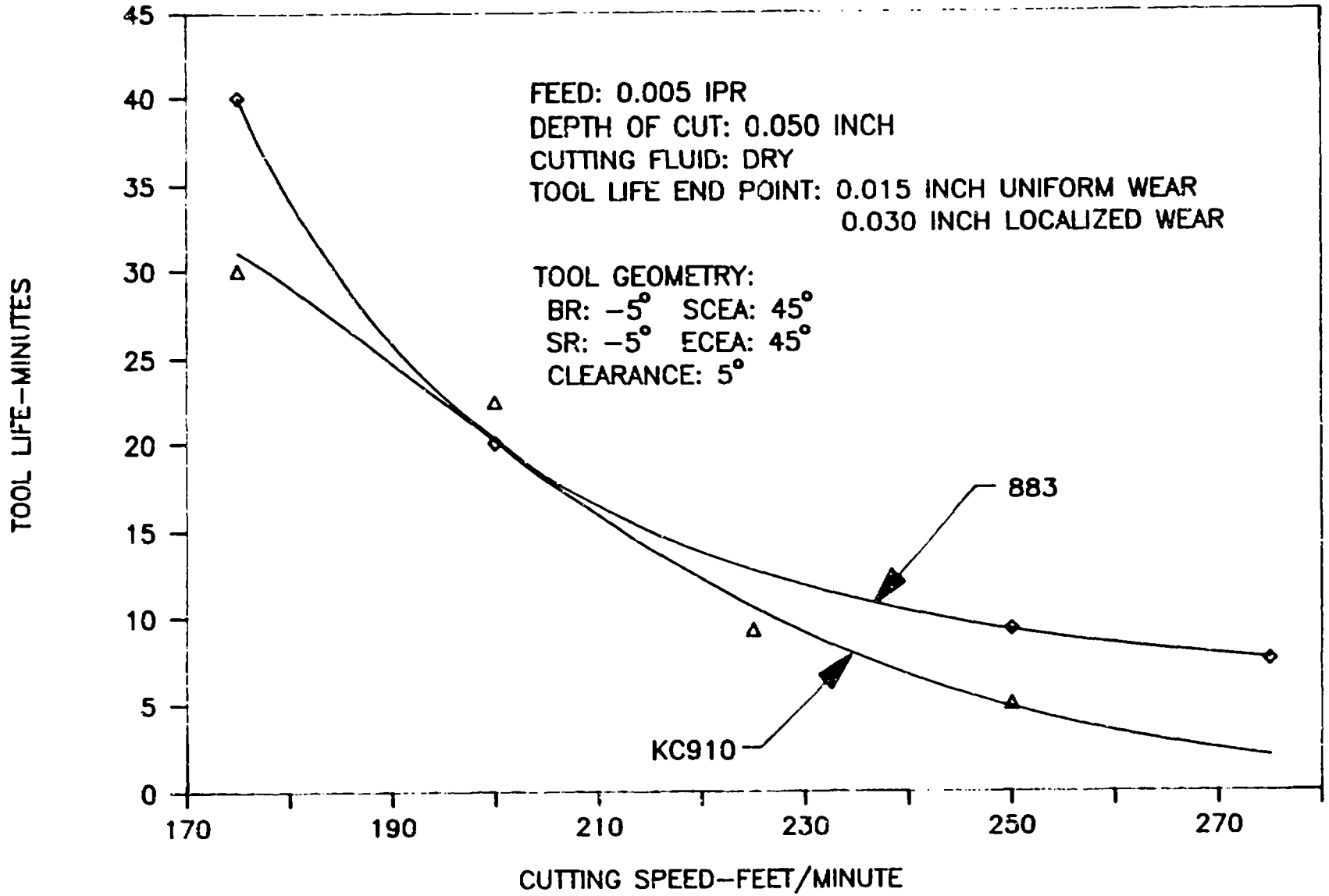

FIGURE 4

TURNING TITANIUM BETA C, 415 BHN
COMPARISON OF CARBOLOY 883 VERSUS KENNAMETAL K313

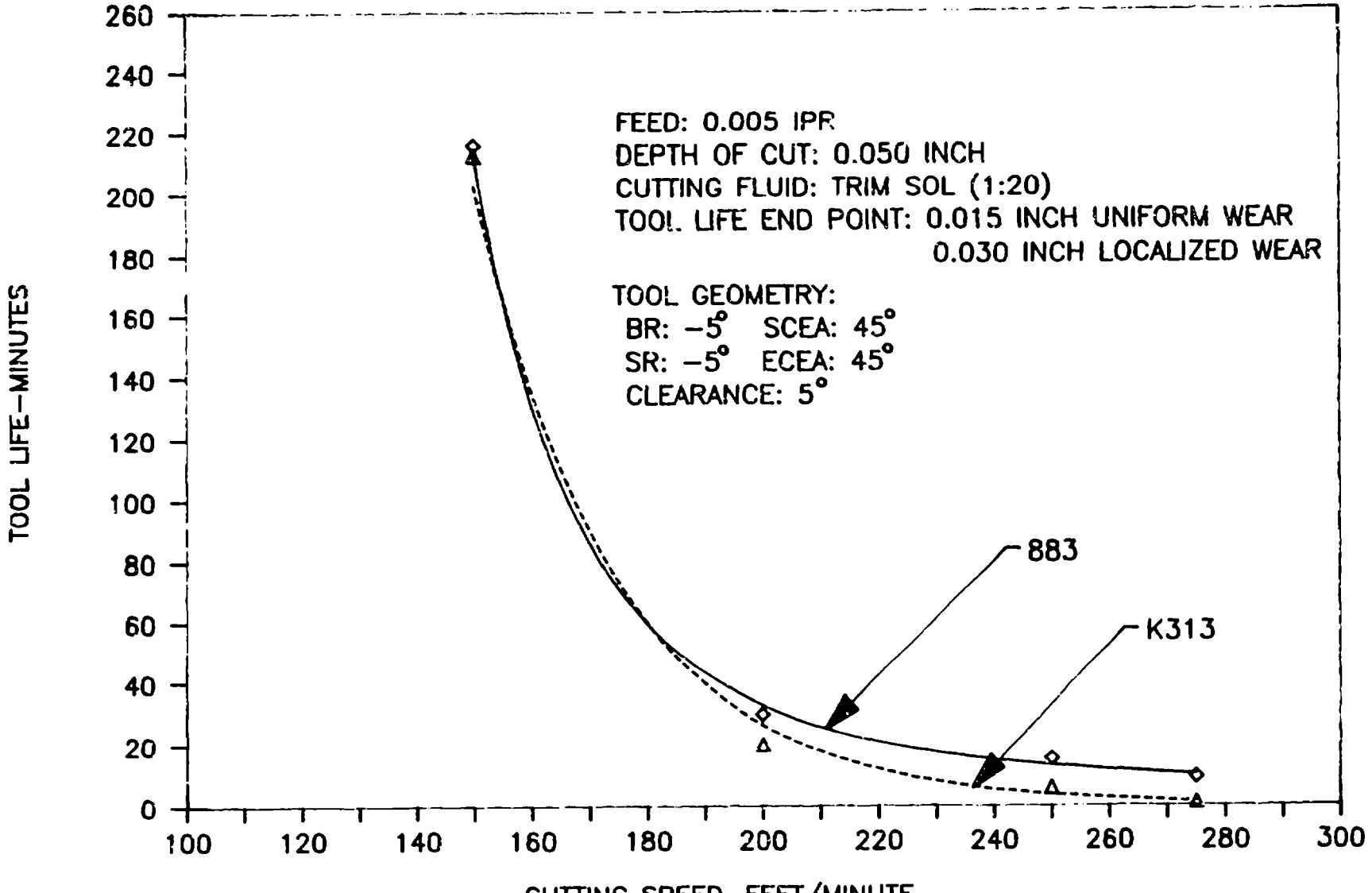

FIGURE 5

TURNING TITANIUM BETA C, 415 BHN
COMPARISON OF 883 VERSUS K313--FEED CURVES

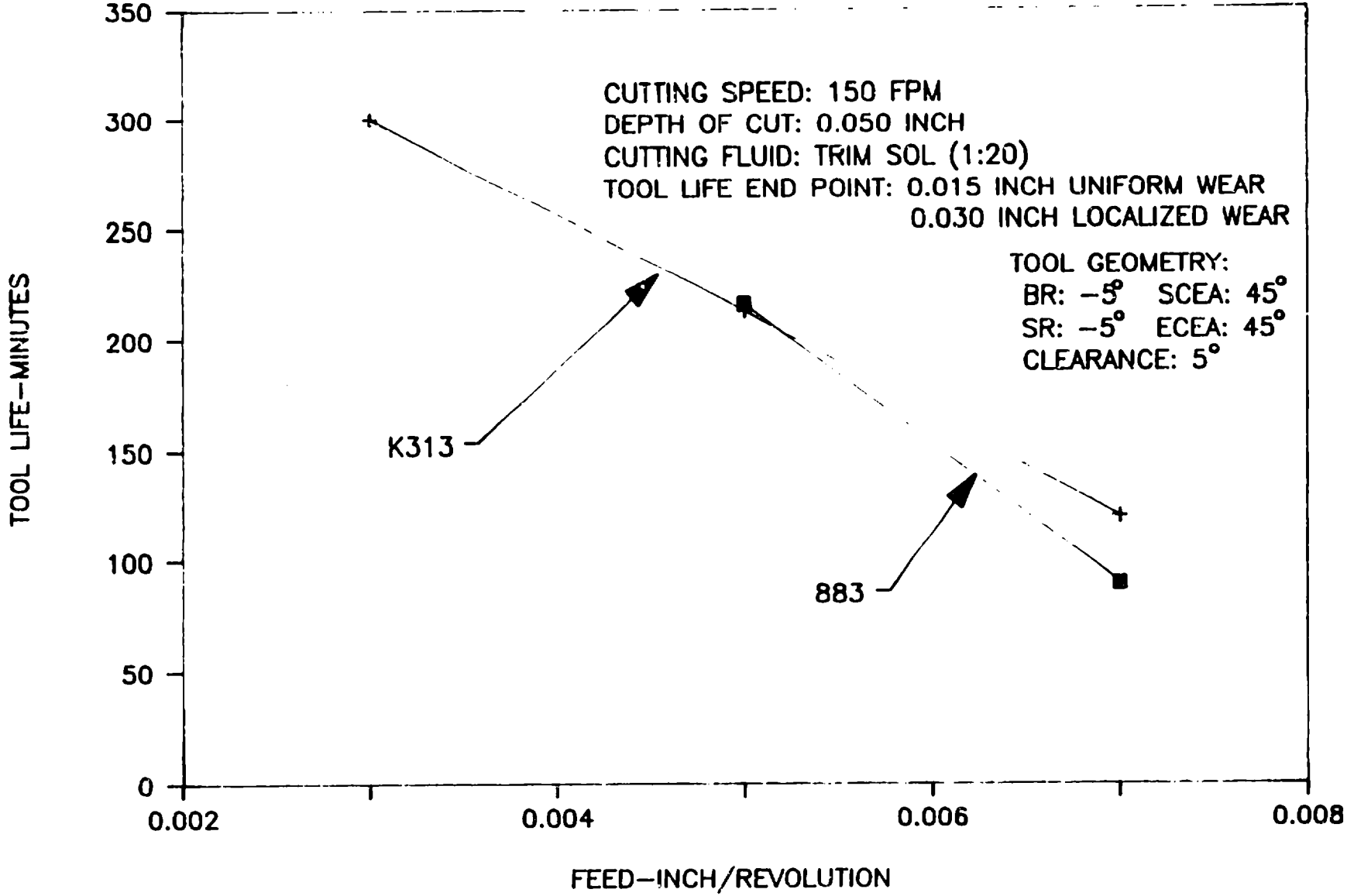

FIGURE 6

TURNING TITANIUM BETA C, 415 BHN

NEGATIVE RAKE 15° SCEA VERSUS NEGATIVE RAKE 45° SCEA

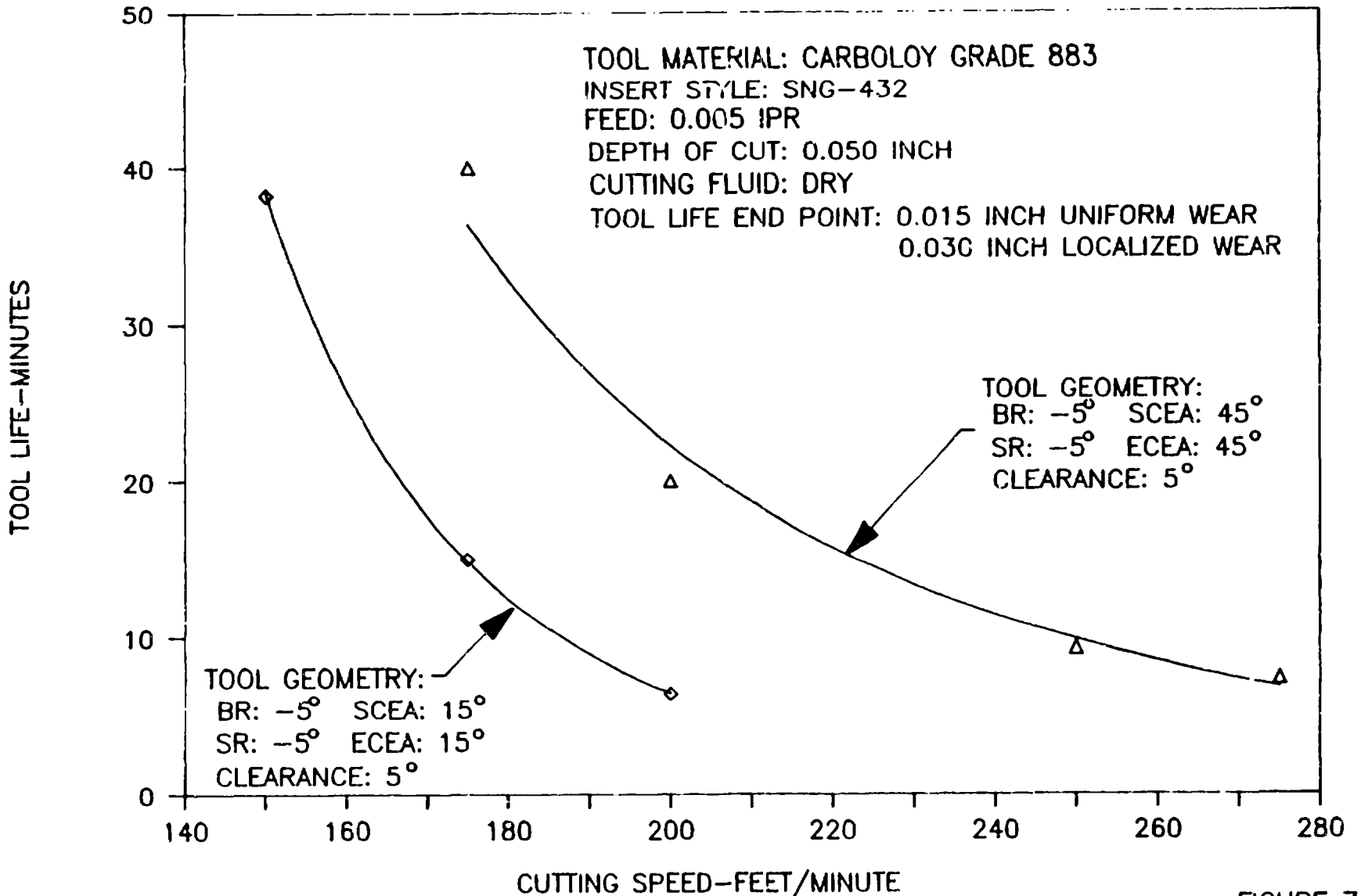

FIGURE 7

TURNING TITANIUM BETA C, 415 BHN

NEGATIVE RAKE 15° SCEA VERSUS NEGATIVE RAKE 45° SCEA

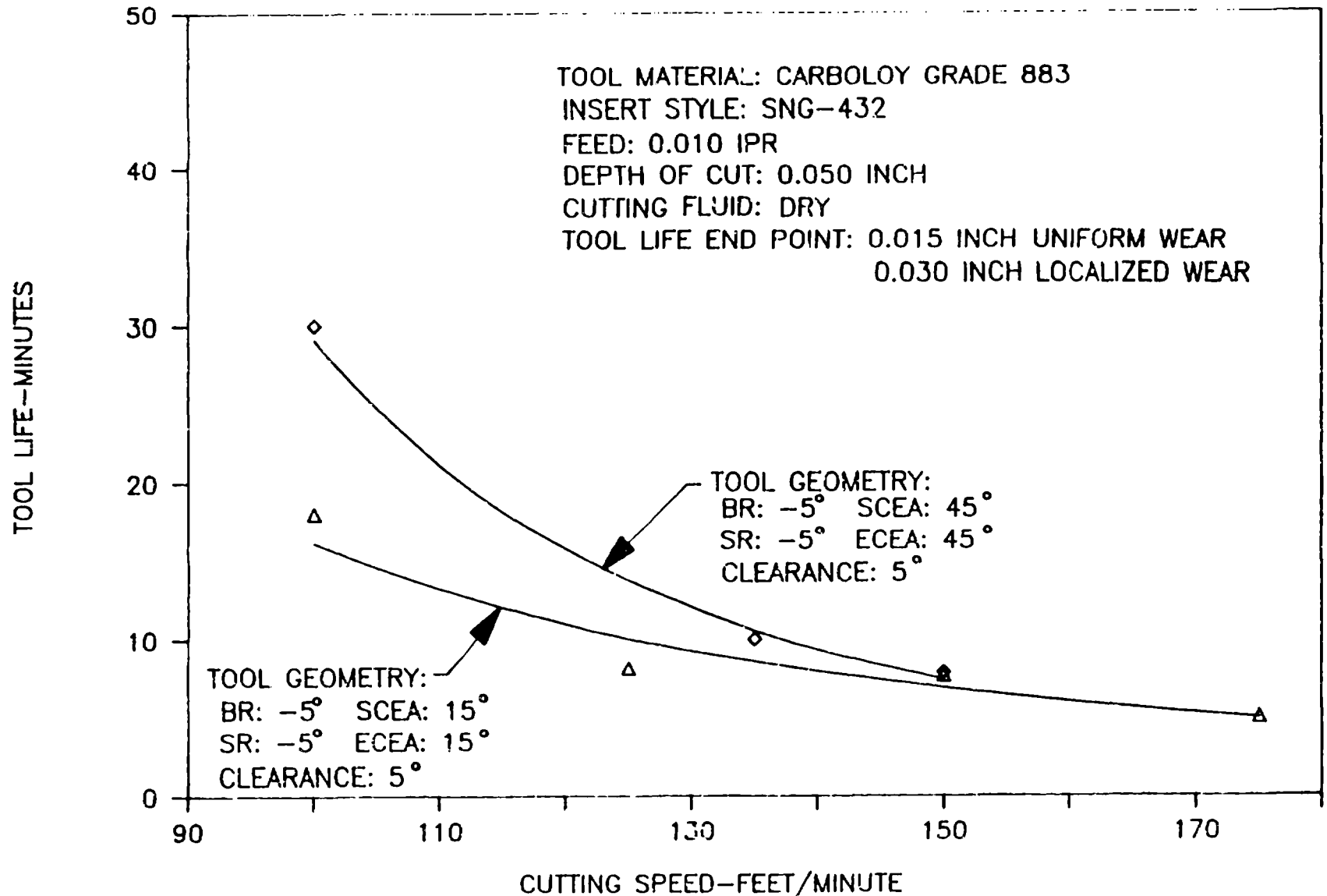

FIGURE 8

TURNING TITANIUM BETA C, 415 BHN
TOOL GEOMETRY EVALUATION
NEGATIVE BACK RAKE VERSUS POSITIVE BACK RAKE

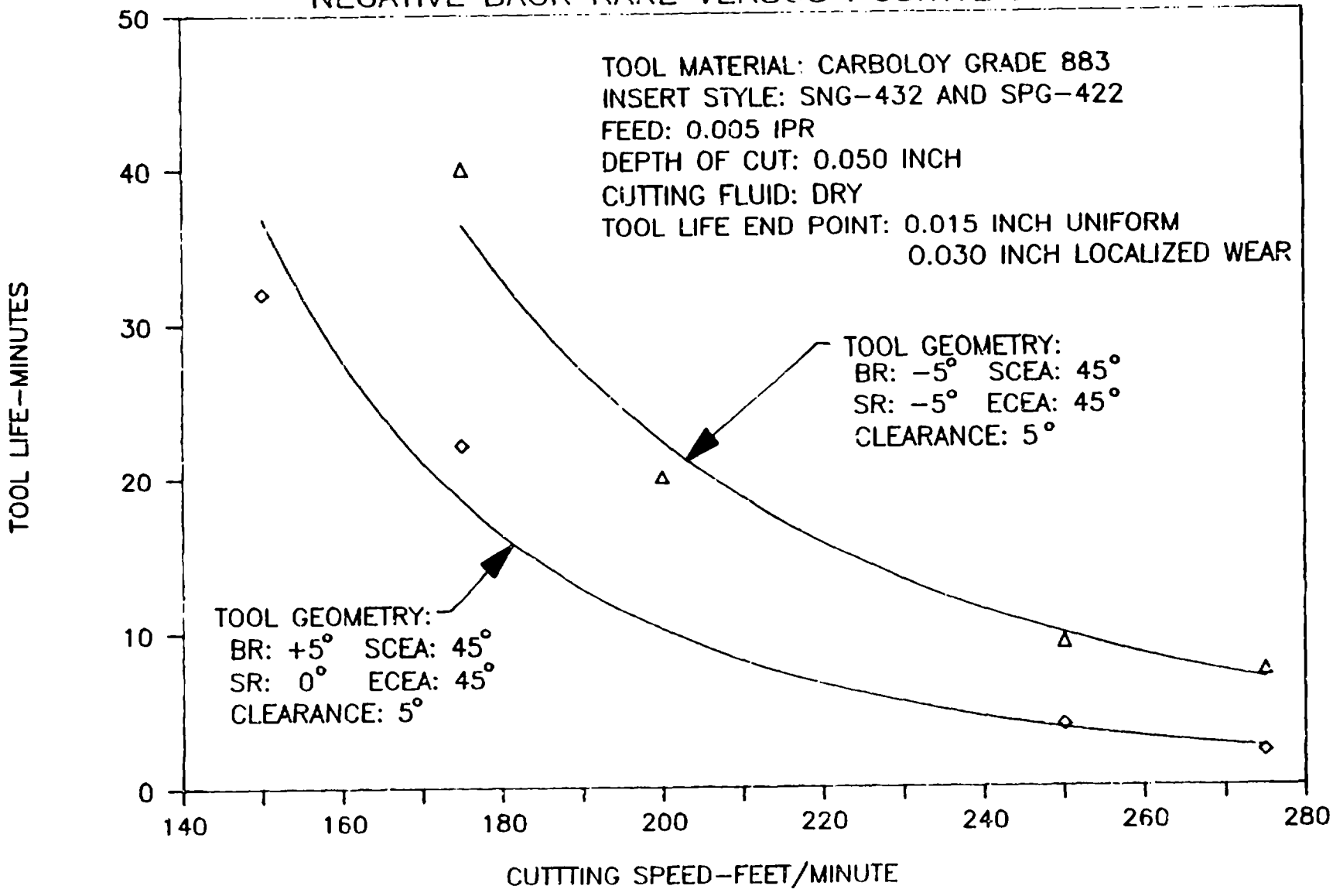

FIGURE 9

TURNING TITANIUM BETA C, 415 BHN
FEED RATE EVALUATION
45° SIDE CUTTING EDGE ANGLE

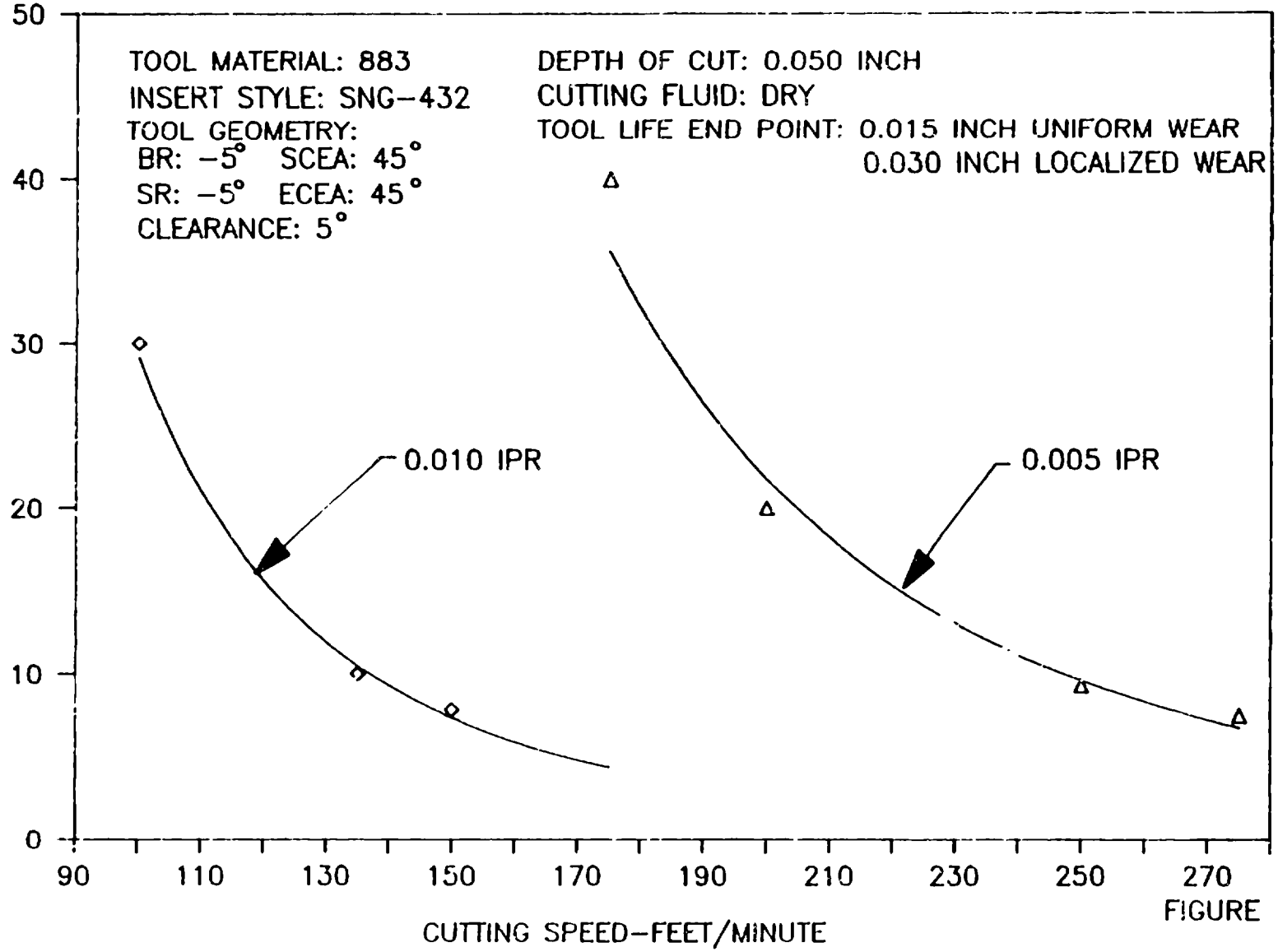

FIGURE 10

TURNING TITANIUM BETA C, 415 BHN
FEED RATE EVALUATION
15° SIDE CUTTING EDGE ANGLE

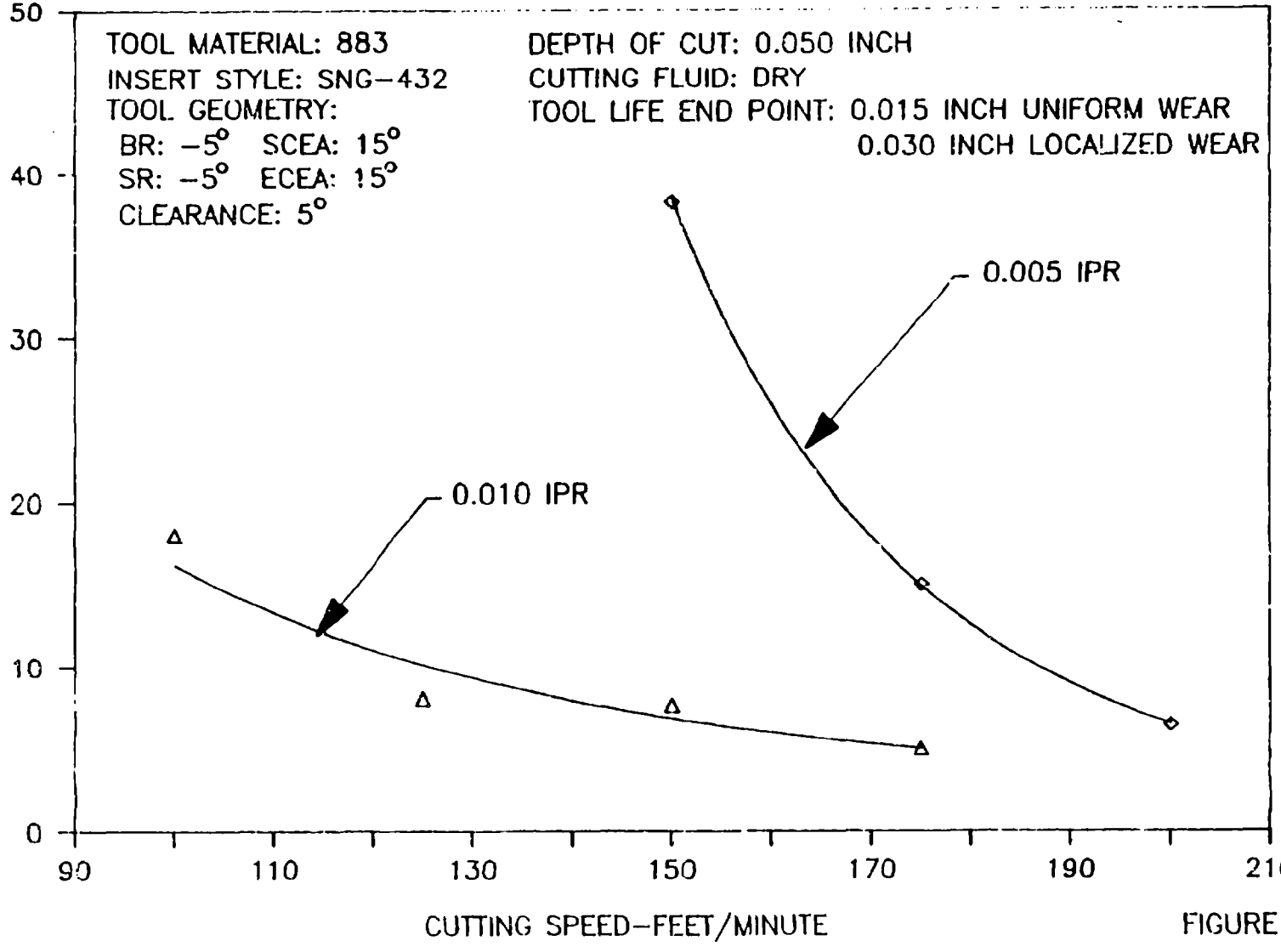

FIGURE 11

TURNING TITANIUM BETA C, 415 BHN
CUTTING FLUID EVALUATION

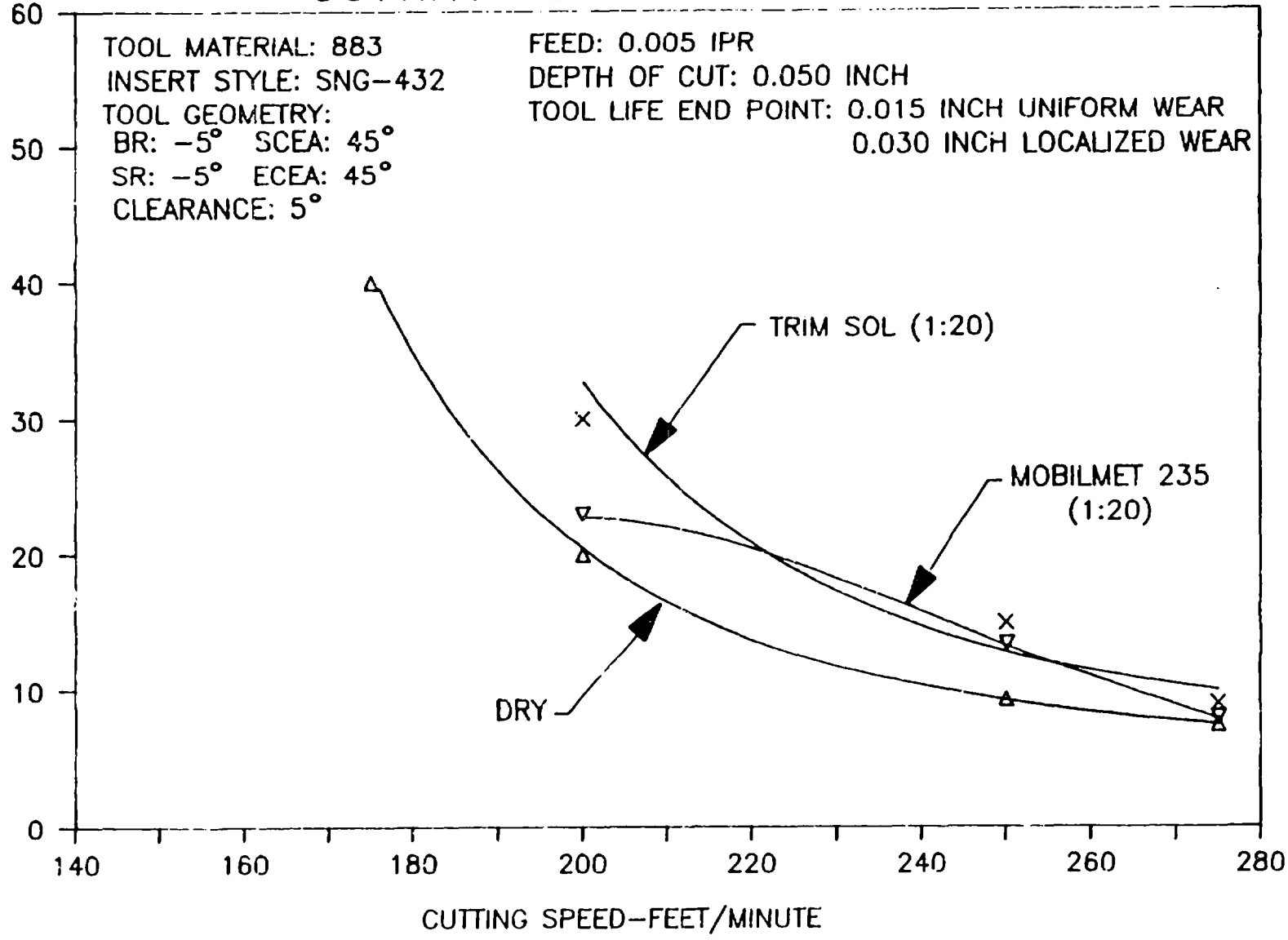

FIGURE 12

TURNING TITANIUM BETA C, 415 BHN
EFFECT OF FEED AT 0.150 INCH DEPTH

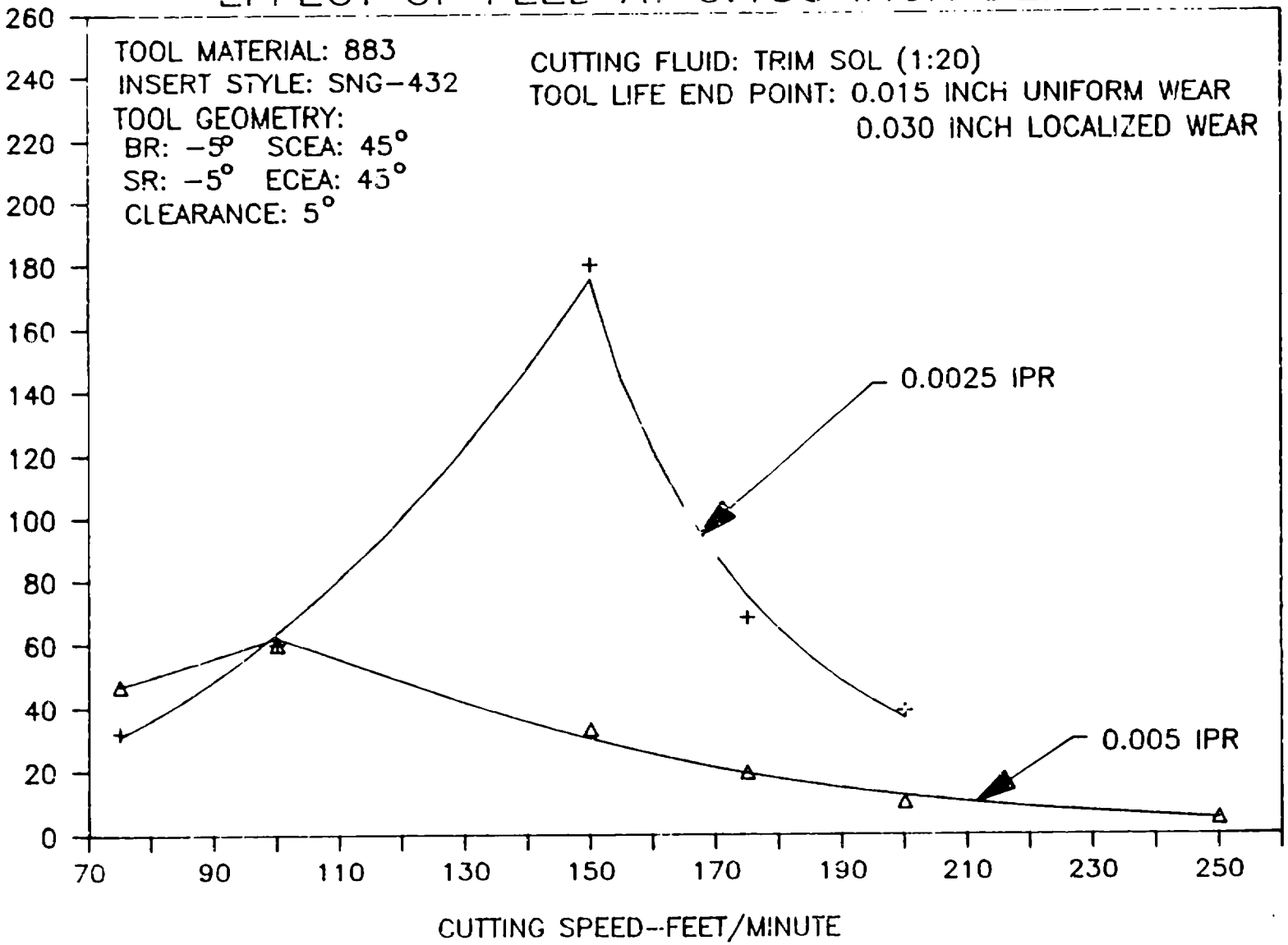

FIGURE 13

TURNING TITANIUM BETA C, 415 BHN
EFFECT OF DEPTH OF CUT

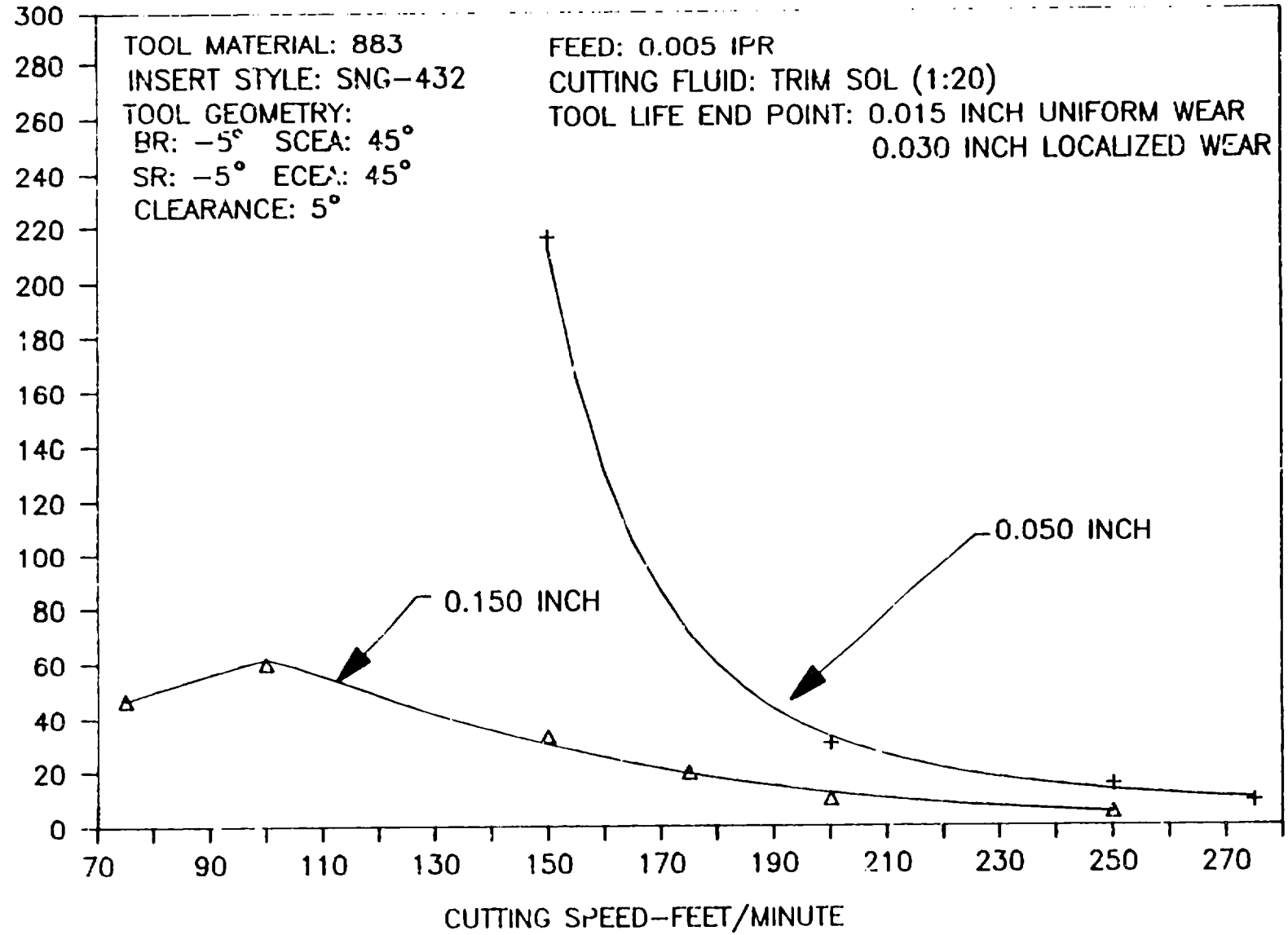

FIGURE 14

TURNING TITANIUM BETA C, 415 BHN
COMPARSION OF CARBOLOY 883 VERSUS NEWCOMER N22

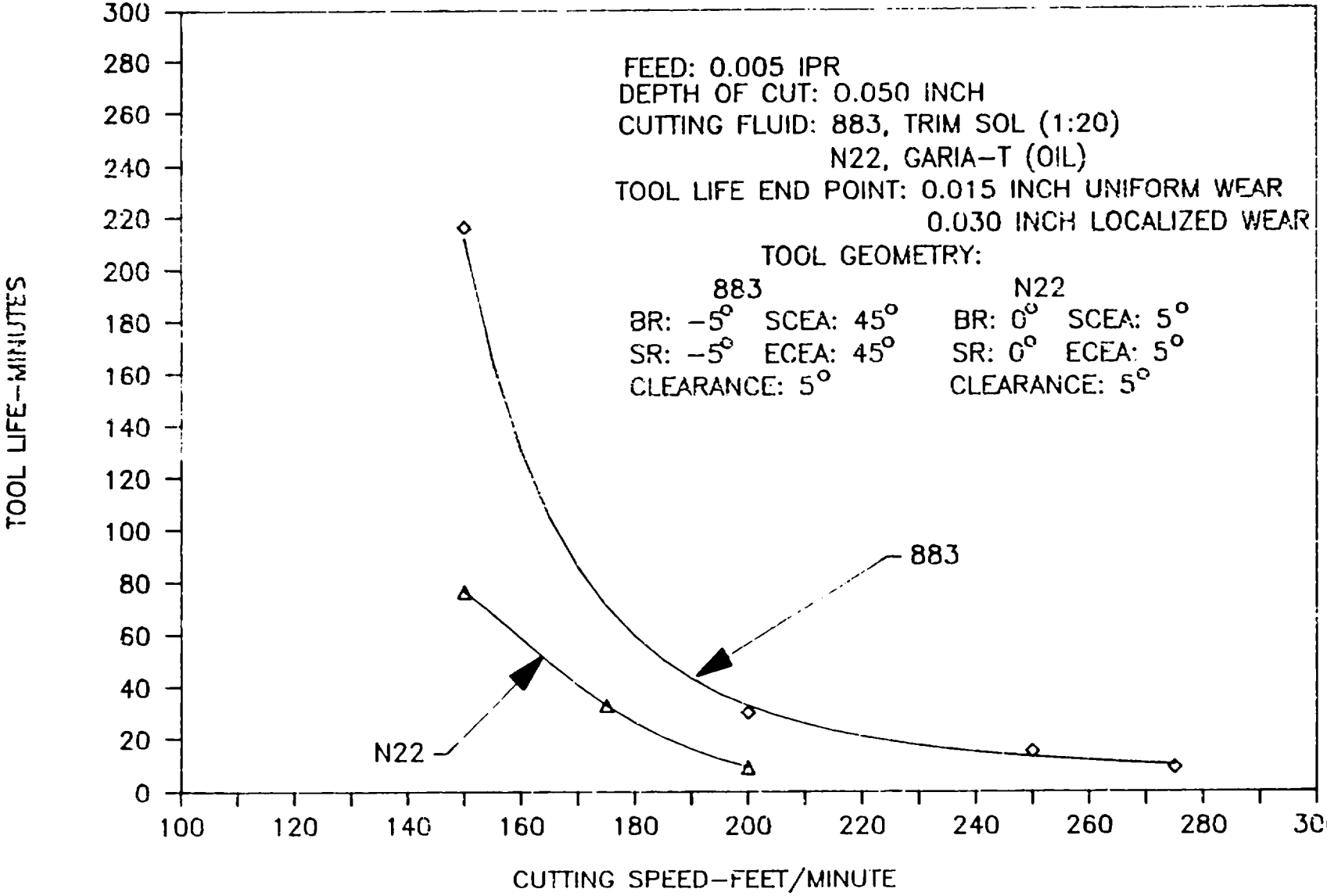

FIGURE 15

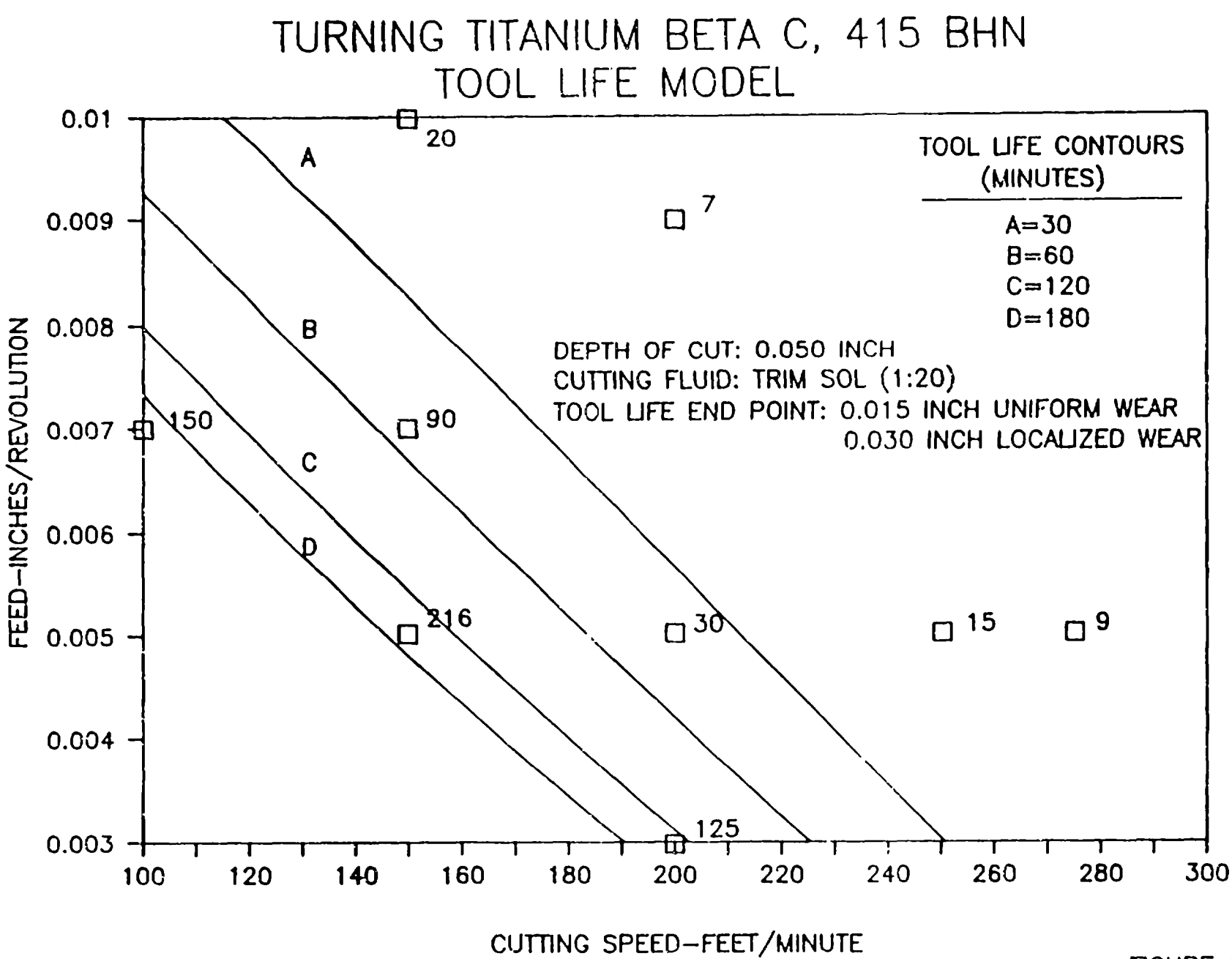
TURNING TITANIUM BETA C, 415 BHN
TOOL LIFE MODEL
TOOL LIFE CONTOURS
(MINUTES)
A=30
B=60
C=120
D=180
DEPTH OF CUT: 0.050 INCH
CUTTING FLUID: TRIM SOL (1:20)
TOOL LIFE END POINT: 0.015 INCH UNIFORM WEAR
0.030 INCH LOCALIZED WEAR
FEED-INCHES/REVOLUTION
CUTTING SPEED-FEET/MINUTE
0.01
0.009
0.008
0.007
0.006
0.005
0.004
0.003
100
120
140
160
180
200
220
240
260
280
300
A
B
C
D
20
7
90
150
216
30
15
9
125

FIGURE 16

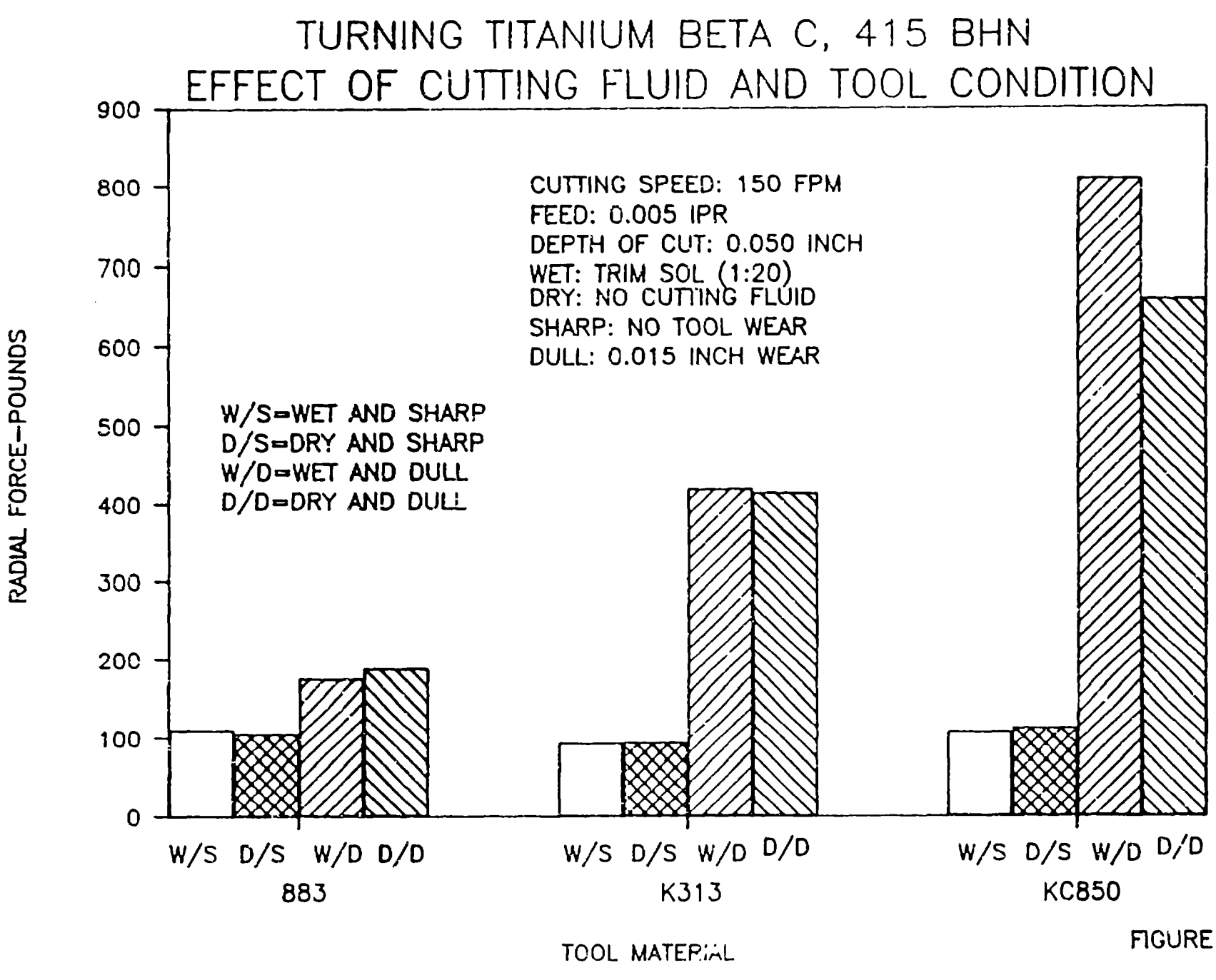
TURNING TITANIUM BETA C, 415 BHN
EFFECT OF CUTTING FLUID AND TOOL CONDITION
RADIAL FORCE-POUNDS
900
800
700
600
500
400
300
200
100
0
CUTTING SPEED: 150 FPM
FEED: 0.005 IPR
DEPTH OF CUT: 0.050 INCH
WET: TRIM SOL (1:20)
DRY: NO CUTTING FLUID
SHARP: NO TOOL WEAR
DULL: 0.015 INCH WEAR
W/S=WET AND SHARP
D/S=DRY AND SHARP
W/D=WET AND DULL
D/D=DRY AND DULL
W/S D/S W/D D/D
883
W/S D/S W/D D/D
K313
W/S D/S W/D D/D
KC850
TOOL MATERIAL

FIGURE 17

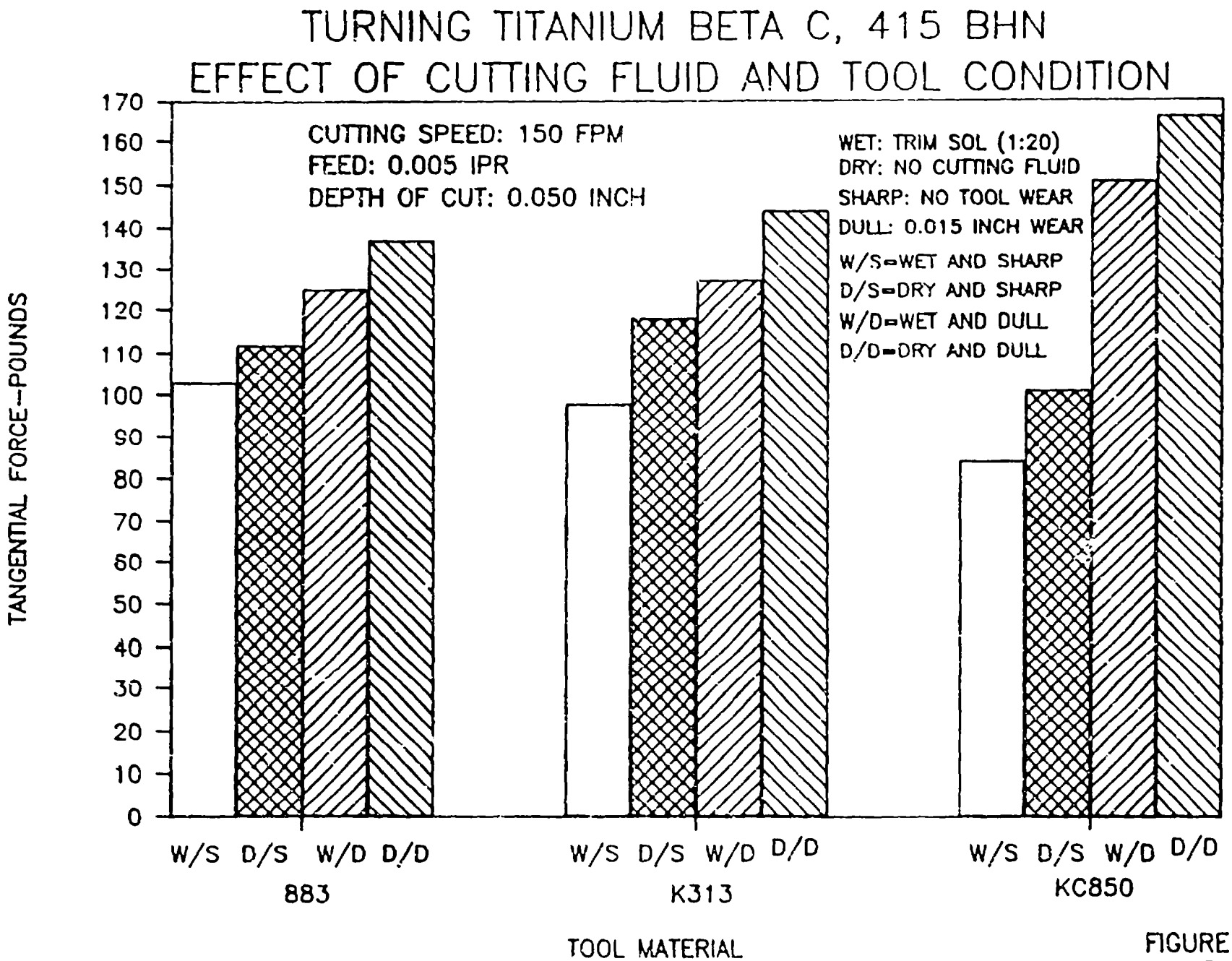
TURNING TITANIUM BETA C, 415 BHN
EFFECT OF CUTTING FLUID AND TOOL CONDITION
CUTTING SPEED: 150 FPM
FEED: 0.005 IPR
DEPTH OF CUT: 0.050 INCH
WET: TRIM SOL (1:20)
DRY: NO CUTTING FLUID
SHARP: NO TOOL WEAR
DULL: 0.015 INCH WEAR
W/S=WET AND SHARP
D/S=DRY AND SHARP
W/D=WET AND DULL
D/D=DRY AND DULL
TANGENTIAL FORCE-POUNDS
170
160
150
140
130
120
110
100
90
80
70
60
50
40
30
20
10
0
W/S D/S W/D D/D
883
W/S D/S W/D D/D
K313
W/S D/S W/D D/D
KC850
TOOL MATERIAL

FIGURE 18

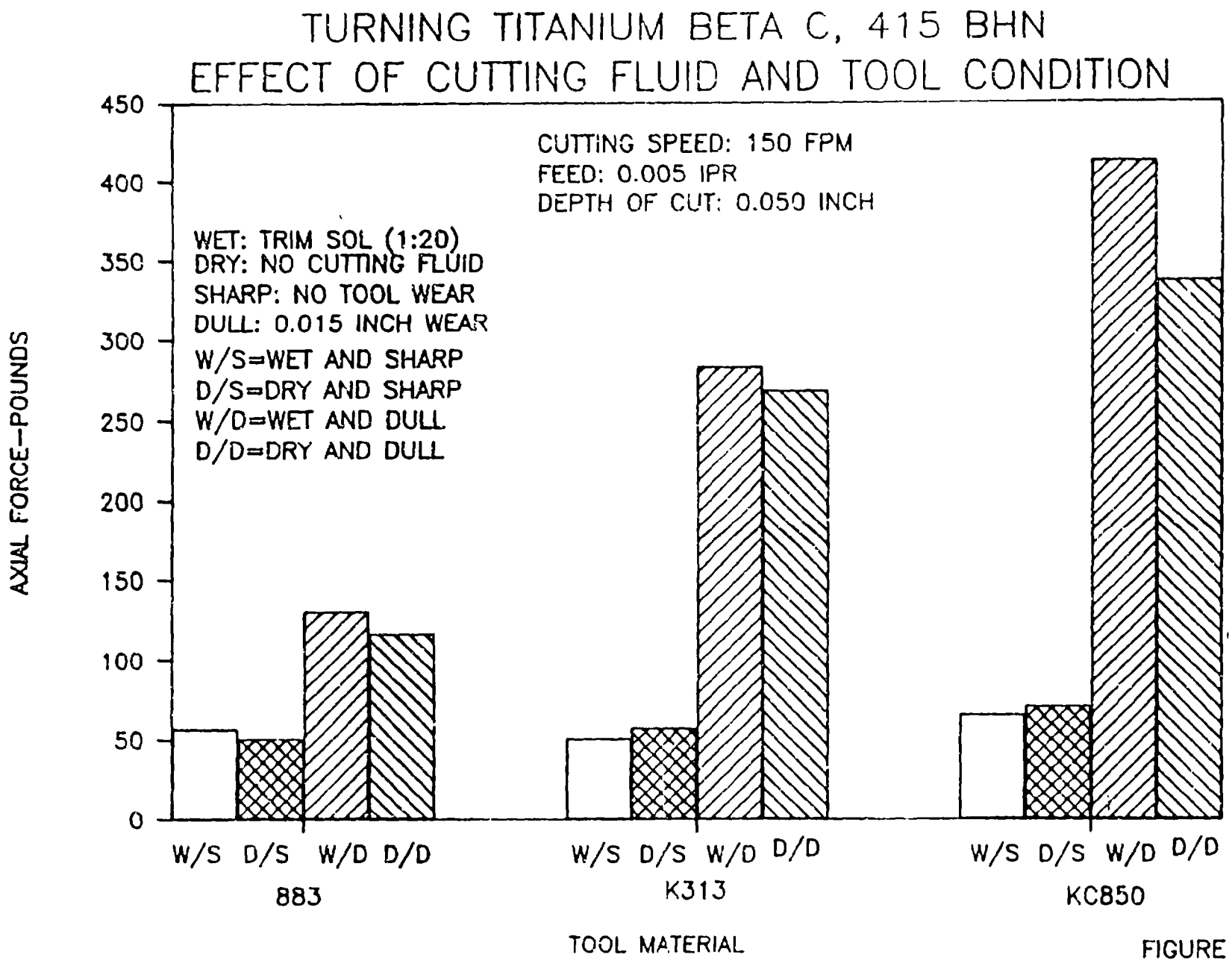
TURNING TITANIUM BETA C, 415 BHN
EFFECT OF CUTTING FLUID AND TOOL CONDITION
CUTTING SPEED: 150 FPM
FEED: 0.005 IPR
DEPTH OF CUT: 0.050 INCH
WET: TRIM SOL (1:20)
DRY: NO CUTTING FLUID
SHARP: NO TOOL WEAR
DULL: 0.015 INCH WEAR
W/S=WET AND SHARP
D/S=DRY AND SHARP
W/D=WET AND DULL
D/D=DRY AND DULL
AXIAL FORCE—POUNDS
450
400
350
300
250
200
150
100
50
0
W/S D/S W/D D/D
883
W/S D/S W/D D/D
K313
W/S D/S W/D D/D
KC850
TOOL MATERIAL

FIGURE 19

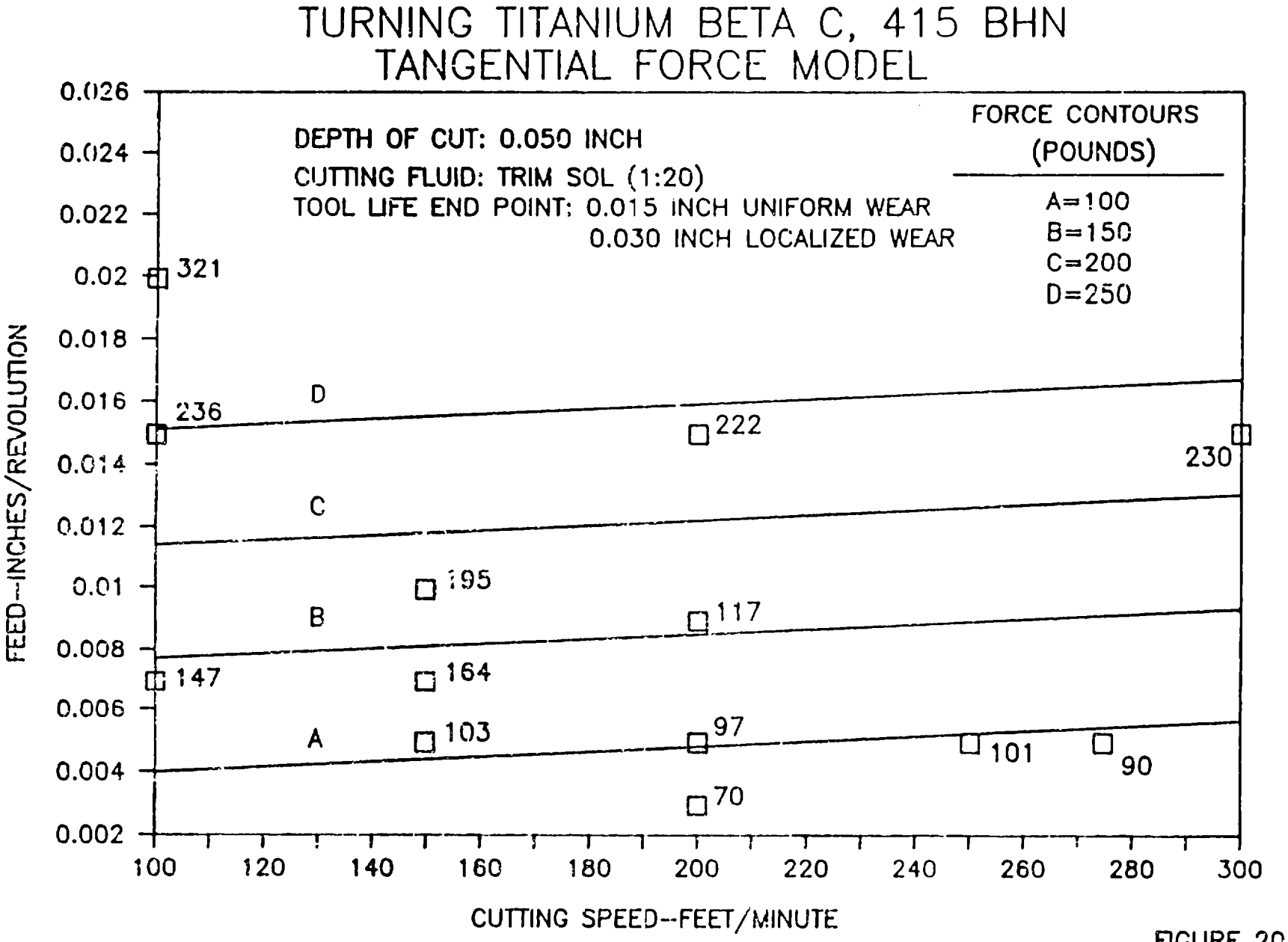
TURNING TITANIUM BETA C, 415 BHN
TANGENTIAL FORCE MODEL
DEPTH OF CUT: 0.050 INCH
CUTTING FLUID: TRIM SOL (1:20)
TOOL LIFE END POINT: 0.015 INCH UNIFORM WEAR
0.030 INCH LOCALIZED WEAR
FORCE CONTOURS
(POUNDS)
A=100
B=150
C=200
D=250
FEED--INCHES/REVOLUTION
0.026
0.024
0.022
0.02
0.018
0.016
0.014
0.012
0.01
0.008
0.006
0.004
0.002
100
120
140
160
180
200
220
240
260
280
300
CUTTING SPEED--FEET/MINUTE
321
236
222
230
195
117
147
164
103
97
101
90
70
A
B
C
D

FIGURE 20

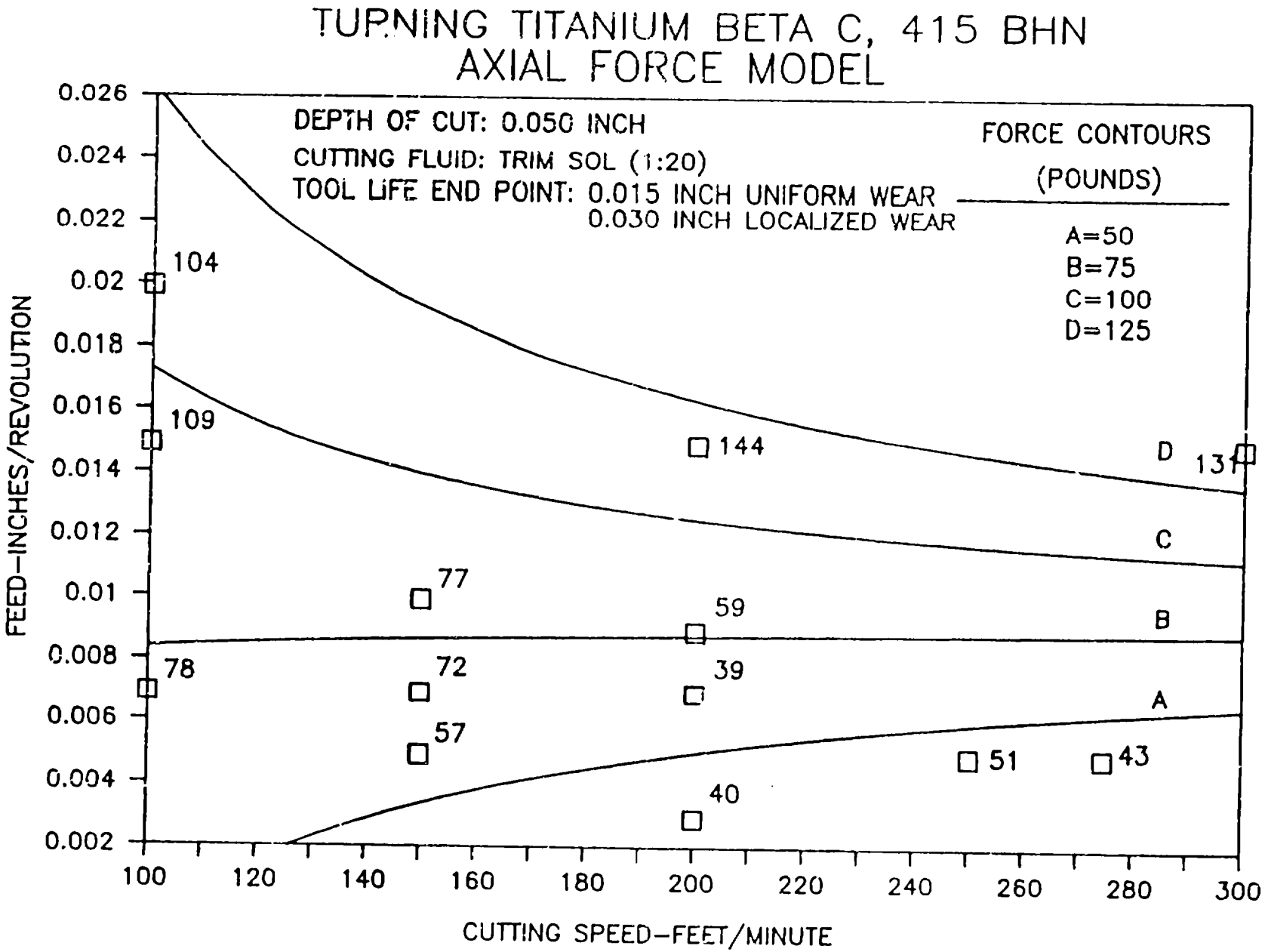
TURNING TITANIUM BETA C, 415 BHN
AXIAL FORCE MODEL
DEPTH OF CUT: 0.050 INCH
CUTTING FLUID: TRIM SOL (1:20)
TOOL LIFE END POINT: 0.015 INCH UNIFORM WEAR
0.030 INCH LOCALIZED WEAR
FORCE CONTOURS
(POUNDS)
A=50
B=75
C=100
D=125
FEED-INCHES/REVOLUTION
CUTTING SPEED-FEET/MINUTE
0.026
0.024
0.022
0.02
0.018
0.016
0.014
0.012
0.01
0.008
0.006
0.004
0.002
100
120
140
160
180
200
220
240
260
280
300
104
109
144
131
77
59
78
72
39
57
51
43
40
D
C
B
A

FIGURE 21

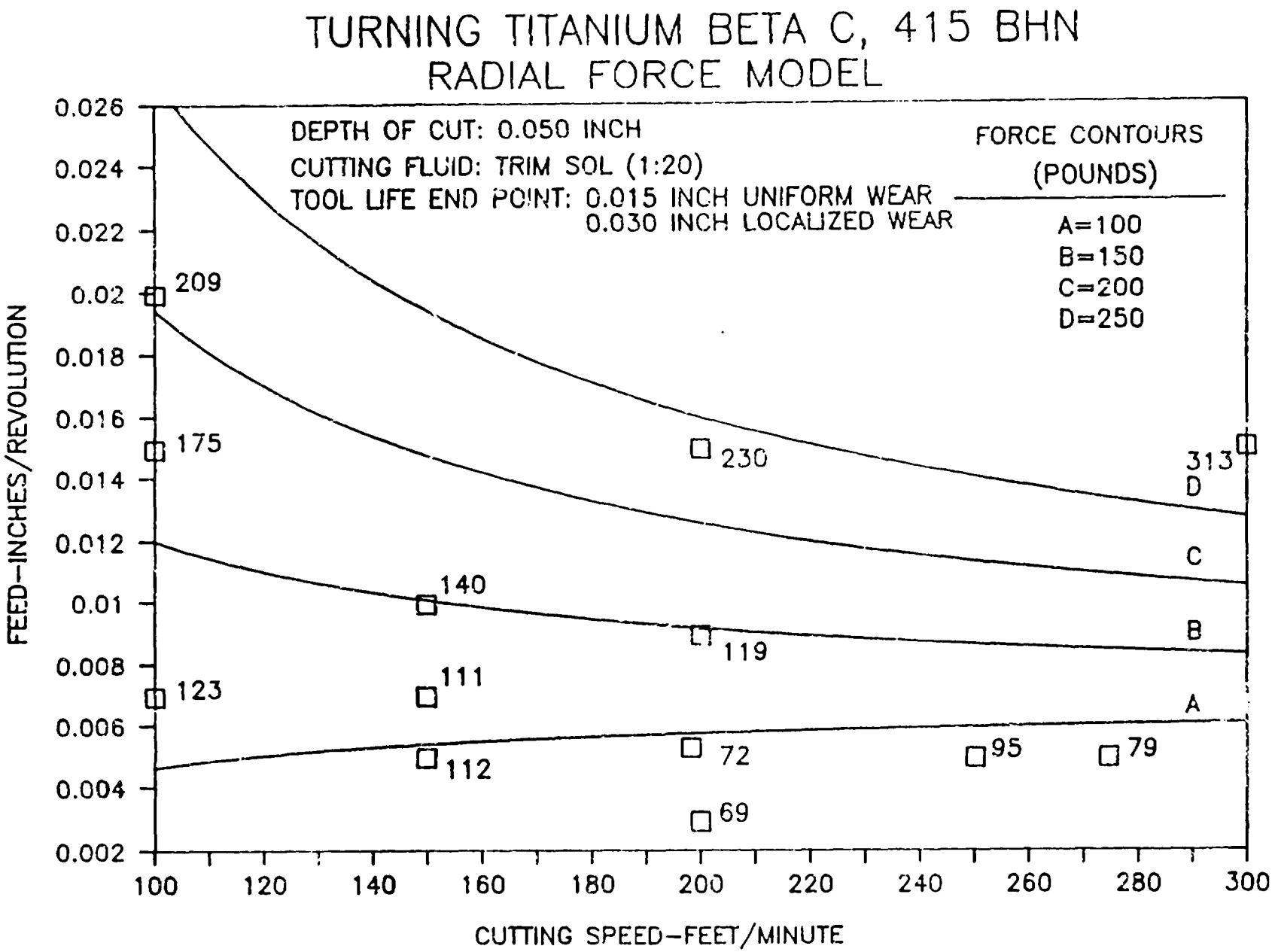
TURNING TITANIUM BETA C, 415 BHN
RADIAL FORCE MODEL
DEPTH OF CUT: 0.050 INCH
CUTTING FLUID: TRIM SOL (1:20)
TOOL LIFE END POINT: 0.015 INCH UNIFORM WEAR
0.030 INCH LOCALIZED WEAR
FORCE CONTOURS
(POUNDS)
A=100
B=150
C=200
D=250
FEED-INCHES/REVOLUTION
CUTTING SPEED-FEET/MINUTE
0.026
0.024
0.022
0.02
0.018
0.016
0.014
0.012
0.01
0.008
0.006
0.004
0.002
100
120
140
160
180
200
220
240
260
280
300
209
175
230
313
D
C
140
119
B
123
111
A
112
72
95
79
69

FIGURE 22

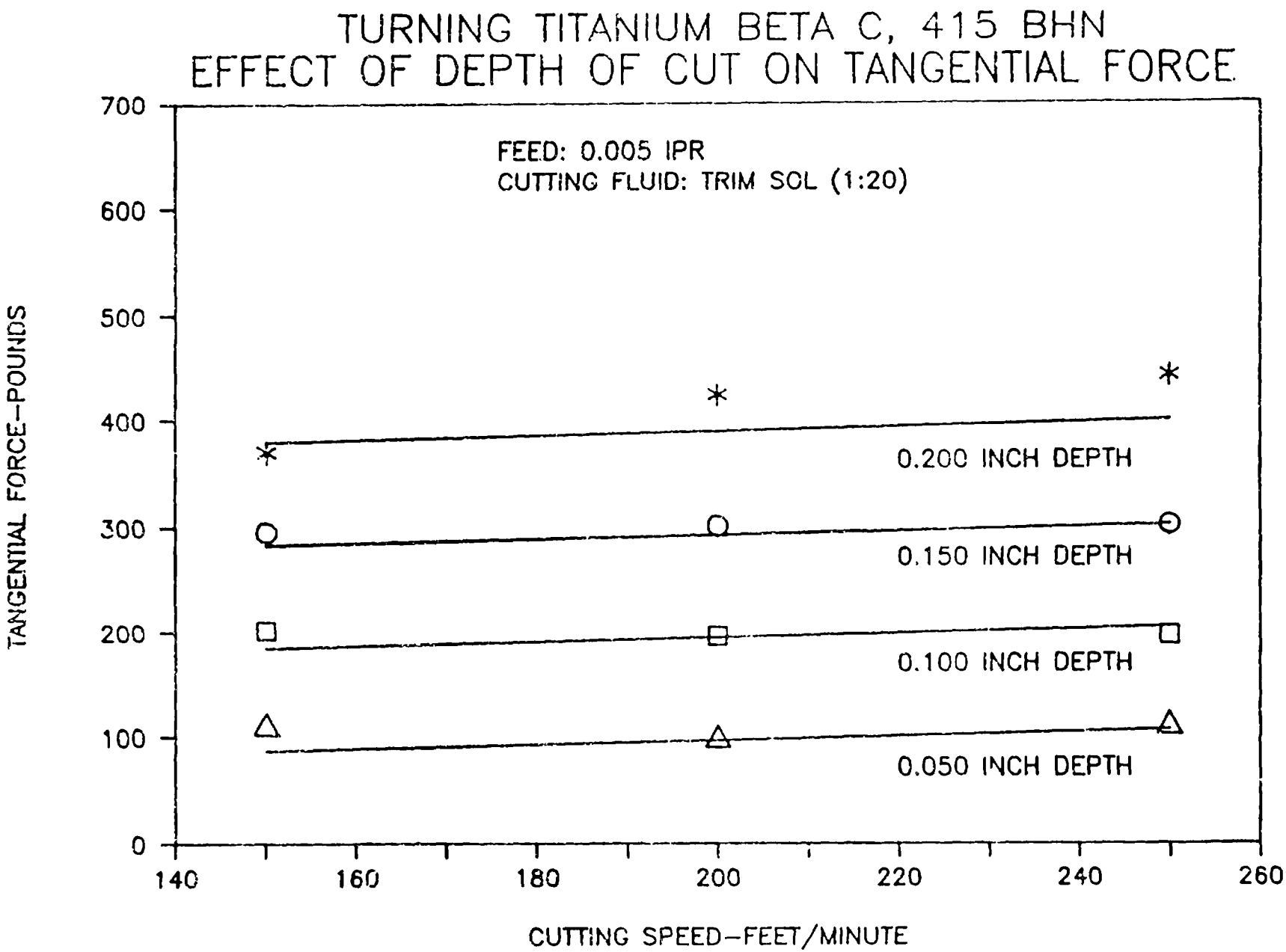
TURNING TITANIUM BETA C, 415 BHN
EFFECT OF DEPTH OF CUT ON TANGENTIAL FORCE
FEED: 0.005 IPR
CUTTING FLUID: TRIM SOL (1:20)
0.200 INCH DEPTH
0.150 INCH DEPTH
0.100 INCH DEPTH
0.050 INCH DEPTH
TANGENTIAL FORCE–POUNDS
CUTTING SPEED–FEET/MINUTE
0
100
200
300
400
500
600
700
140
160
180
200
220
240
260

FIGURE 23

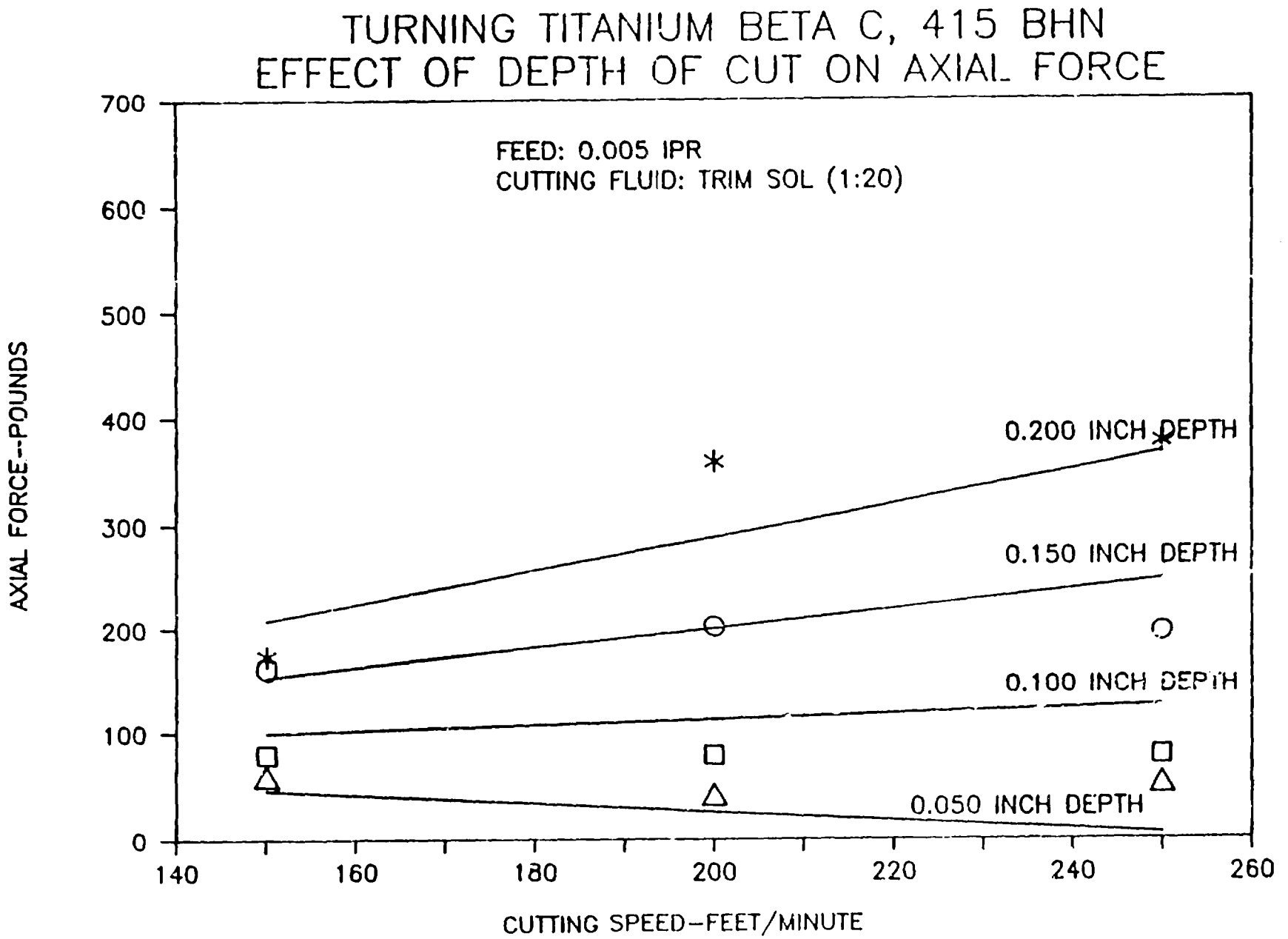
TURNING TITANIUM BETA C, 415 BHN
EFFECT OF DEPTH OF CUT ON AXIAL FORCE
FEED: 0.005 IPR
CUTTING FLUID: TRIM SOL (1:20)
0.200 INCH DEPTH
0.150 INCH DEPTH
0.100 INCH DEPTH
0.050 INCH DEPTH
AXIAL FORCE--POUNDS
CUTTING SPEED-FEET/MINUTE
700
600
500
400
300
200
100
0
140
160
180
200
220
240
260

FIGURE 24

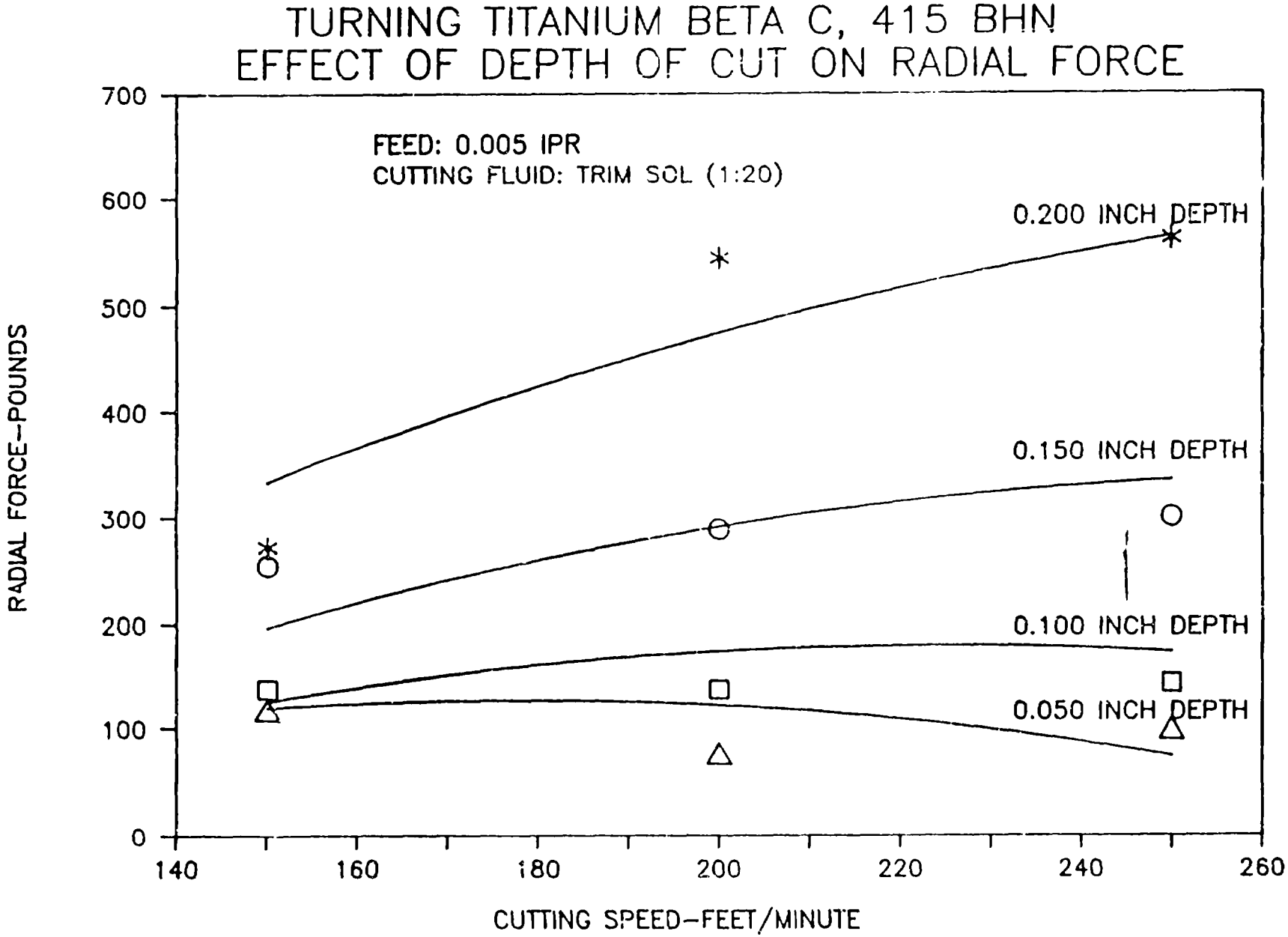
TURNING TITANIUM BETA C, 415 BHN
EFFECT OF DEPTH OF CUT ON RADIAL FORCE
FEED: 0.005 IPR
CUTTING FLUID: TRIM SOL (1:20)
0.200 INCH DEPTH
0.150 INCH DEPTH
0.100 INCH DEPTH
0.050 INCH DEPTH
RADIAL FORCE-POUNDS
CUTTING SPEED-FEET/MINUTE
0
100
200
300
400
500
600
700
140
160
180
200
220
240
260

FIGURE 25

TURNING TITANIUM BETA C, 415 BHN
EFFECT OF FEED AND DEPTH OF CUT ON AXIAL FORCE

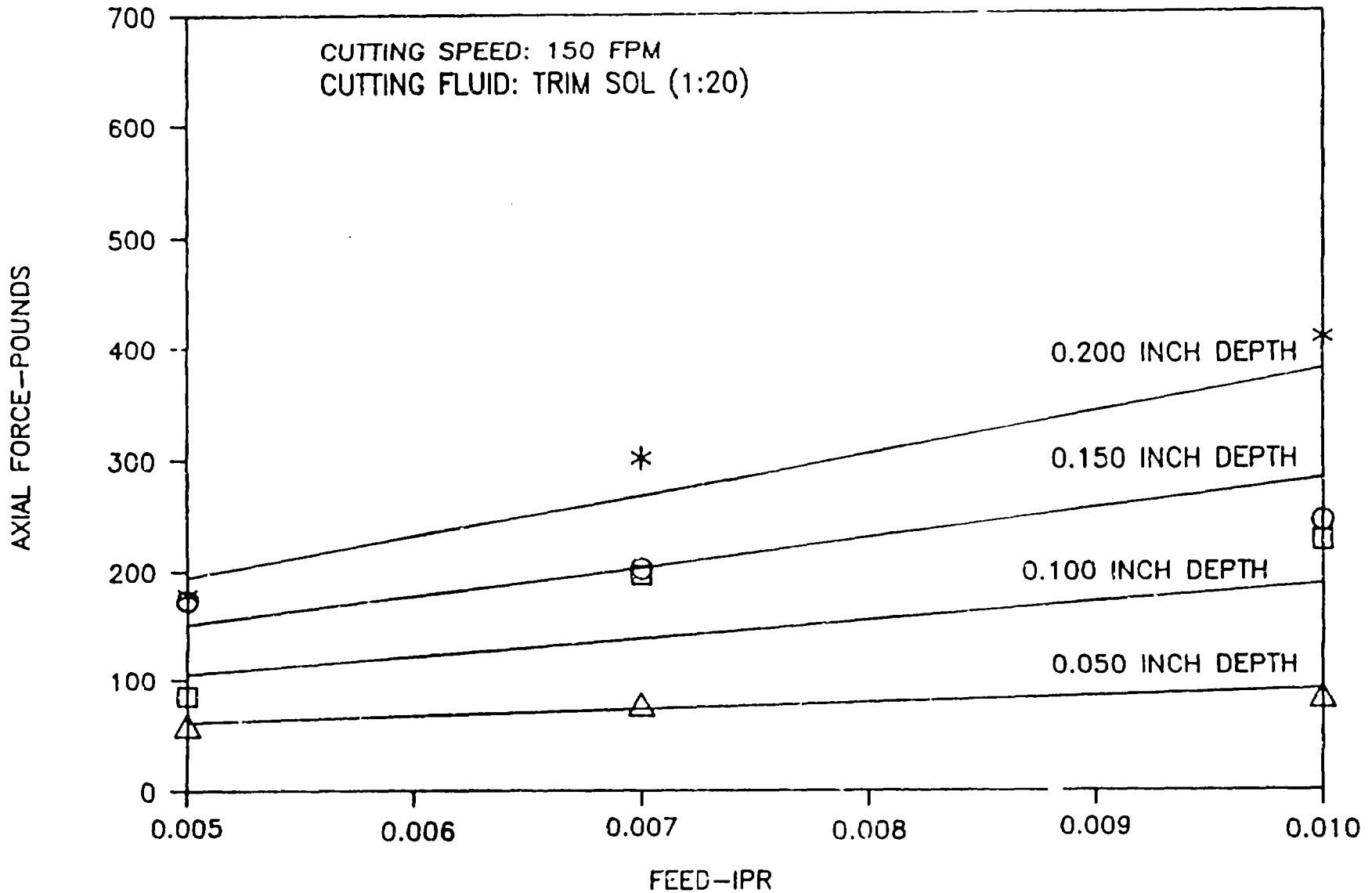

FIGURE 26

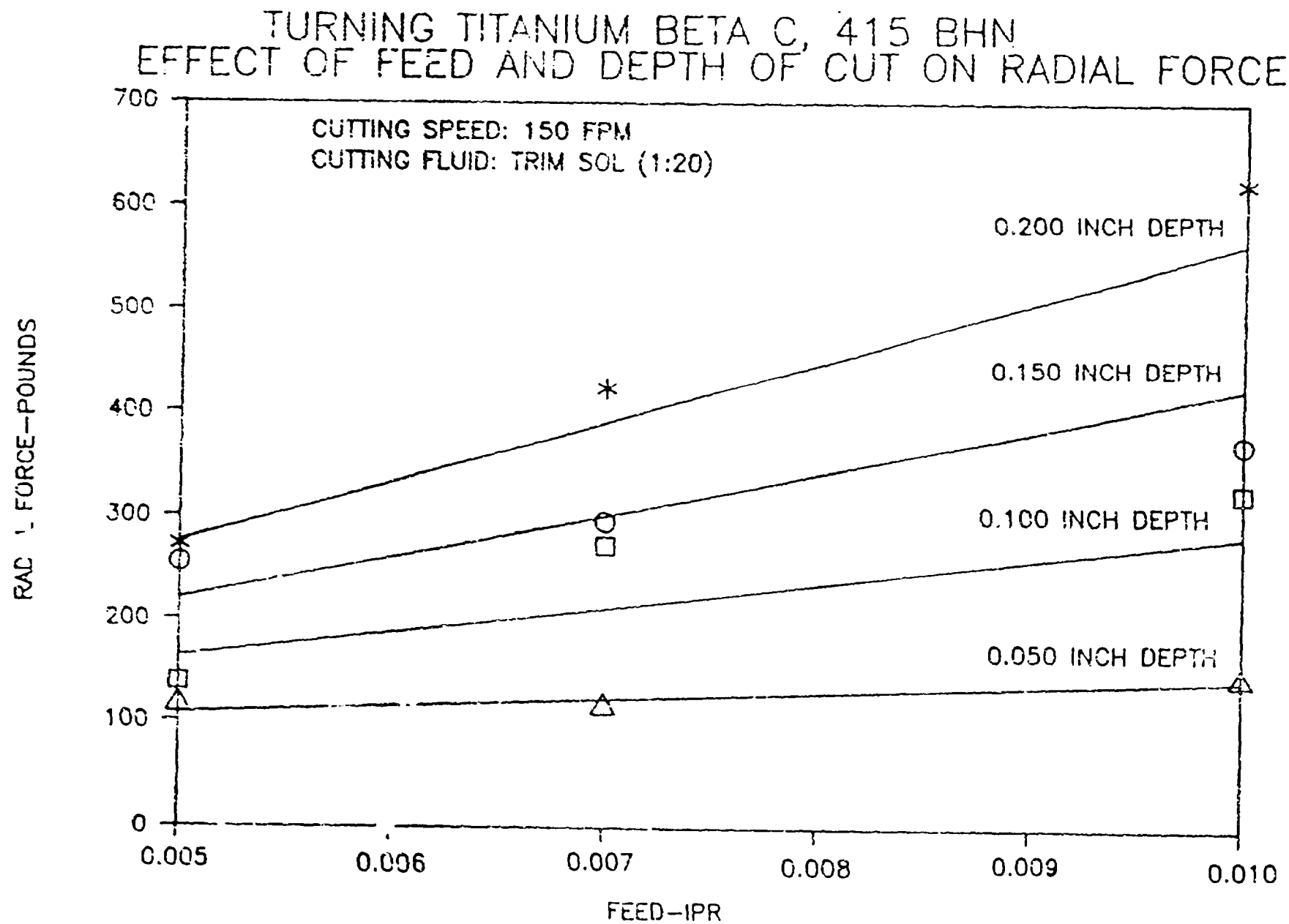
TURNING TITANIUM BETA C, 415 BHN
EFFECT OF FEED AND DEPTH OF CUT ON RADIAL FORCE
CUTTING SPEED: 150 FPM
CUTTING FLUID: TRIM SOL (1:20)
0.200 INCH DEPTH
0.150 INCH DEPTH
0.100 INCH DEPTH
0.050 INCH DEPTH
RAD L FORCE—POUNDS
700
600
500
400
300
200
100
0
0.005
0.006
0.007
0.008
0.009
0.010
FEED—IPR

FIGURE 27

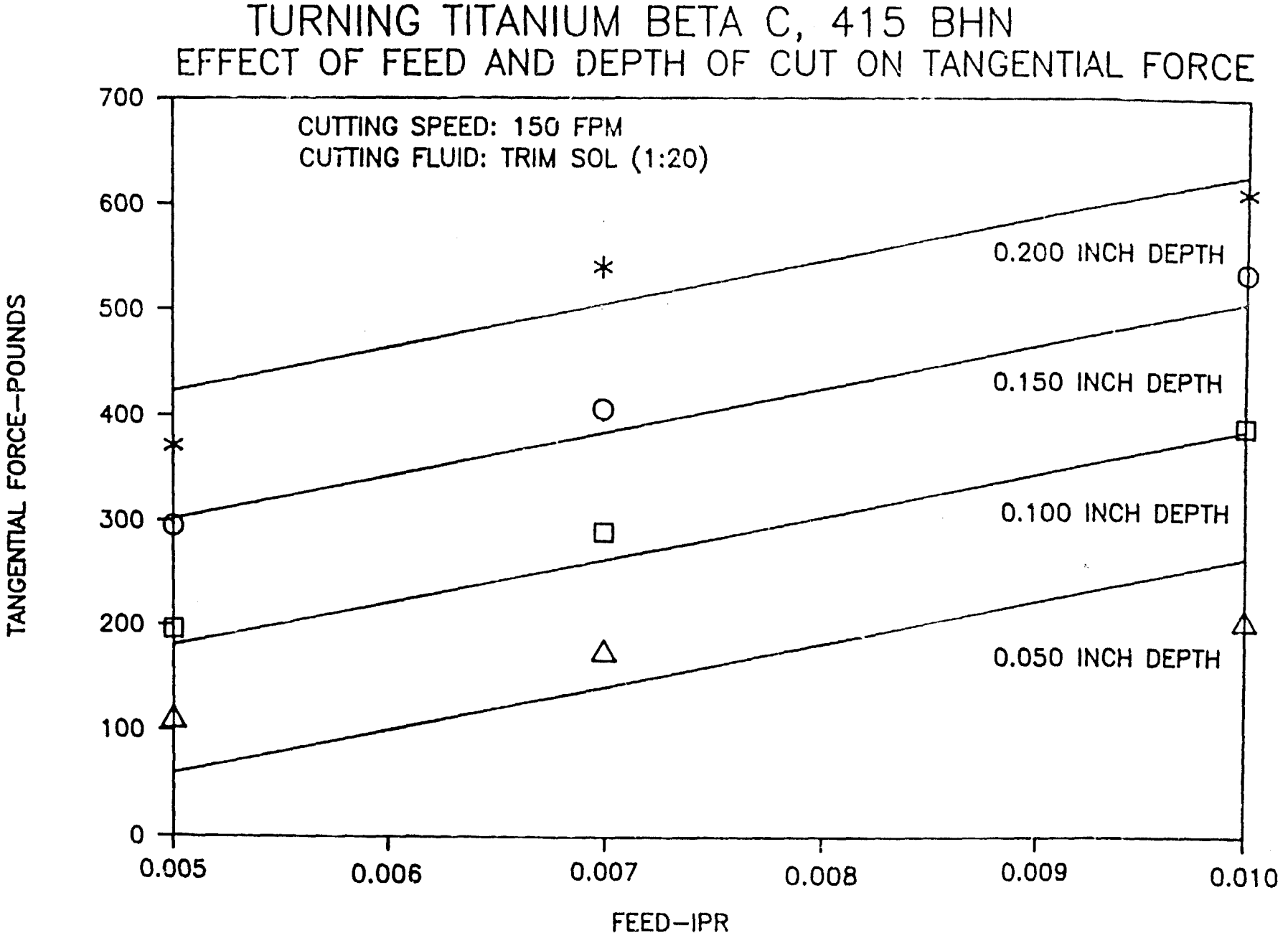
TURNING TITANIUM BETA C, 415 BHN
EFFECT OF FEED AND DEPTH OF CUT ON TANGENTIAL FORCE
CUTTING SPEED: 150 FPM
CUTTING FLUID: TRIM SOL (1:20)
0.200 INCH DEPTH
0.150 INCH DEPTH
0.100 INCH DEPTH
0.050 INCH DEPTH
TANGENTIAL FORCE—POUNDS
700
600
500
400
300
200
100
0
0.005
0.006
0.007
0.008
0.009
0.010
FEED—IPR

FIGURE 28

TURNING TITANIUM BETA C, 415 BHN
EFFECT OF CUTTING SPEED AND DEPTH OF CUT ON AXIAL FORCE

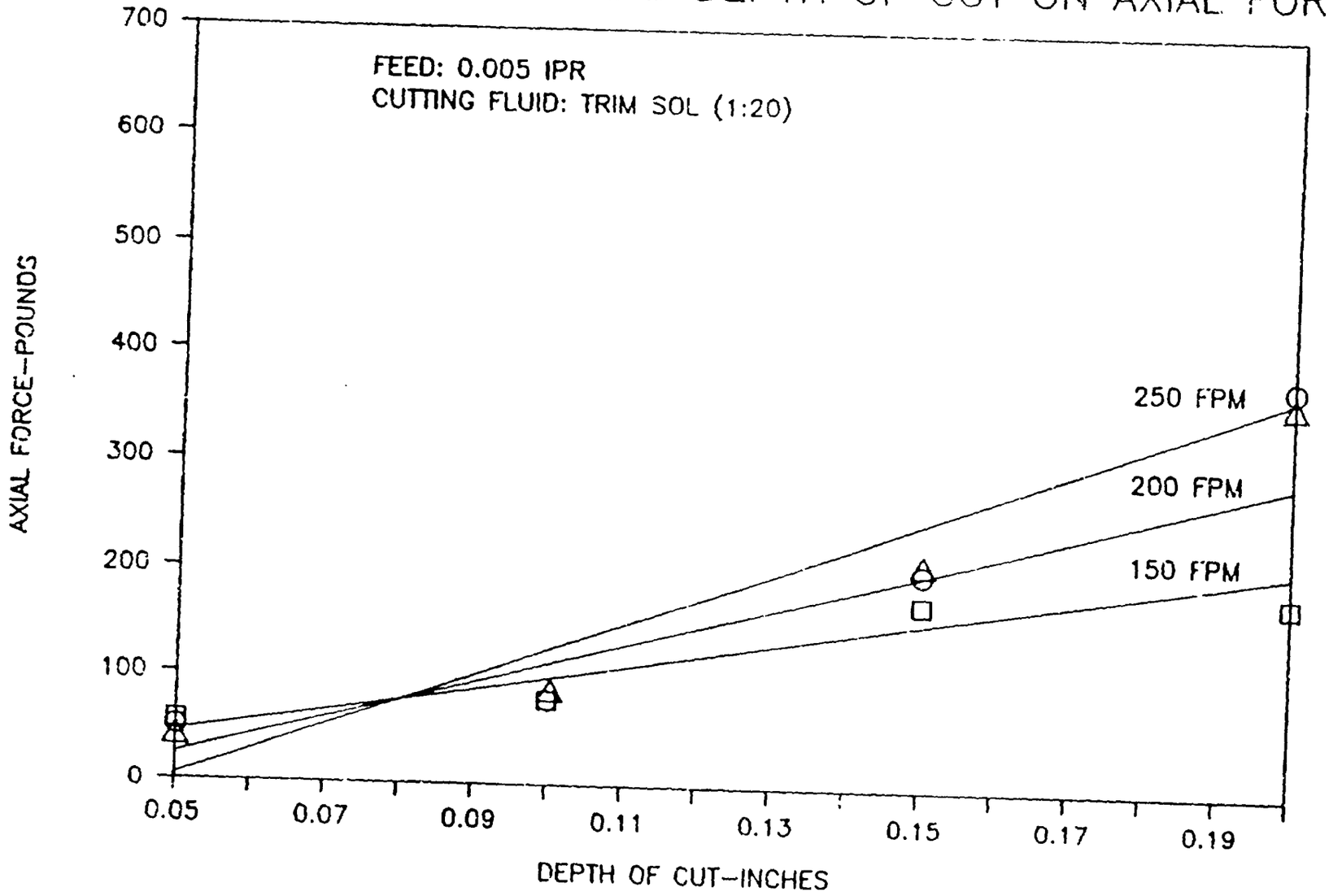

FIGURE 29

TURNING TITANIUM BETA C, 415 BHN
EFFECT OF FEED AND DEPTH OF CUT ON AXIAL FORCE

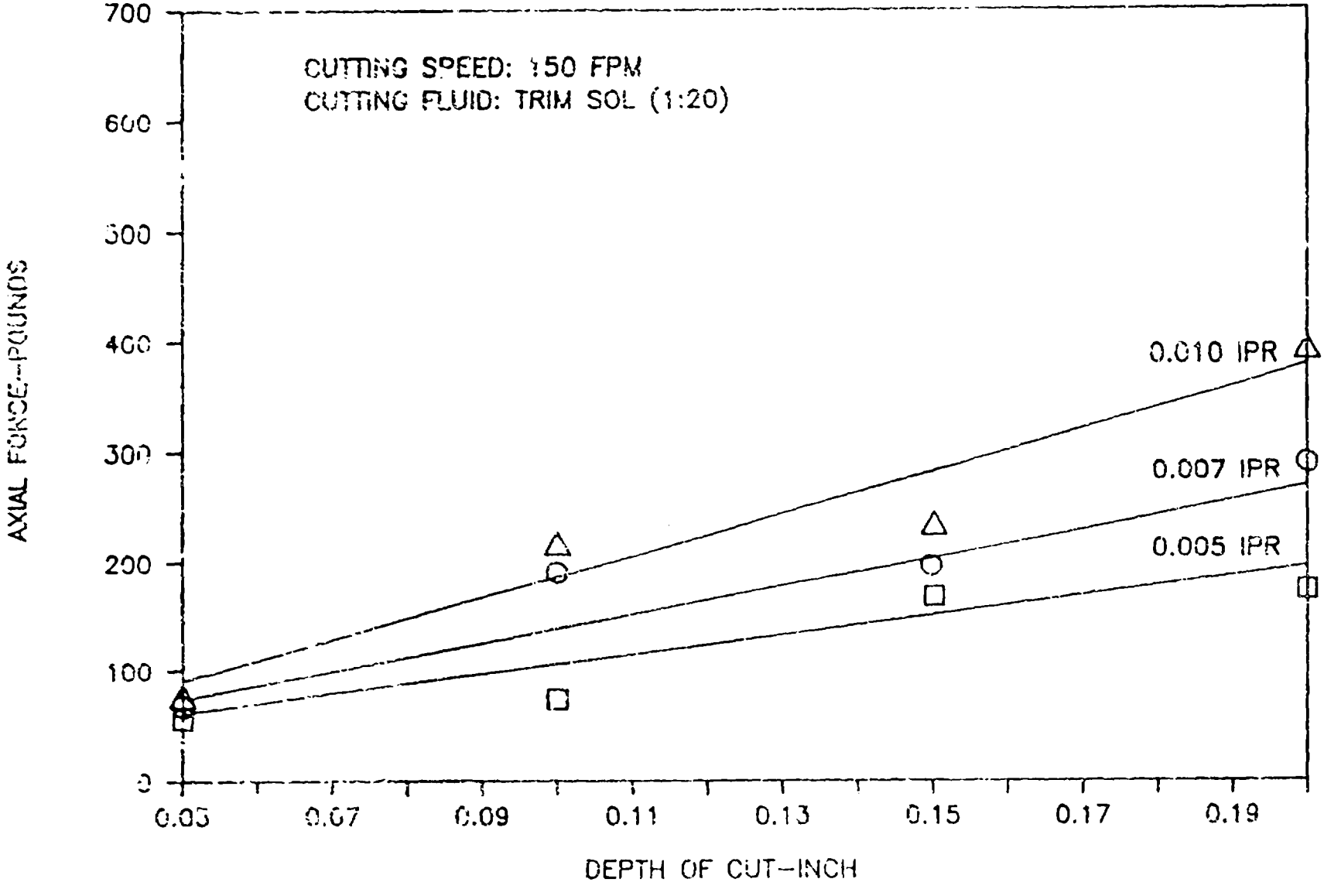

FIGURE 30

TURNING TITANIUM BETA C, 415 BHN
EFFECT OF CUTTING SPEED AND DEPTH OF CUT ON RADIAL FORCE

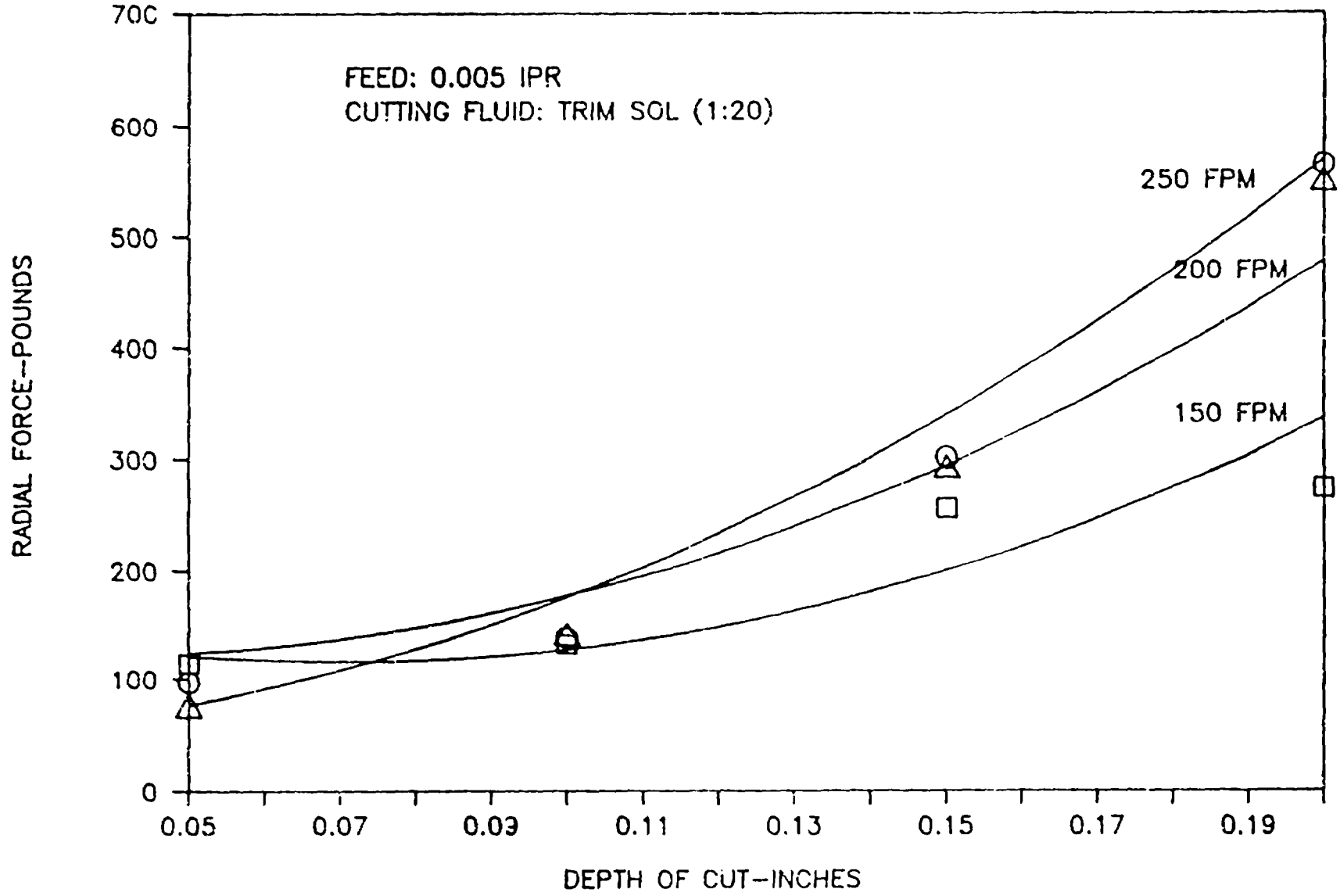

FIGURE 31

TURNING TITANIUM BETA C, 415 BHN
EFFECT OF FEED AND DEPTH OF CUT ON RADIAL FORCE

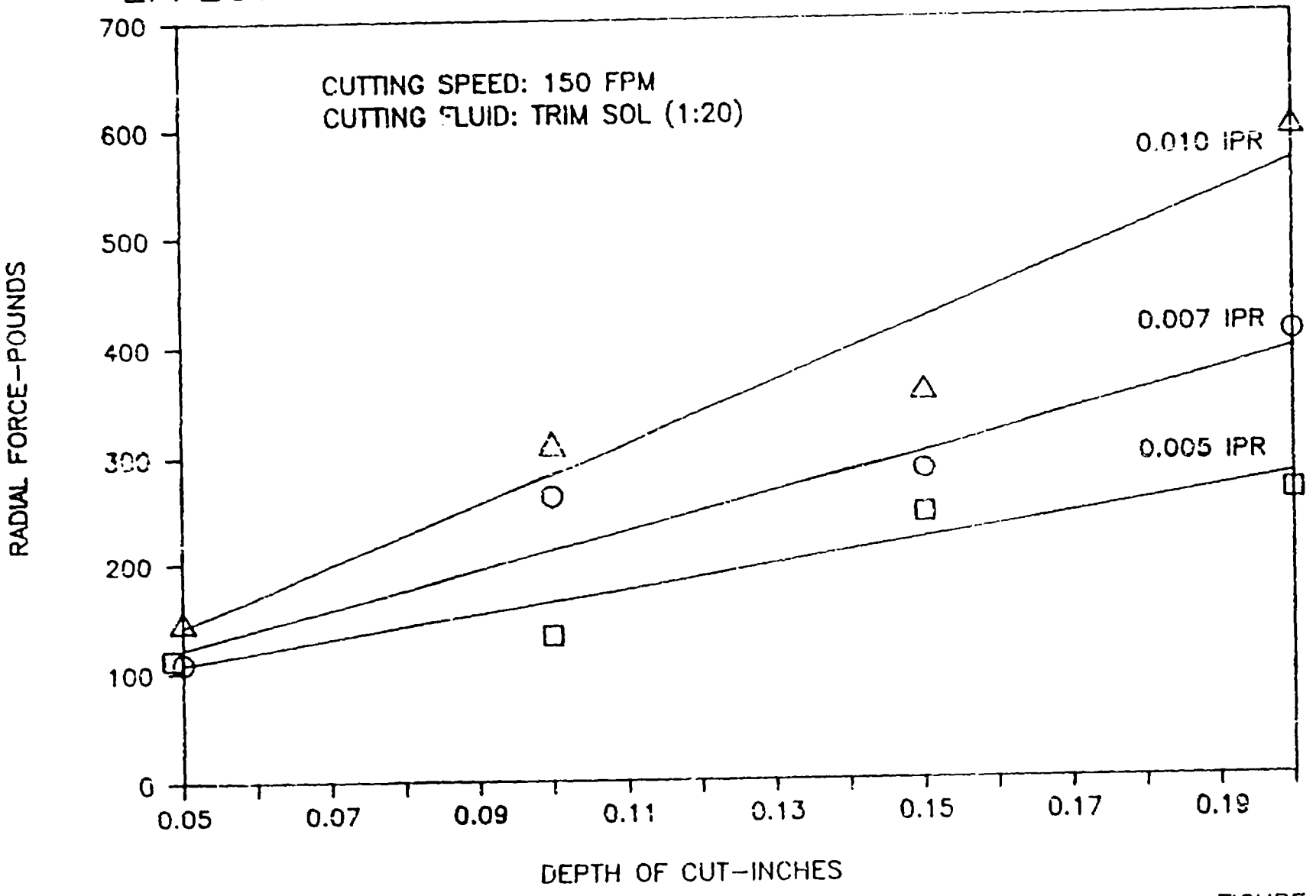

FIGURE 32

TURNING TITANIUM BETA C, 415 BHN

EFFECT OF CUTTING SPEED AND DEPTH OF CUT ON TANGENTIAL FORCE

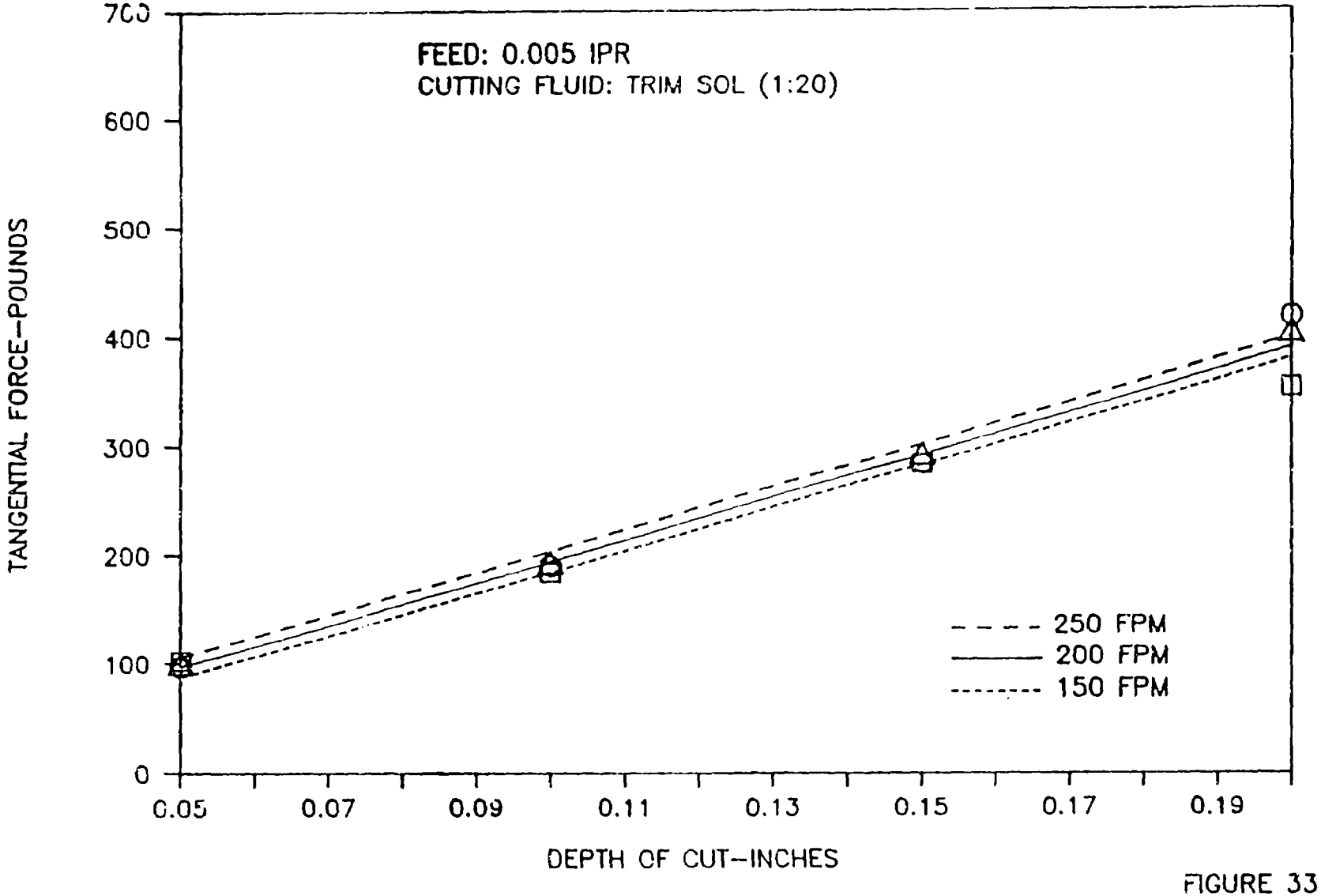

FIGURE 33

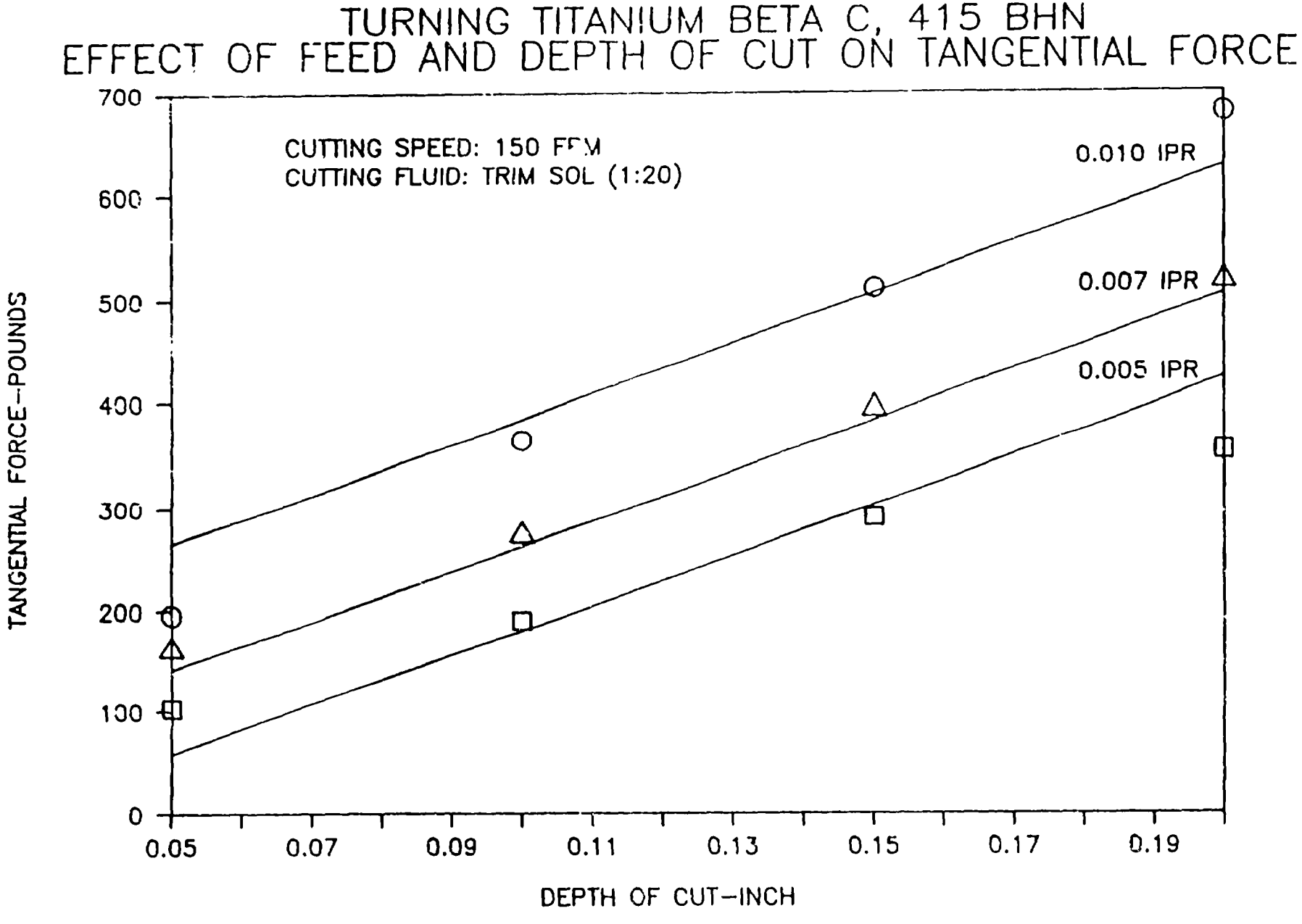
TURNING TITANIUM BETA C, 415 BHN
EFFECT OF FEED AND DEPTH OF CUT ON TANGENTIAL FORCE
CUTTING SPEED: 150 FPM
CUTTING FLUID: TRIM SOL (1:20)
0.010 IPR
0.007 IPR
0.005 IPR
TANGENTIAL FORCE-POUNDS
700
600
500
400
300
200
100
0
0.05
0.07
0.09
0.11
0.13
0.15
0.17
0.19
DEPTH OF CUT-INCH

FIGURE 34

WEAR PHOTOGRAPH SHOWING DEPTH OF CUT NOTCH

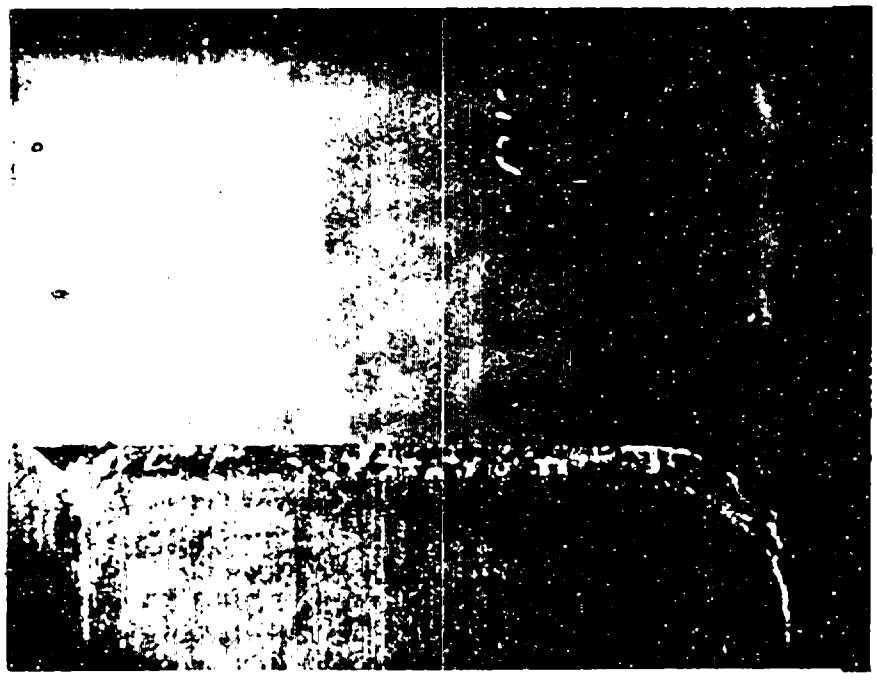

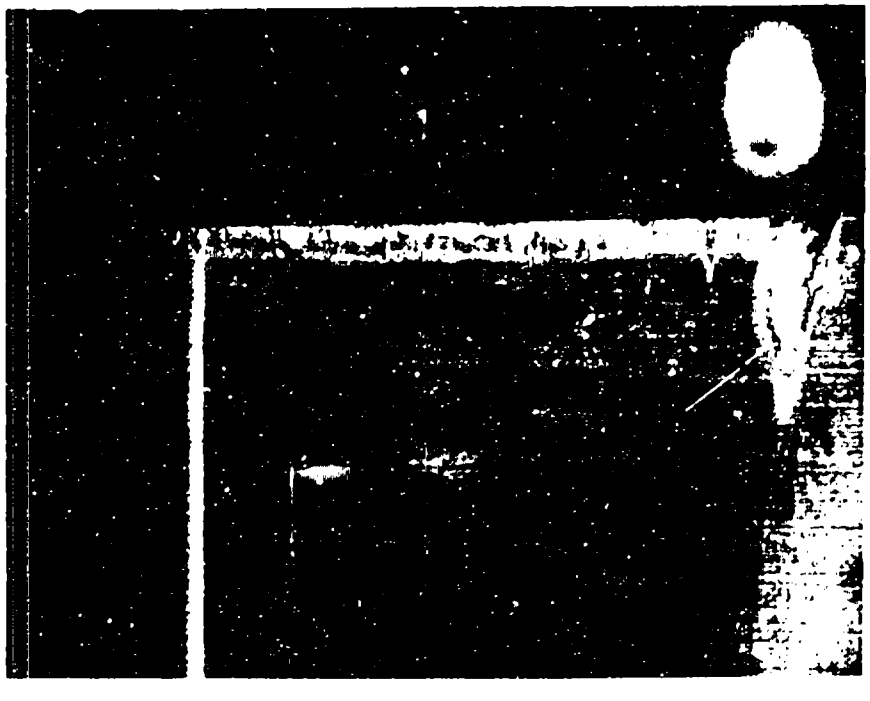

TOP VIEW

SIDE CUTTING EDGE VIEW

0 0.050 0.100 0.150

INCH

MAG 26X

CUTTING SPEED: 200 FPM
FEED: 0.0025 IPR
DEPTH OF CUT: 0.150 INCH
TOOL LIFE: 38.8

FIGURE 35

WEAR PHOTOGRAPH SHOWING CHIPPED CUTTING EDGE

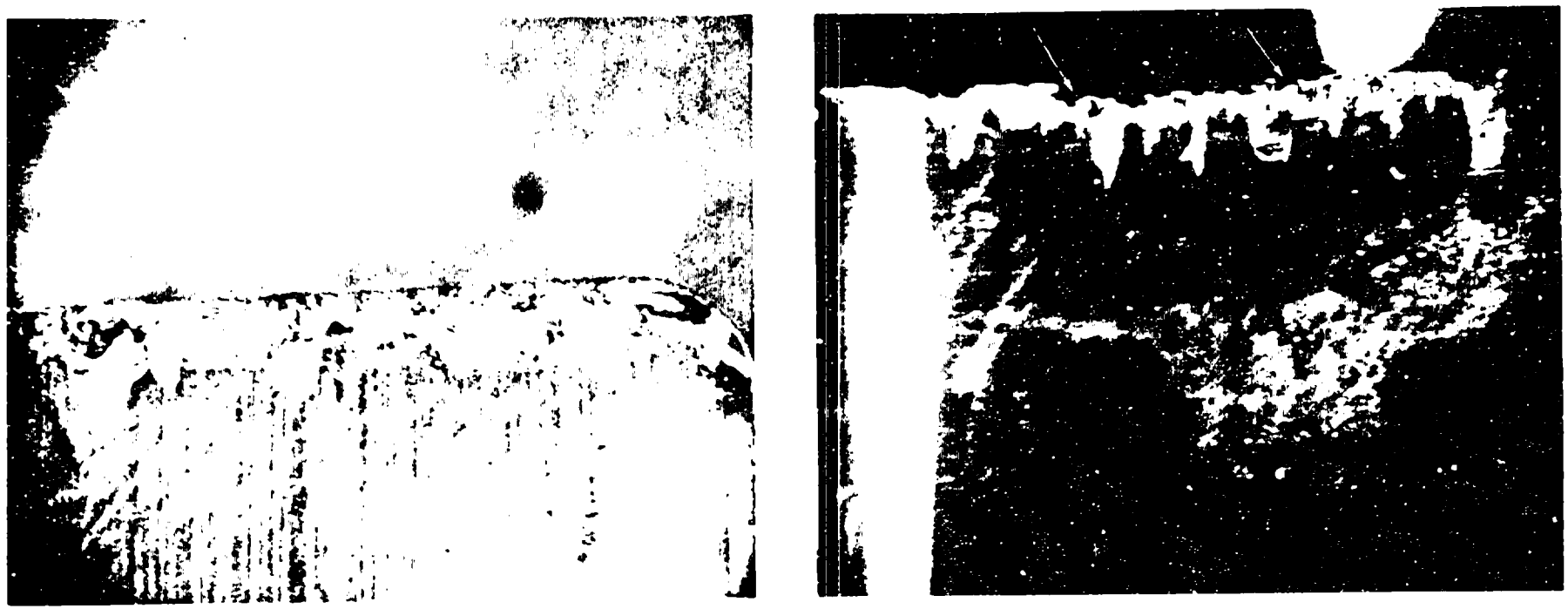

TOP VIEW

SIDE CUTTING EDGE VIEW

0 0.050 0.100 0.150

INCH

MAG 26X

CUTTING SPEED: 100 FPM
FEED: 0.005 IPR
DEPTH OF CUT: 0.150 INCH
TOOL LIFE: 60 MINUTES

FIGURE 36

TYPICAL WEAR AT 60 MINUTES

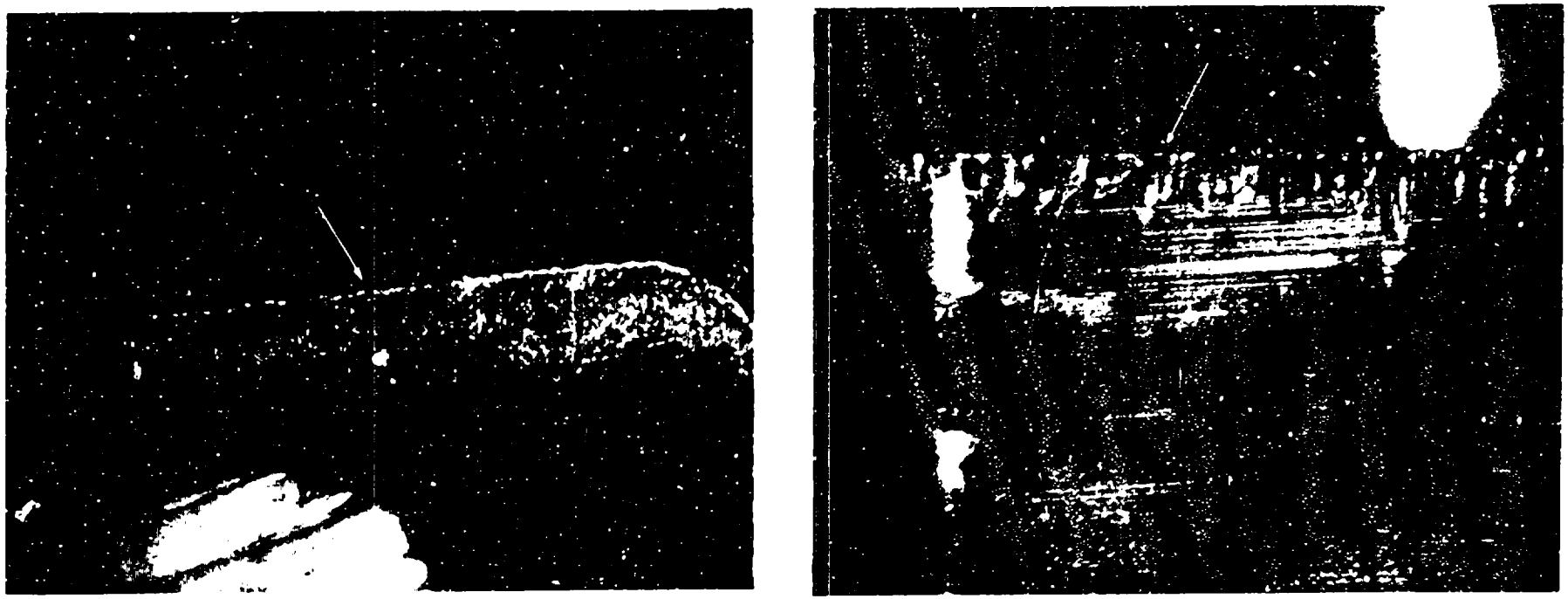

TOP VIEW

SIDE CUTTING EDGE VIEW

0 0.050 0.100 0.150

INCH

MAG 26X

CUTTING SPEED: 100 FPM
FEED: 0.0025 IPR
DEPTH OF CUT: 0.150 INCH
TOOL LIFE: 60 MINUTES

FIGURE 37

TYPICAL WEAR AT 90 MINUTES

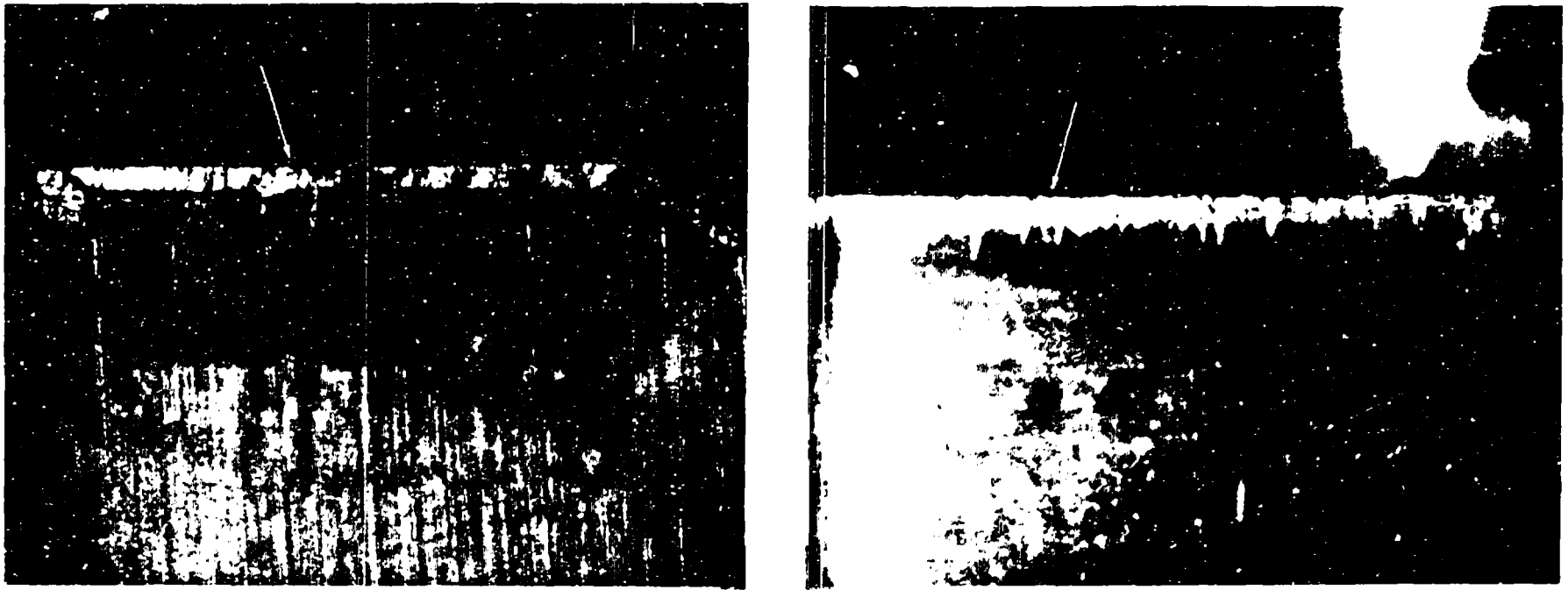

TOP VIEW

SIDE CUTTING EDGE VIEW

0 0.050 0.100

INCH

MAG 26X

CUTTING SPEED: 150 FPM
FEED: 0.0025 IPR
DEPTH OF CUT: 0.150 INCH
TOOL LIFE: 90.0 MINUTES

FIGURE 38

TYPICAL WEAR AT 120 MINUTES

TOP VIEW

0 0.050 0.100 0.150

INCH

SIDE CUTTING EDGE VIEW

MAG 26X

CUTTING SPEED: 150 FPM
FEED: 0.0025 IPR
DEPTH OF CUT: 0.150 INCH
TOOL LIFE: 120 MINUTES

FIGURE 39

TYPICAL WEAR AT 180.0 MINUTES

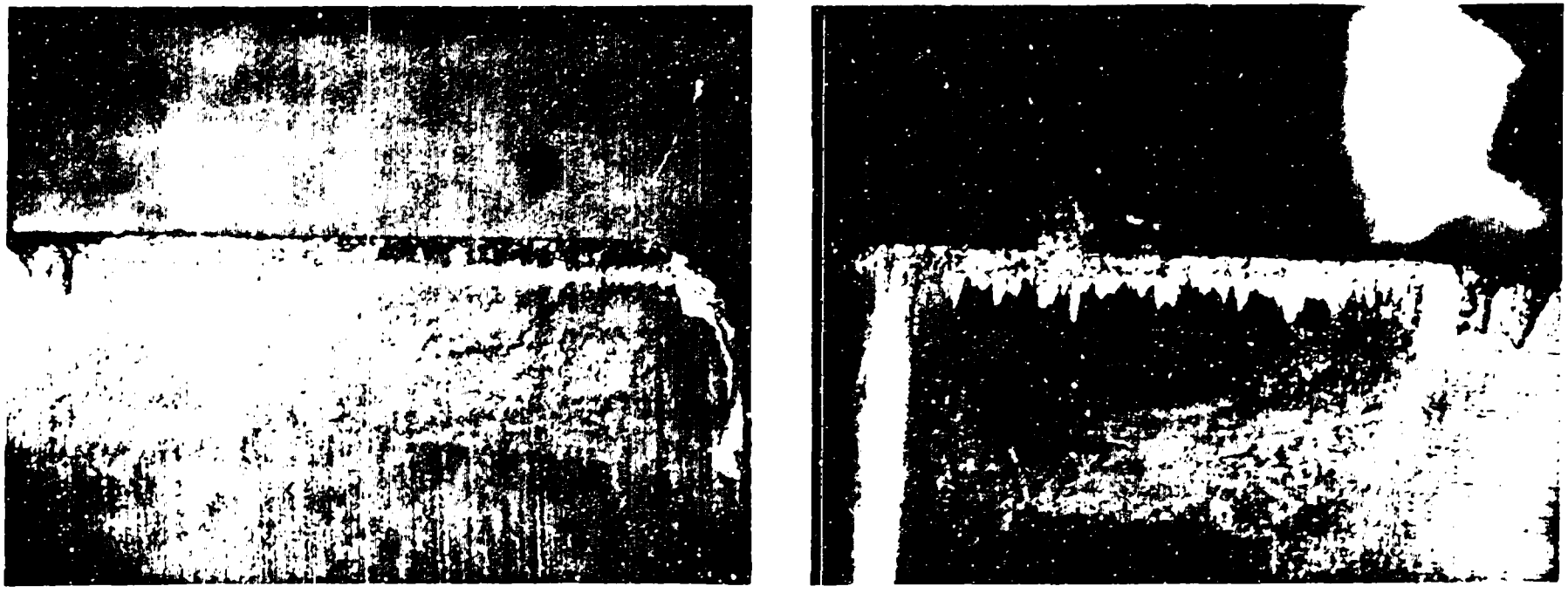

TOP VIEW — SIDE CUTTING EDGE VIEW

0 0.050 0.100 0.150

INCH

MAG 26X

CUTTING SPEED: 150 FPM
FEED: 0.0025 IPR
DEPTH OF CUT: 0.150 INCH
TOOL LIFE: 180.0 MINUTES

FIGURE 40

PHOTOGRAPH OF TOOL USED IN A BORING TEST

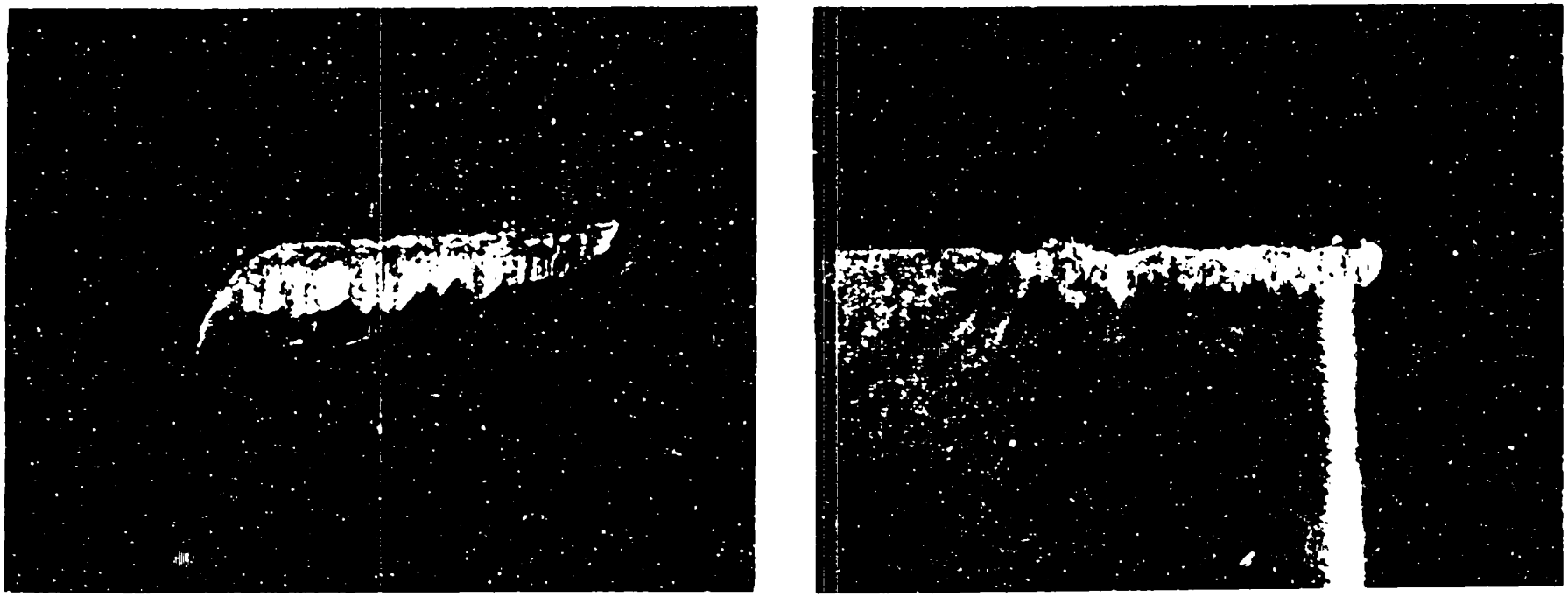

MAG 26X

CUTTING SPEED: 150 FPM
FEED: 0.0025 IPR
DEPTH OF CUT: 0.050 INCH
TOOL LIFE: 428.3 MINUTES

FIGURE 41

SURFACE INTEGRITY OF 0.050 INCH DEPTH OF CUT WITH A SHARP TOOL

MAG: 30X

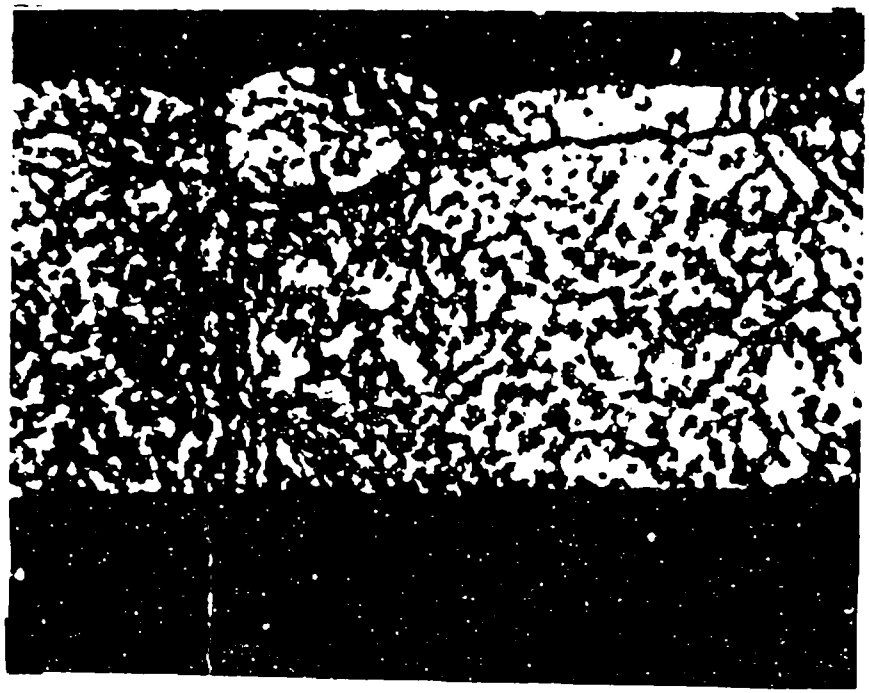

MAG: 200X

MOUNT NUMBER 31229

CUTTING SPEED: 150 FPM
FEED: 0.005 IPR
CUTTING FLUID: TRIM SOL (1:20)

FIGURE 42

SURFACE INTEGRITY OF 0.050 INCH DEPTH OF CUT WITH A DULL TOOL

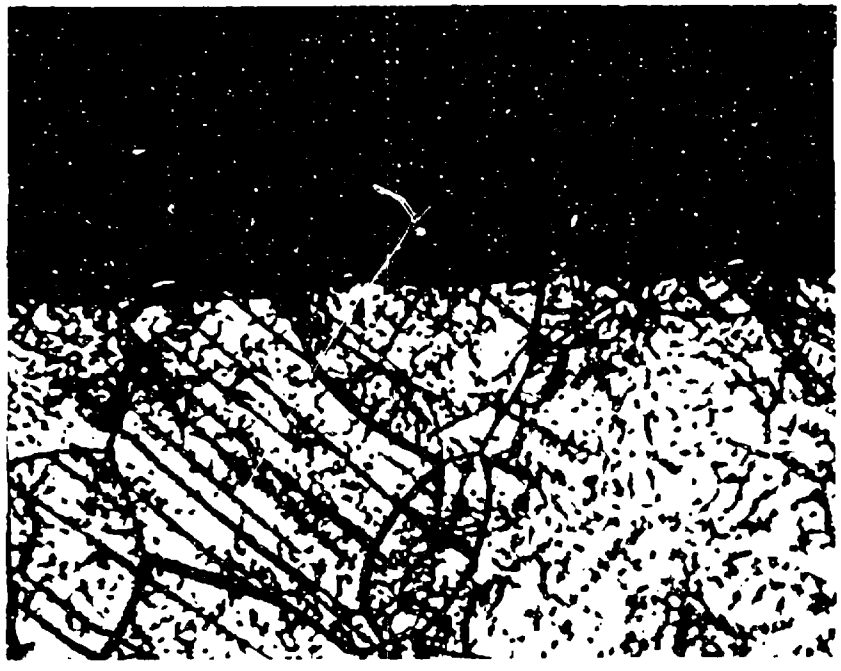

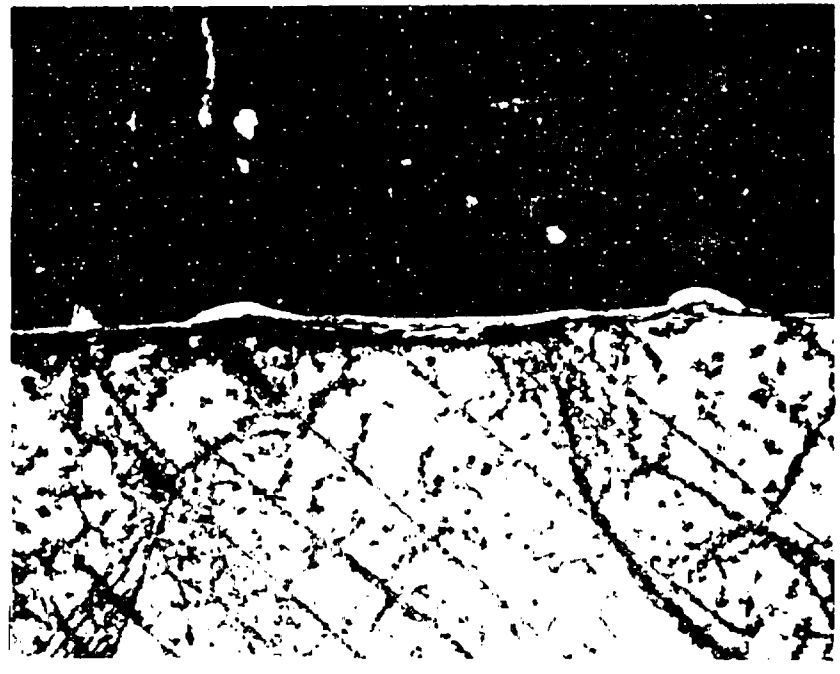

MAG: 200X

MOUNT NUMBER 31233

MAG: 500X

CUTTING SPEED: 150 FPM
FEED: 0.005 IPR
CUTTING FLUID: TRIM SOL (1:20)

FIGURE 43

SURFACE INTEGRITY OF 0.100 INCH DEPTH OF CUT WITH A SHARP TOOL

MAG: 10X

MAG: 50X

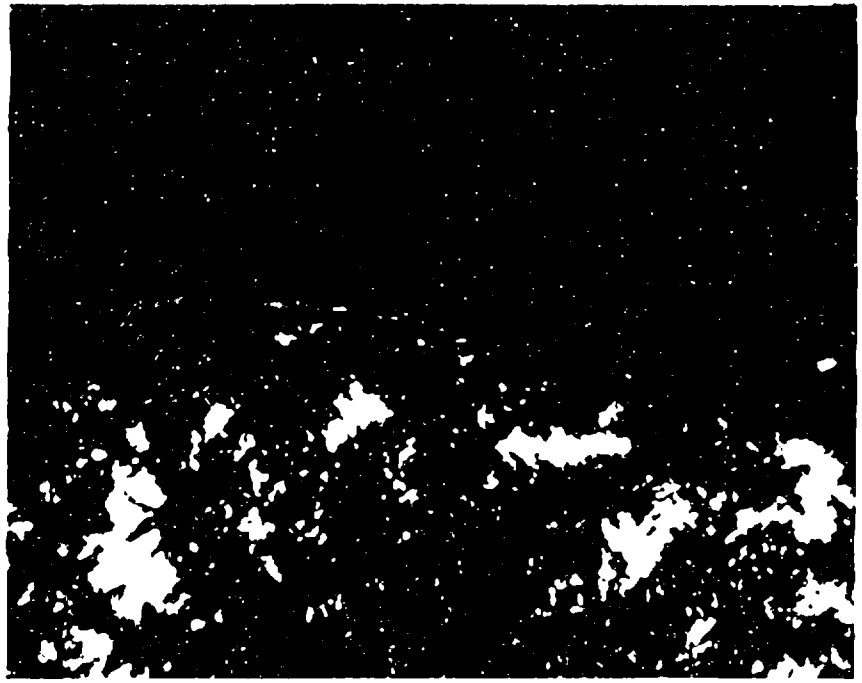

MAG: 1000X

MOUNT NUMBER 31230

CUTTING SPEED: 150 FPM
FEED: 0.005 IPR
CUTTING FLUID: TRIM SOL (1:20)

FIGURE 44

SURFACE INTEGRITY OF 0.100 INCH DEPTH OF CUT WITH A DULL TOOL

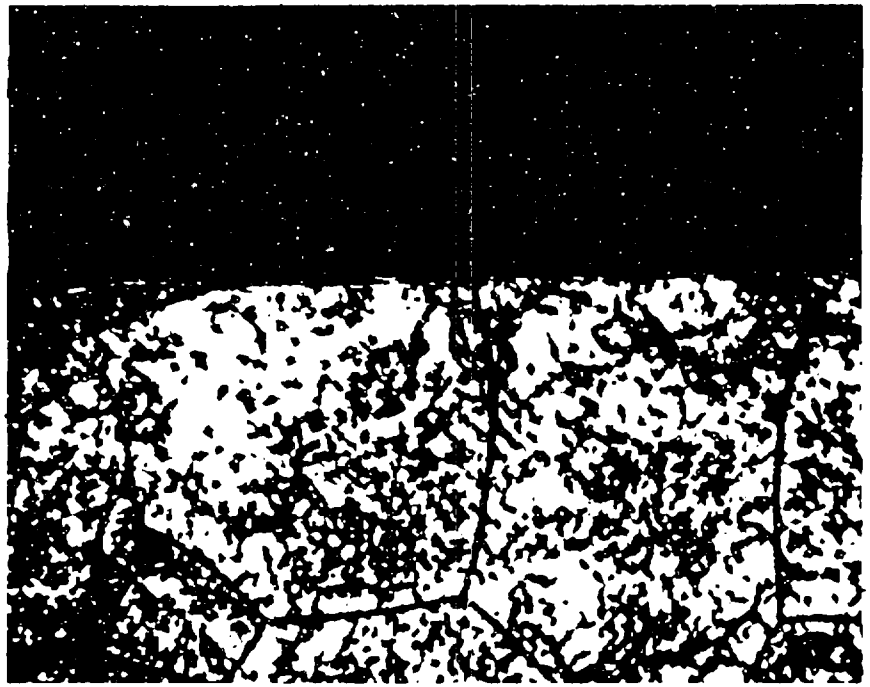

MOUNT NUMBER 31234

MAG: 200X

CUTTING SPEED: 150 FPM
FEED: 0.005 IPR
CUTTING FLUID: TRIM SOL (1:20)

FIGURE 45

SURFACE INTEGRITY OF 0.150 INCH DEPTH OF CUT WITH A SHARP TOOL

MOUNT NUMBER 31231

MAG: 500X

CUTTING SPEED: 150 FPM
FEED: 0.005 IPR
CUTTING FLUID: TRIM SOL (1:20)

FIGURE 46

SURFACE INTEGRITY OF 0.150 INCH DEPTH OF CUT WITH A DULL TOOL

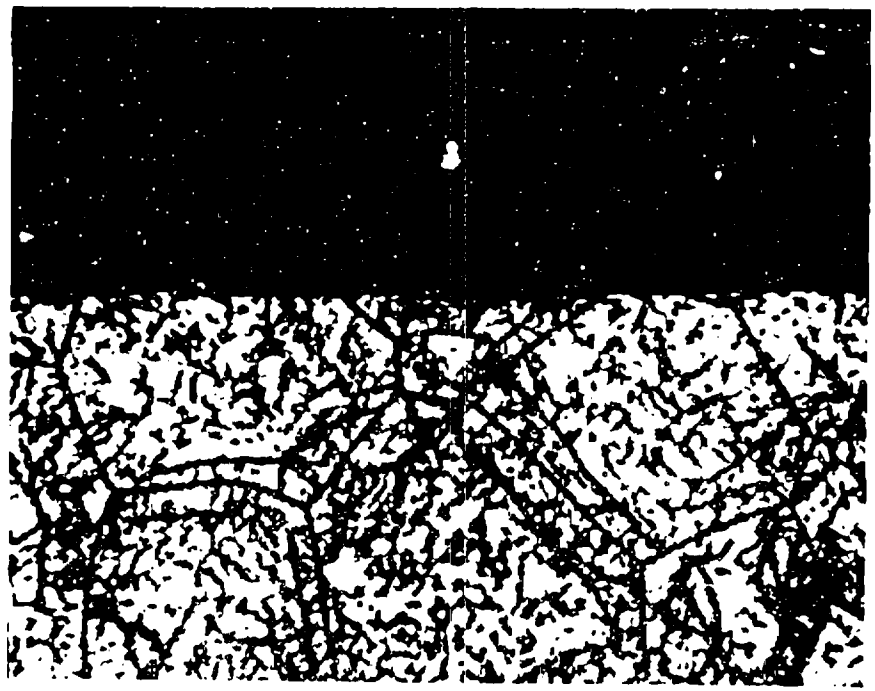

MOUNT NUMBER 31235

MAG: 200X

CUTTING SPEED: 150 FPM
FEED: 0.005 IPR
CUTTING FLUID: TRIM SOL (1:20)

FIGURE 47

SURFACE INTEGRITY OF 0.200 INCH DEPTH OF CUT WITH A SHARP TOOL

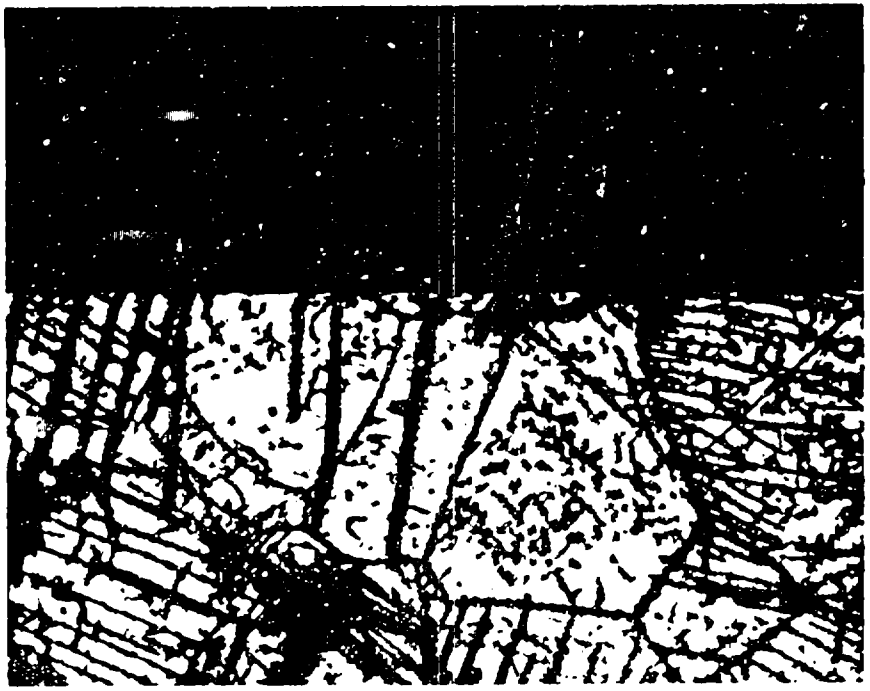

MOUNT NUMBER 31232

MAG: 200X

CUTTING SPEED: 150 FPM
FEED: 0.005 IPR
CUTTING FLUID: TRIM SOL (1:20)

FIGURE 48

SURFACE INTEGRITY OF 0.200 INCH DEPTH OF CUT WITH A DULL TOOL

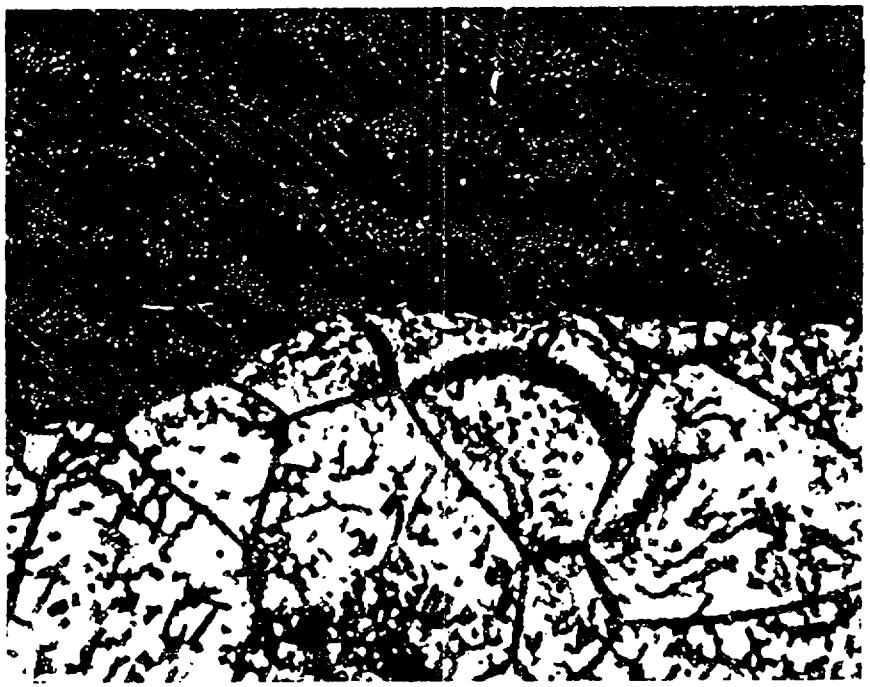

MOUNT NUMBER 31236 MAG: 200X

CUTTING SPEED: 150 FPM
FEED: 0.005 IPR
CUTTING FLUID: TRIM SOL (1:20)

FIGURE 49

SCANNING ELECTRON MICROSCOPE ENERGY DISPERSIVE SPECTROSCOPY ANALYSIS OF MACHINED TITANIUM CHIPS

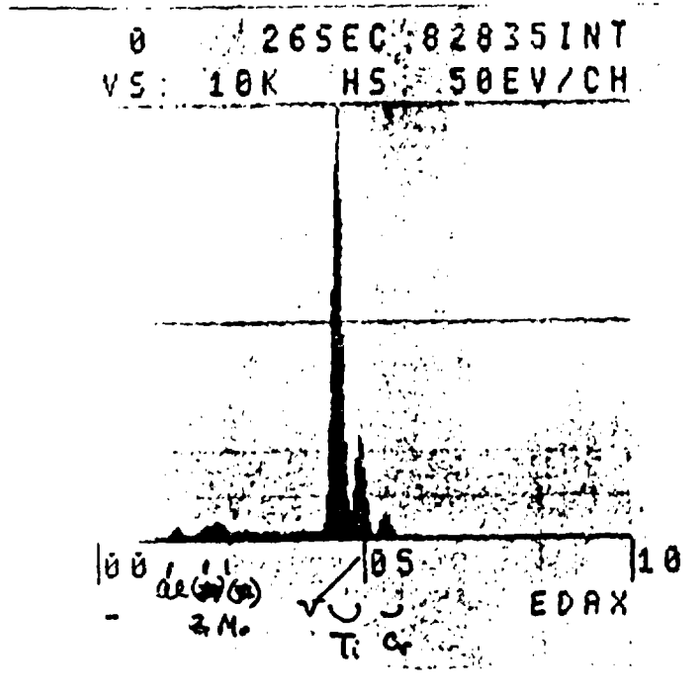

TOOL: KC910
CUTTING FLUID: TRIM SOL (1:20)
CUTTING SPEED: 200 FPM

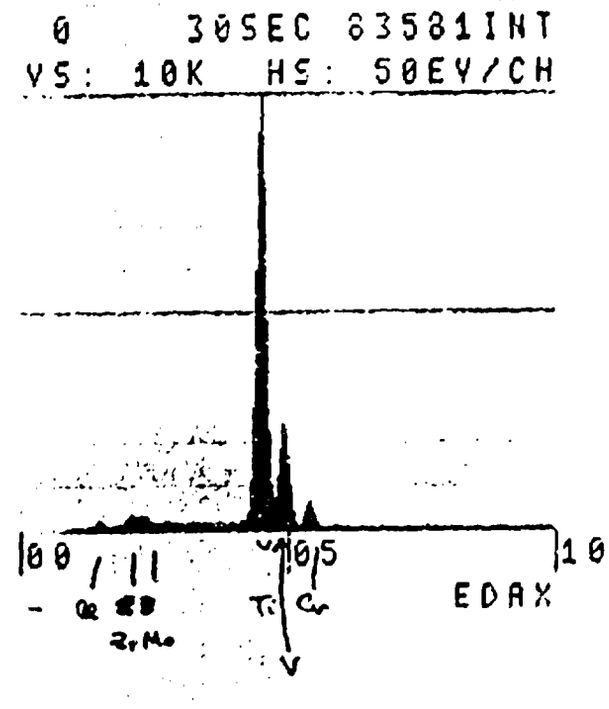

TOOL: 883
CUTTING FLUID: TRIM SOL (1:20)
CUTTING SPEED: 200 FPM

FIGURE 50

SCANNING ELECTRON MICROSCOPE ENERGY DISPERSIVE SPECTROSCOPY

ANALYSIS OF MACHINED TITANIUM CHIPS

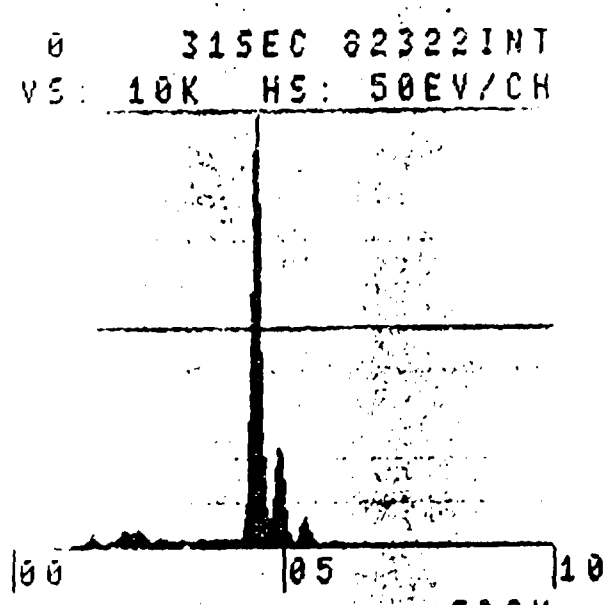

TOOL: KC910
CUTTING FLUID: DRY
CUTTING SPEED: 200 FPM

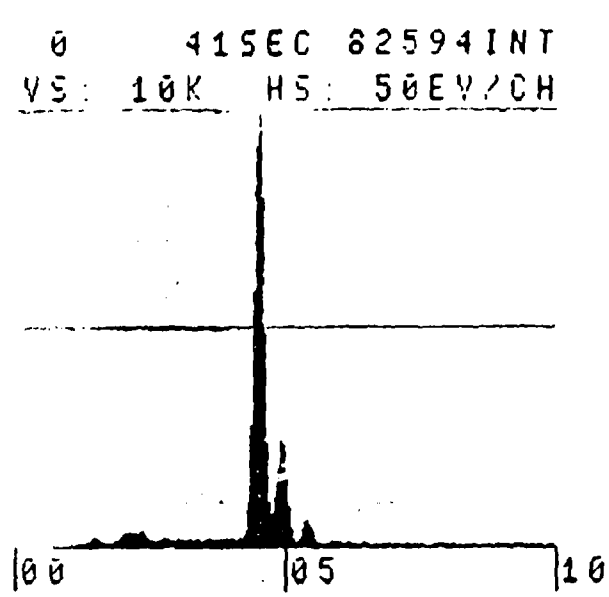

TOOL: 883
CUTTING FLUID: DRY
CUTTING SPEED: 200 FPM

FIGURE 51

SCANNING ELECTRON MICROSCOPE ENERGY DISPERSIVE SPECTROSCOPY ANALYSIS OF MACHINED TITANIUM CHIPS

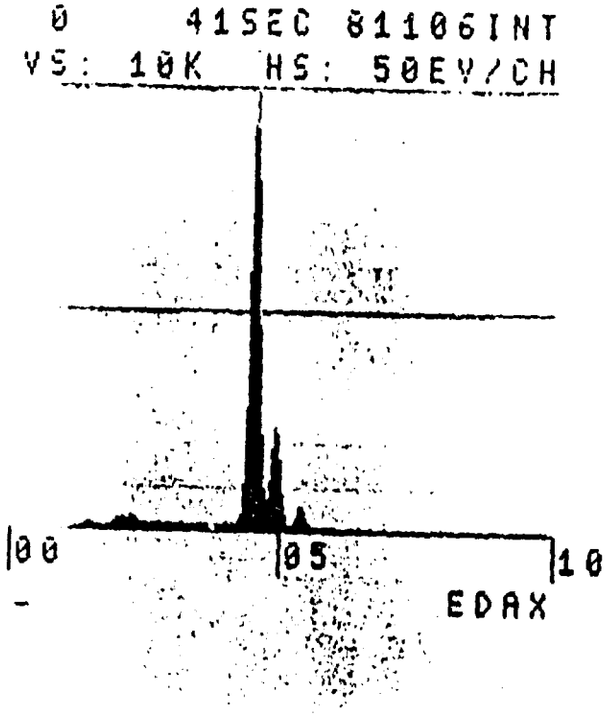

TOOL: KC910
CUTTING FLUID: TRIM SOL (1:20)
CUTTING SPEED: 150 FPM

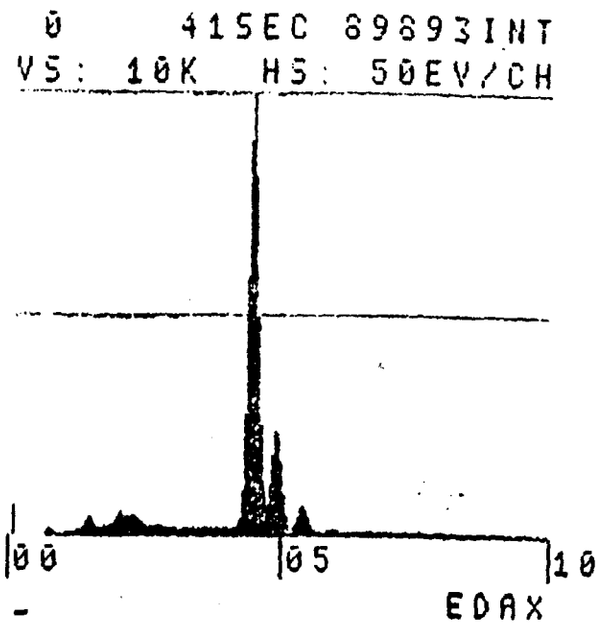

TOOL: 883
CUTTING FLUID: TRIM SOL (1:20)
CUTTING SPEED: 150 FPM

FIGURE 52

SCANNING ELECTRON MICROSCOPE ENERGY DISPERSIVE SPECTROSCOPY

ANALYSIS OF MACHINED TITANIUM CHIPS

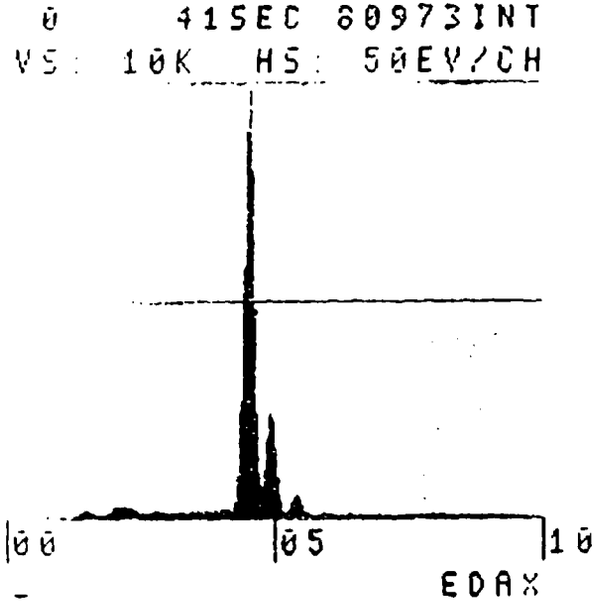

TOOL: KC910
CUTTING FLUID: DRY
CUTTING SPEED: 150 FPM

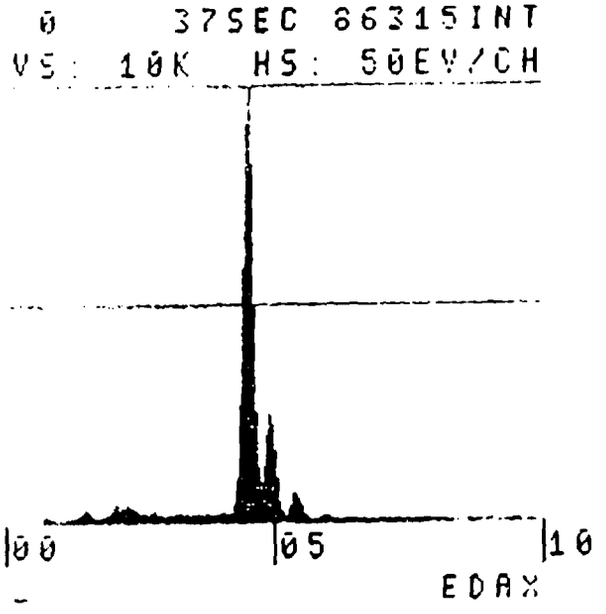

TOOL: 883
CUTTING FLUID: DRY
CUTTING SPEED: 150 FPM

FIGURE 53

SCANNING ELECTRON MICROSCOPE ENERGY DISPERSIVE SPECTROSCOPY

ANALYSIS OF AN 883 CARBIDE INSERT

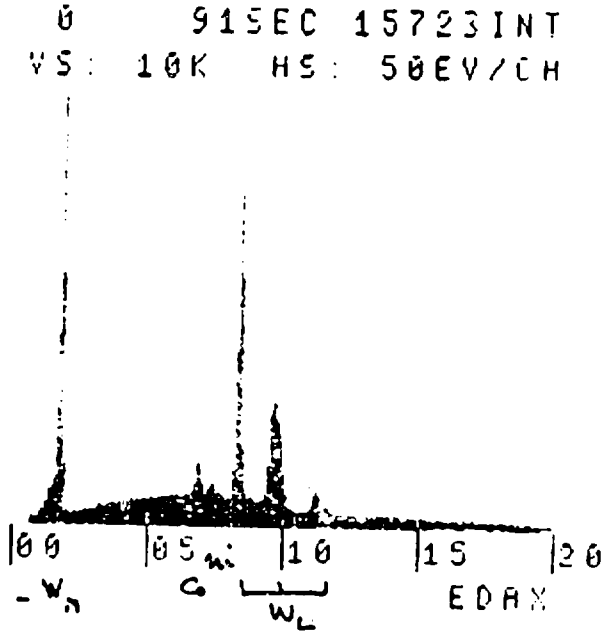

TOOL: 883 (USED FOR REFERENCE)

FIGURE 54

SCANNING ELECTRON MICROSCOPE IMAGE OF A TYPICAL CHIP

TOOL: 883
CUTTING FLUID: DRY
CUTTING SPEED: 200 FPM
MAG: 500X

FIGURE 55

SCHEMATIC OF BORING HEAD FACE VIEW

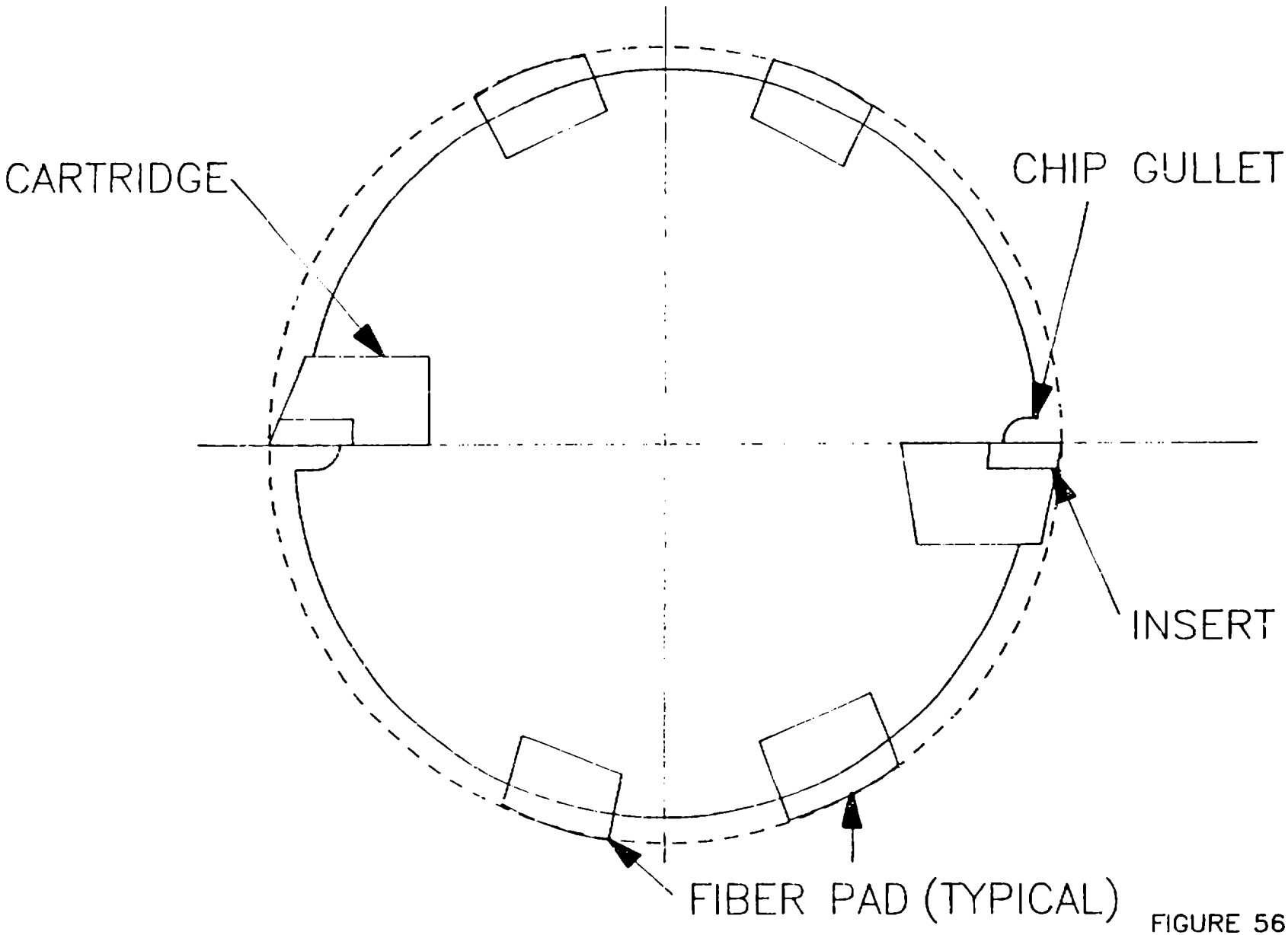

FIGURE 56

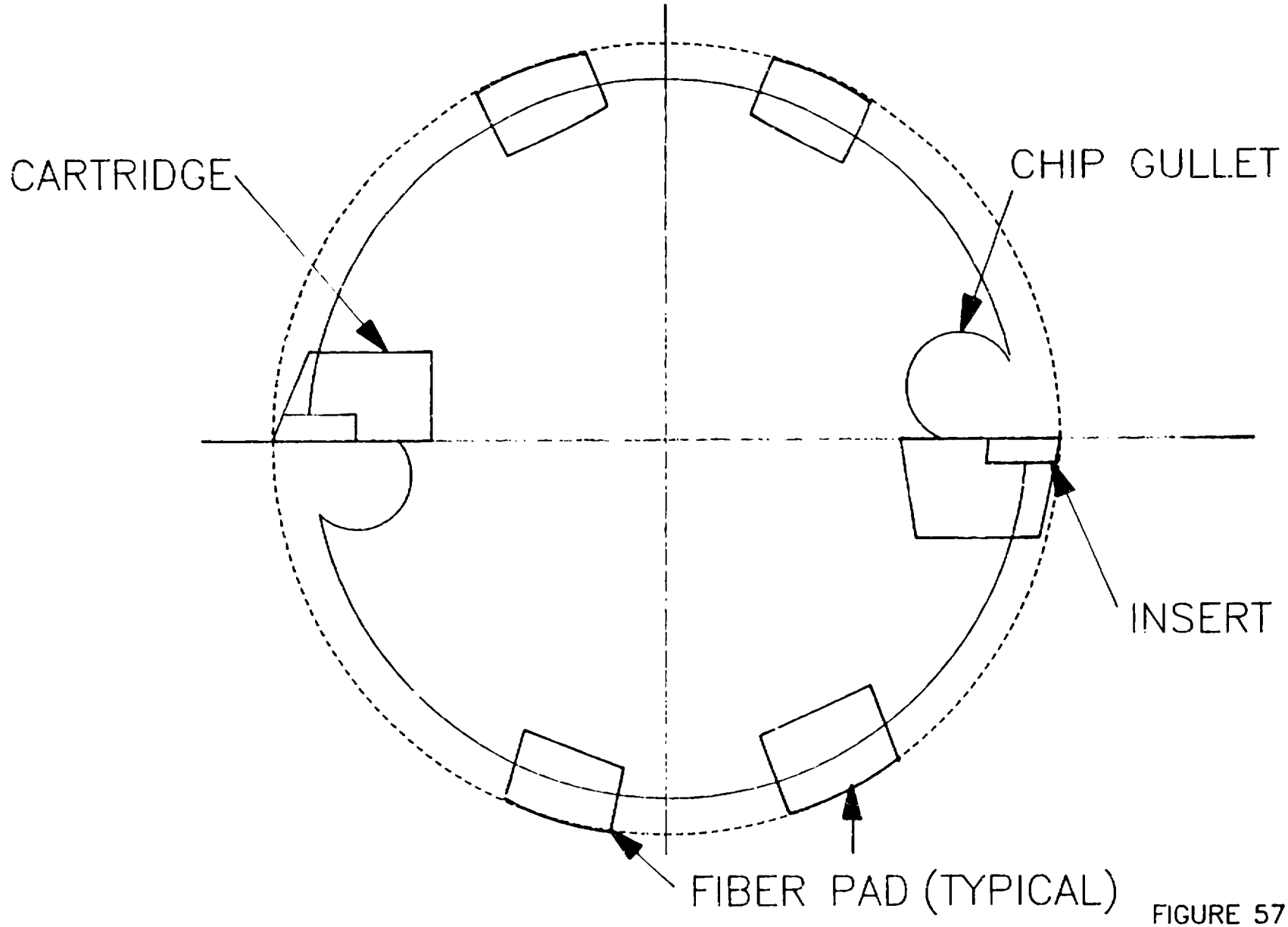
SCHEMATIC OF BORING HEAD FACE VIEW
WITH CHIP GULLET ENLARGED
CARTRIDGE
CHIP GULLET
INSERT
FIBER PAD (TYPICAL)

FIGURE 57

PHOTOGRAPHS OF AMERICAN HELLER BTA BORING HEAD

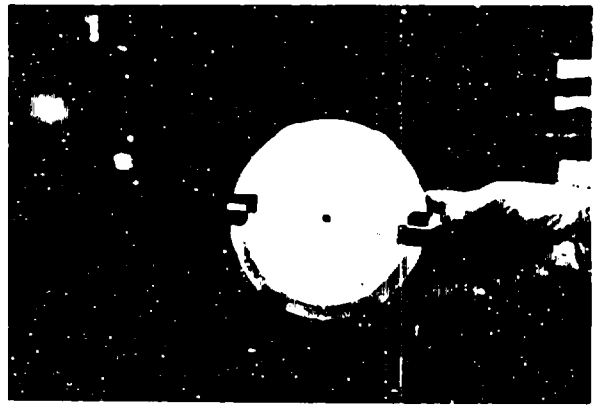

ORIGINAL HEAD
FACE VIEW

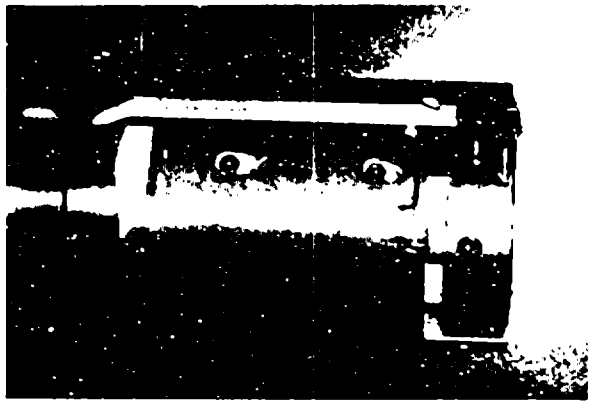

ORIGINAL HEAD
SIDE VIEW

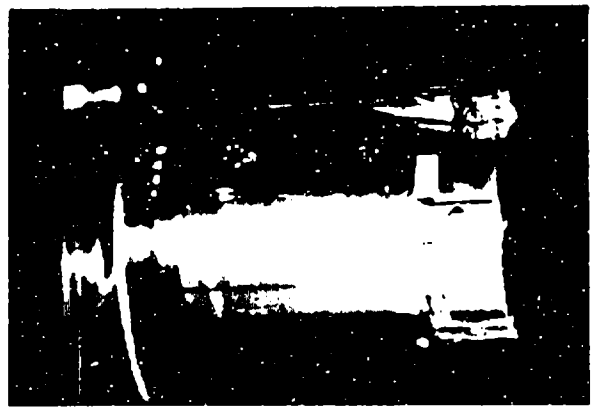

MODIFIED HEAD
SIDE VIEW

FIGURE 58

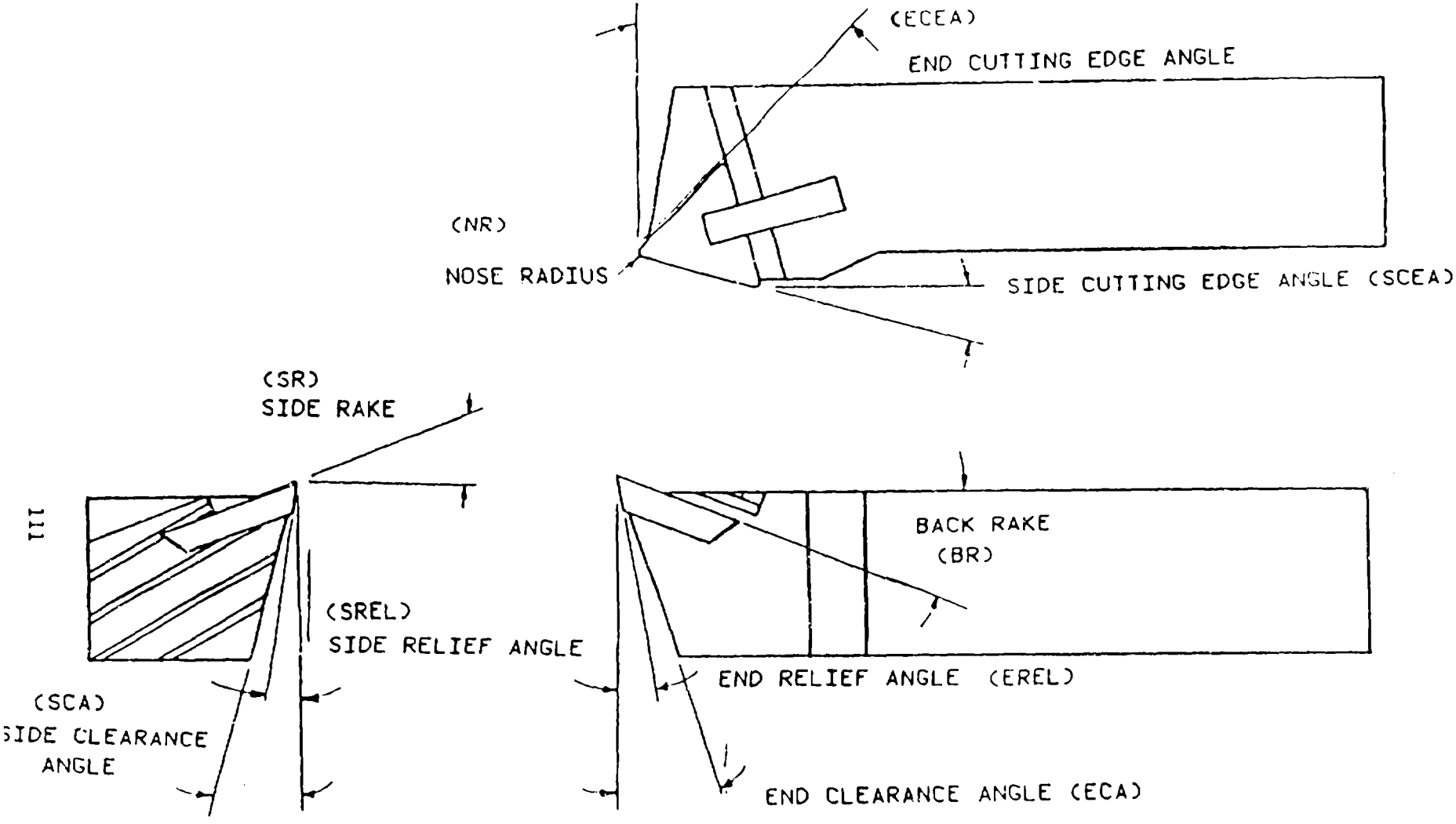

TOOL GEOMETRY

FIGURE 59

SKETCH OF TYPICAL INDEXABLE CARBIDE INSERT WITH MOLDED CHIP CONTROL GROOVES

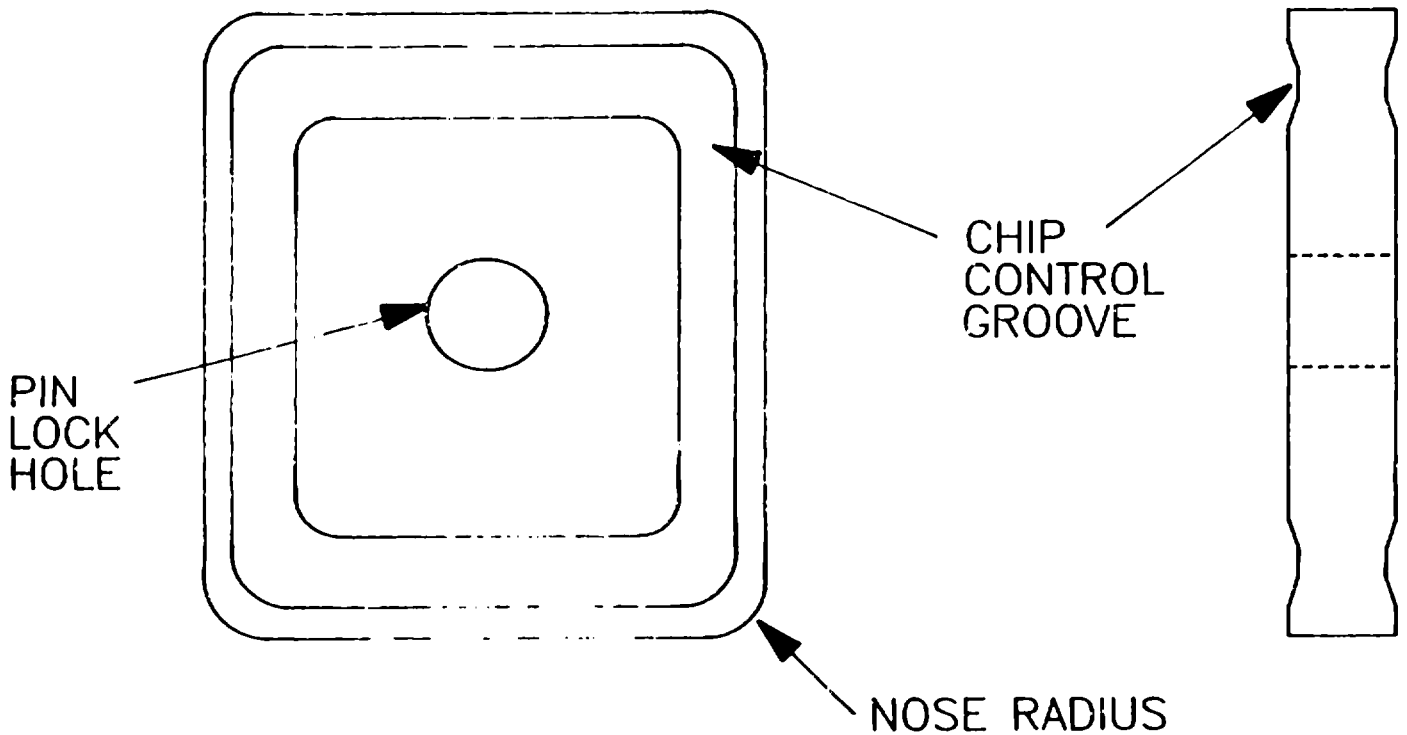

FIGURE 60

APPENDIX A

"Chip Control in Turning"

CHIP CONTROL IN TURNING

By

Sadayuki Nakamura*
John D. Christopher**
Garry J. Wuebbling***

Presented at
SME 1982 International Tool &
Manufacturing Engineering Conference
May 17-20, 1982
Philadelphia, Pennsylvania

*Visiting Engineer, Metcut Research Associates Inc., Cincinnati, Ohio
(Research Engineer, Daido Steel Company, Ltd., Nagoya, Japan)

**Manager, Machinability Testing, Metcut Research Associates Inc., Cincinnati, Ohio

***Project Engineer, Metcut Research Associates Inc., Cincinnati, Ohio

ABSTRACT

Chip control in a turning operation is one of the serious problems that must be addressed in operating an unmanned machine tool. The chip control performance of five different tool shapes and the chip breakability of four different workpiece materials: AISI 4140 (three different hardness levels), AISI 8620, Inconel 718, and Ti-6Al-4V alloy are discussed based on laboratory experiments. The results show that the chip shapes are independently influenced by tool geometry and by workpiece material. From this fact, two methods were devised to estimate acceptable chip shapes. The first method is based on tool geometry and workpiece material constants, and the second method is based on proposed experimental results.

INTRODUCTION

Continuous chips produced in turning operations can damage the workpiece finished surface, chip the tool, and create difficulty in chip handling. In an unmanned manufacturing plant which is one of the ultimate goals of manufacturing, the control of chip shape is a key factor which will determine the successful operation.

A review of literature reveals that there are three primary methods of chip control as follows:

1. Selection of appropriate depth of cut, feed rate and cutting speed.

2. Application of chip breakers on the tool.

3. Selection of workpiece materials whose chips are easily broken, such as free-machining materials.

The influence of cutting conditions on chip breakage has been discussed in terms of chip flow diameter,[1-4] chip flow direction[5] and fracture strain of chips,[6] all of which have been studied based on the fundamental theory on chip formation. Storing the cutting conditions for well controlled chips which have been determined from turning tests under various cutting conditions is another aspect of this kind of study designed for more practical use.[7] Development of a chip-shape sensor for use in an adaptive control system has also been attempted.[8]

There are many reports on the relationship between the geometry of obstruction-type chip breakers and the radius of chips,[1,3] optimum configuration of the obstruction-type chip breaker,[1] and functions of the groove-type chip breaker,[4,9] and the non-groove-type (land-angle) chip breakers.[10]

One work material with good chip breakability (chip breakability being that characteristic of chip breakage from the viewpoint of the workpiece material) is free-machining brass whose chips tend to be small fragments. Steels containing additional sulfur and/or lead show better chip breakability over a wide range of cutting conditions and can be machined without a chip breaker using normal cutting conditions.

Necessary information for engine lathe operators and NC lathe programmers includes suitable cutting tools and optimum cutting conditions. In order to provide such information, it is necessary to collect and store data in advance, which is the goal of this study. Since the combinations of workpiece materials, cutting tools, and cutting conditions are infinite, estimation of chip breakage by experimental or theoretical equations is useful toward saving man-hours and reducing cost.

This study consists of two parts: First, an experimental study on the effect of side cutting edge angle, cutting speed, workpiece material, and chip-breaker shape on chip breakage phenomena; second, a discussion of the ways to estimate chip breakage for the combination of workpiece material and cutting tool using the experimental constants which are obtained from the first step.

CHIP CLASSIFICATION

Several ways to classify chip shapes have been proposed. The primary difference among them is the number of groups into which the chips are classified. Similar definitions on acceptable and unacceptable chips are specified in all cases.

For this study, the chip-shape classification described by E. K. Henriksen[1] was modified to include snarling chips not exceeding 2" in diameter and compressed crescent-shaped chips which were suggested by D. G. Jones, et. al.[10] Figure 1 gives a representation of those different types of chips. Of these chips, No. 4 through No. 7 are judged acceptable, and No. 1 through No. 3 are considered unacceptable. No. 8 chips are not too harmful from the viewpoint of disposal. However, they are classified as unacceptable because they are accompanied by a high cutting force which reduces tool life.[10]

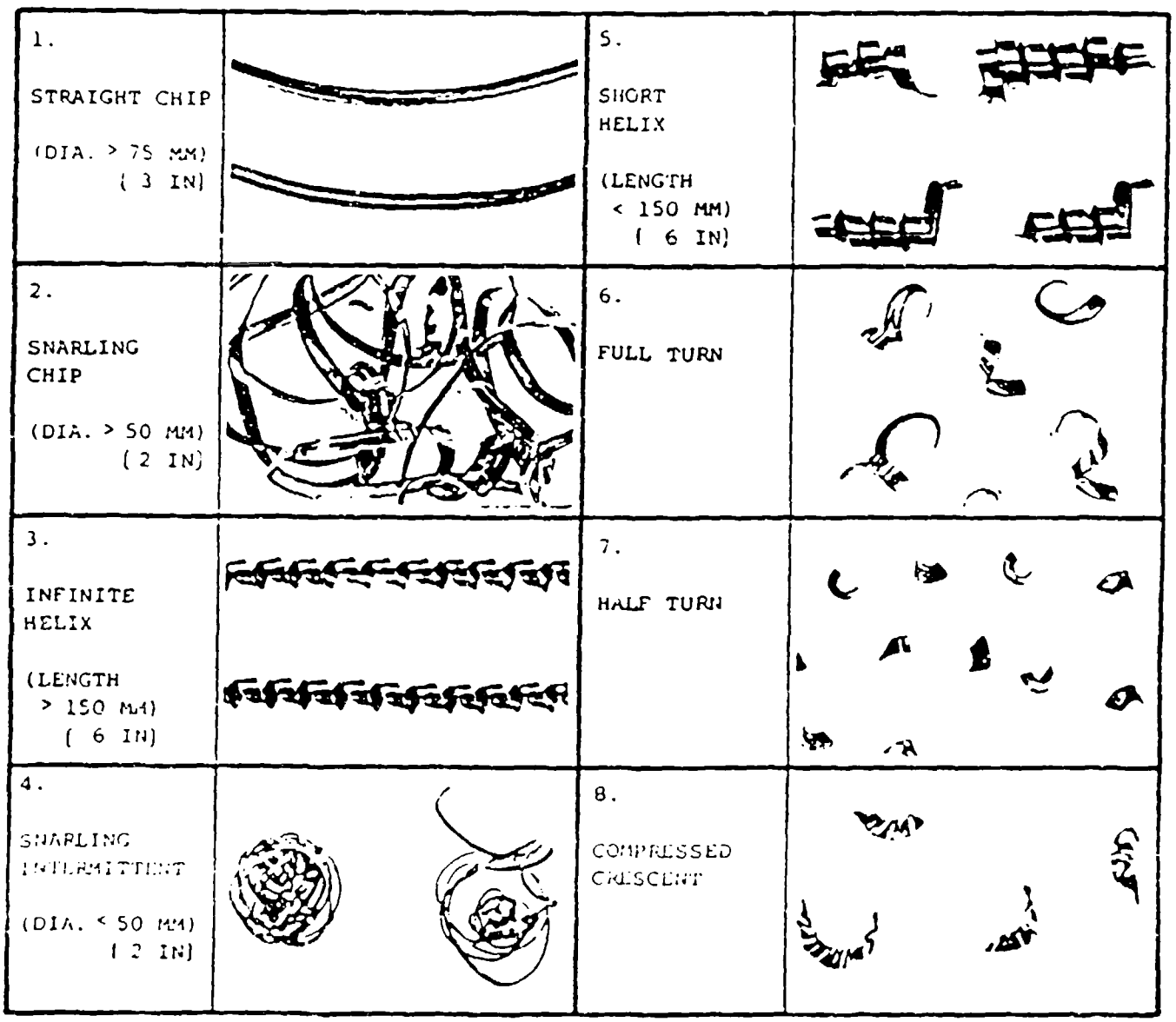

FIGURE 1. CHIP CLASSIFICATION

EXPERIMENTAL PROCEDURE

AISI 4140, AISI 8620, Inconel 718 and Ti-6Al-4V were used as workpiece materials for this study. Their chemical compositions are given in Table 1. The materials were procured as three-inch-diameter, hot-rolled round bars and were subsequently heat treated. Three levels of heat treatments were given to AISI 4140 in order to examine the influence of hardness on chip-breakage phenomena. The Brinell Hardness after heat treatment is listed in Table 1. A multi-phase TiN-coated carbide was used for AISI 4140 and AISI 8620, but a C-2 grade carbide was used with Inconel 718 and Ti-6Al-4V as indicated in Table 2.

TABLE 1. DETAILS OF WORKPIECE MATERIALS

WORKPIECE MATERIAL	CHEMICAL COMPOSITION (%)								HEAT TREATMENT*	HARDNESS (HB)
	C	Si	Mn	P	S	Ni	Cr	Mo		
AISI 4140	0.41	0.20	0.83	0.010	0.010	0.05	1.10	0.25	ANN	179
									Q&T	341
									Q&T	415
AISI 8620	0.20	0.28	0.67	0.021	0.018	0.42	0.44	0.16	ANN	156
	C	Ni	Cr	Mo	Nb+Ta	Ti	Al	Fe		
INCONEL 718	0.05	53.17	18.07	3.11	5.16	1.02	0.67	BAL.	STA	376
	C	Al	V	Fe	O	N	H	Ti		
Ti-6Al-4V	0.006	6.02	4.12	0.13	0.18	0.006	0.002	BAL.	STA	302

* ANN: Annealed
Q&T: Quenched and Tempered
STA: Solution Treated and Aged

A set of cutting tests which was composed of a combination of five different tools (four tools for Inconel 718 and Ti-6Al-4V), five depth-of-cut levels, and five feed-rate levels was regarded as "a unit of test". In other words, 'a test' for a workpiece material, a cutting speed, and a side cutting edge consisted of all these combinations. Table 3 shows the detail of the combinations.

TABLE 2. CARBIDE GRADES APPLIED TO WORKPIECE MATERIALS

WORKPIECE MATERIAL	TOOL MATERIAL
AISI 4140, AISI 8620	MULTI-PHASE TiN COATED CARBIDE (KENNAMETAL KC850)
INCONEL 718, Ti-6Al-4V	C-2 CARBIDE (KENNAMETAL K68)

TABLE 3. A UNIT OF TEST

(A unit of test consists of all the combinations of tool, depth of cut, and feed rate.)

TOOL (INDEXABLE INSERT)	A: CNMA432 C: CNMG432 M: CNMM432* P: CNMP432 S: CNMS432
DEPTH OF CUT, MM (IN)	0.25, 0.51, 1.27, 2.5, 5.1 (0.01, 0.02, 0.05, 0.10, 0.20)
FEED RATE, MM/REV (IPR)	0.064, 0.13, 0.25, 0.38, 0.51 (0.0025, 0.005, 0.010, 0.015, 0.020)

* Tool M was not applied to Inconel 718 and Ti-6Al-4V.

All the tools were 80-degree diamond inserts with 1/32-inch nose radius. Figure 2 illustrates the cross-section of the tool describing chip-breaker design. Tool A (CNMA432 as described in this paper) has no chip breaker, but a flat rake face. Tool G (CNMG432) has a groove-type chip breaker. Tool M (CNMM432) has a land-angle type, which was designed to reduce the cutting force at the high feed rates. This insert shape was not used for Inconel 718 and Ti-6Al-4V because the C-2 grade was not commercially available. Tool P (CNMP432) and Tool S (CNMS432) are obstruction types in which the geometry varies along the cutting edge, depending on the distance from the tool point. The side rake angles of the inserts set in the tool holders are also given in Figure 2. The values for chip flow radius will be explained in a later section.

The depth of cut and feed rate were selected to cover both roughing and finishing operations. Other cutting parameters such as side cutting edge angle and cutting speed will be explained later.

The workpiece material was machined until the chip shape stabilized. The chips were collected during each operation and were ranked as previously described.

DESCRIPTION OF ACCEPTABLE CHIP REGION

One of the ways to describe the effect of cutting conditions on chip breakage is to draw an acceptable and unacceptable region on a rate versus feed depth-of-cut diagram. Examples of such diagrams obtained in this study are shown in Figure 3. The boundary lines between under-control and good-control in these diagrams were determined by fourth power linear regression analysis after log transformation. Since the chip shape rating number has no mathematical meaning, this regression method is not mathematically rigid. However, it helps us draw the smooth lines, and the lines drawn by this method are a good representation of the real data. On the other hand, the border lines between good-control and over-control could not be determined by this method because there are only a few data points belonging to the over-control region. These lines were drawn as a smooth curve linking the over-control data.

At the smaller depth of cut, the tool nose has a large effect on chip flow direction, chip curl radius, and eventually chip breakage. Most of the discussion in the following sections will be on the boundaries defining under-control and good-control at a depth of cut larger than 1.27 mm (0.05 inch) where there is little influence by the nose. The average feed rate along the under/good-control control boundary for the depth of cut between 1.27 and 5.1 mm (0.05 and 0.20 inch) is defined as the lower limiting feed in this paper. The average value along the good-control/over-control boundary is the upper limiting feed.

In the following sections, the effect of side cutting edge angle, cutting speed, workpiece material, and cutting tool/chip-breaker geometry on chip breakage will be discussed.

TOOL NAME	CHIP-BREAKER SHAPE		CHIP-BREAKER TYPE	SIDE RAKE	CHIP FLOW RADIUS
A (CNMA432)			NO CHIP BREAKER	-5°	----
G (CNMG432)	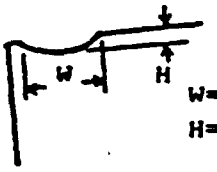	W=1.68 MM H=0.10 MM	GROOVE	-5°	3.6 MM (0.14 IN)
M (CNMM432)	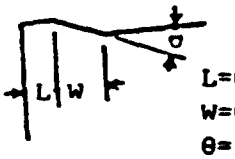	L=0.30 MM W=0.43 MM θ=16°	LAND-ANGLE	-5°	4.1 MM (0.16 IN)
P (CNMP432)	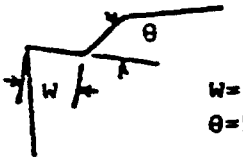	W=1.30 MM* θ=55°	OBSTRUCTION	+5°	2.5 MM (0.10 IN)
S (CNMS432)	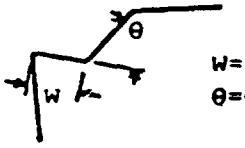	W=1.33 MM* θ=60°	OBSTRUCTION	+15°	2.3 MM (0.09 IN)

*AVERAGE VALUE

FIGURE 2. GEOMETRY OF CHIP-BREAKER CROSS-SECTION

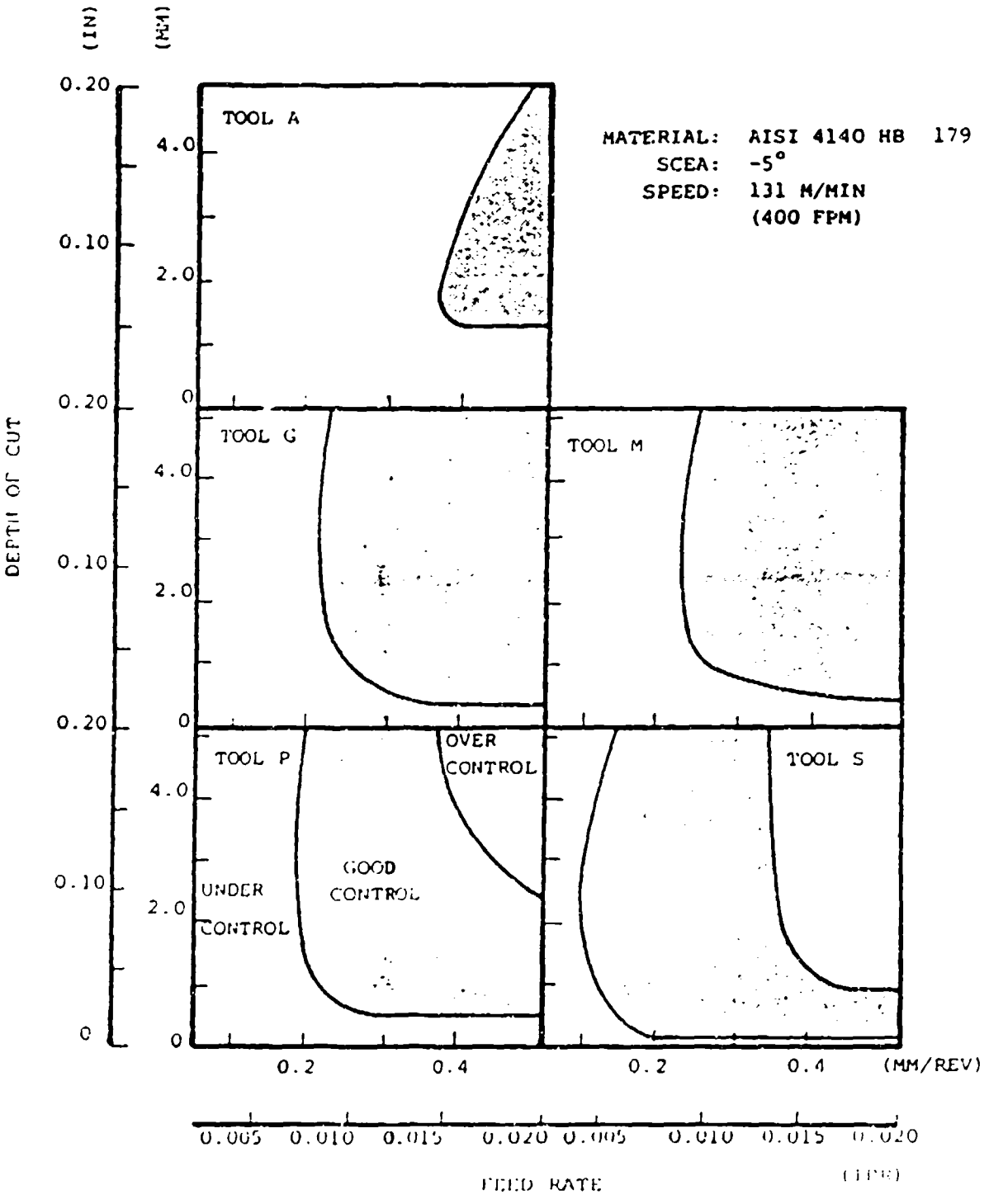

FIGURE 3. ACCEPTABLE CHIP REGION ON FEED-RATE DEPTH-OF-CUT DIAGRAM

EFFECT OF SIDE CUTTING EDGE ANGLE ON LOWER LIMITING FEED

Lower limiting feeds are plotted against side cutting edge angle in Figure 4. Annealed AISI 4140 steel was used for these tests. The cutting speed was 131 m/min (400 fpm). This figure indicates that the side cutting edge angle has no major effect on lower limiting feed, but the increase in side cutting edge angle does slightly reduce the lower limiting feed. The reduction is about 12% over the side cutting edge angle range of -5° to +15°.

While the larger side cutting edge angle (absolute value) produces the thinner chips which are less easily broken, it also gives more opportunity for chips to hit obstacles such as the workpiece or the tool. The results shown in Figure 4 suggest that there is a greater tendency for chips to hit obstacles than for thinner chips to be produced.

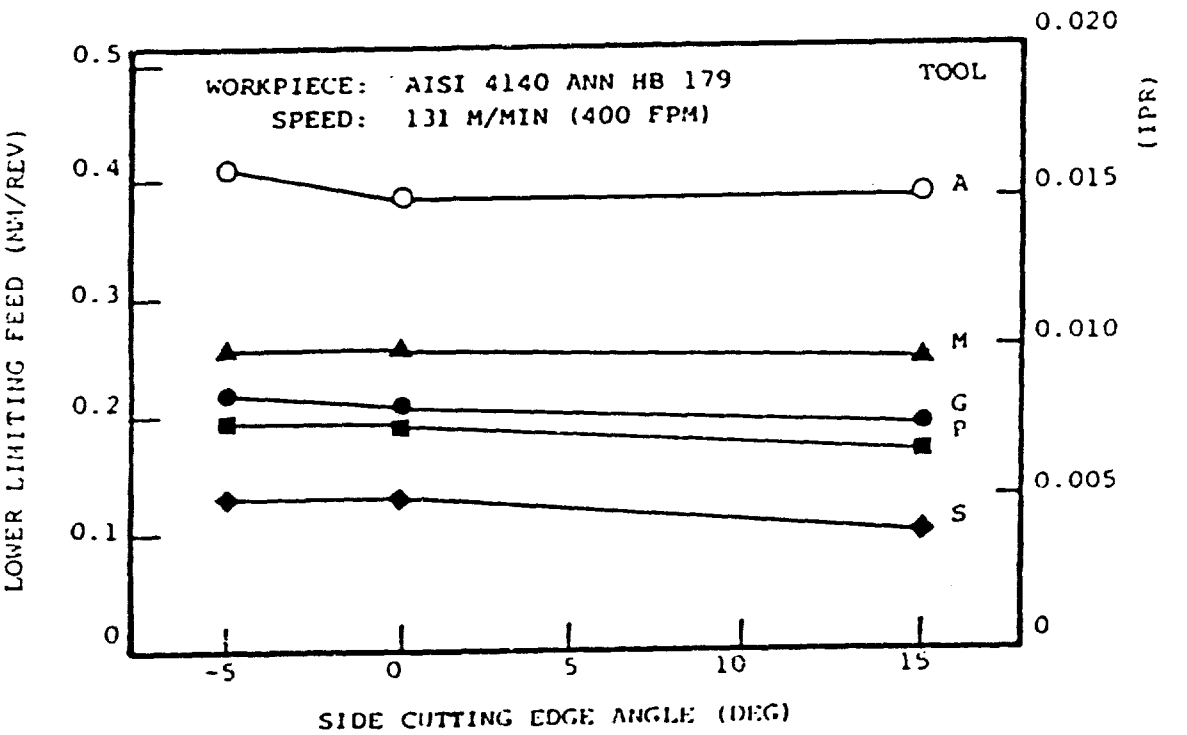

FIGURE 4. EFFECT OF SIDE CUTTING EDGE ANGLE ON LOWER LIMITING FEED

EFFECT OF CUTTING SPEED ON LOWER LIMITING FEED

The relationship between cutting speed and lower limiting feed for chip breakage is given in Figure 5. All tests were carried out with annealed AISI 4140. The side cutting edge angle was -5°. There was no built-up edge observed on the tool rake face during these tests.

The lower limiting feed becomes slightly higher when the cutting speed is increased. The increase of lower limiting feed caused by the increase in cutting speed from 66 to 197 m/min (200 to 600 fpm) is about 22%. The thinner chips are obtained at the higher cutting speeds. The change in measured chip thickness was about 25% within the speed range of this test. The coincidence of these two values indicates that the increase in lower limiting feed brought about by the increase in cutting speed is related to the reduction of chip thickness.

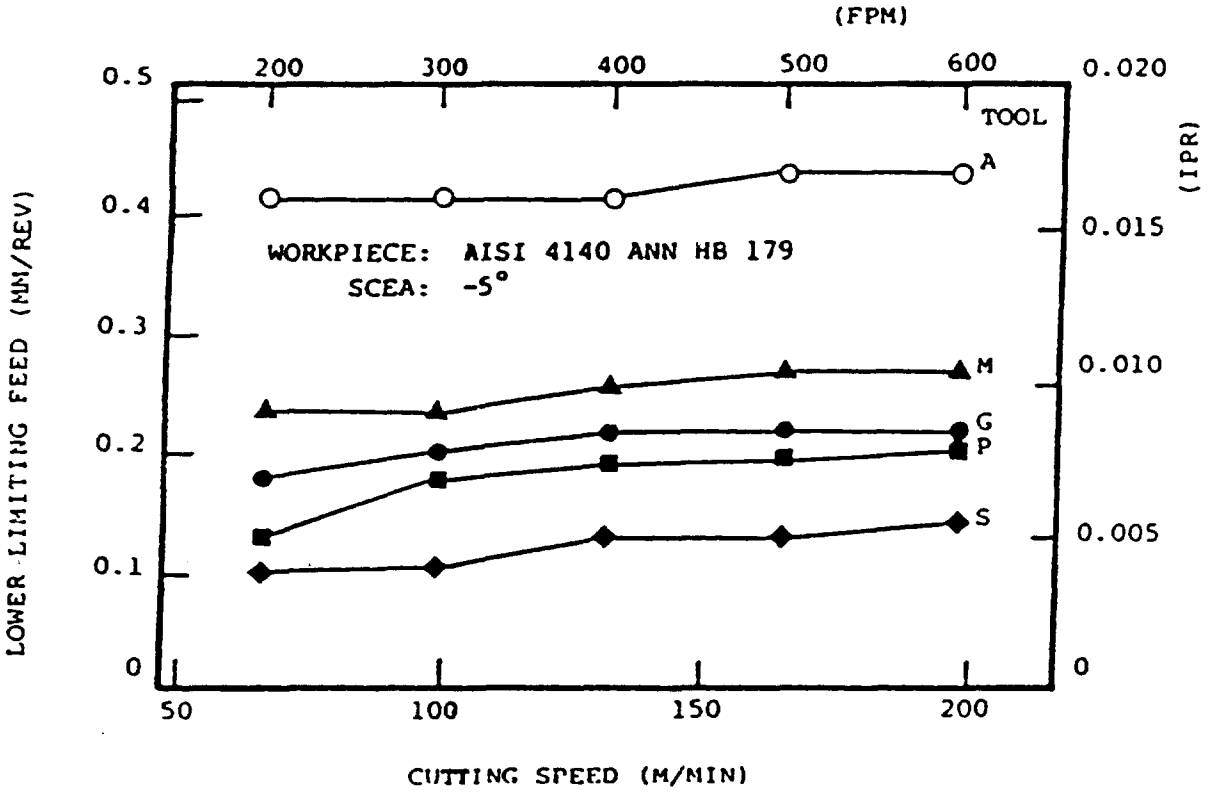

FIGURE 5. EFFECT OF CUTTING SPEED ON LOWER LIMITING FEED

EFFECT OF WORKPIECE MATERIAL ON LOWER LIMITING FEED

Lower limiting feeds for all tested workpiece materials are shown in Figure 6. The cutting speed for each material was selected from the Machining Data Handbook to avoid undesirably high tool wear rate. The values of cutting speed are given in Figure 6. The difference in cutting speed need not be seriously considered when comparing the materials because cutting speed causes little change in the lower limiting feed.

The workpiece material has a significant effect on chip-breakage phenomena. Annealed AISI 4140, AISI 8620 and Inconel 718 have better chip breakability than Ti-6Al-4V and hardened AISI 4140. Since similar trends were observed in all the tests with five different insert configurations, these chip-breakage features can be considered characteristic of the materials themselves.

Lower limiting feeds are plotted against Brinell Hardness in Figure 7 which shows that harder material has poorer chip breakability. This trend is also well explained by the change in chip thickness: harder material produces thinner chips which are less easily broken. The harder material also produces higher strength chips which are more difficult to break.

EFFECT OF CHIP-BREAKER TYPE ON LOWER LIMITING FEED

The effect of chip-breaker type is shown in Figures 4 through 6. In all those cases, Tool S showed the smallest lower limiting feed, followed by Tool P, Tool G and Tool M. Tool A had the poorest chip control as expected from the rake face configuration. Note that the influence of the chip-breaker shape was as great as that of the workpiece material. From the fact that the chip control ranking of the tools does not change for different side cutting edge angles, cutting speeds, and work materials, the effect of chip-breaker type may be described by a parameter related to its geometry. Details of this consideration will be discussed later in this paper.

UPPER LIMITING FEED

Over-controlled chips were only observed in turning with Tool P and Tool S. Quantitative discussion is not possible because there are not enough data. However, it appears that the higher the lower limiting feeds of a tool or a material, the higher their upper limiting ...is.

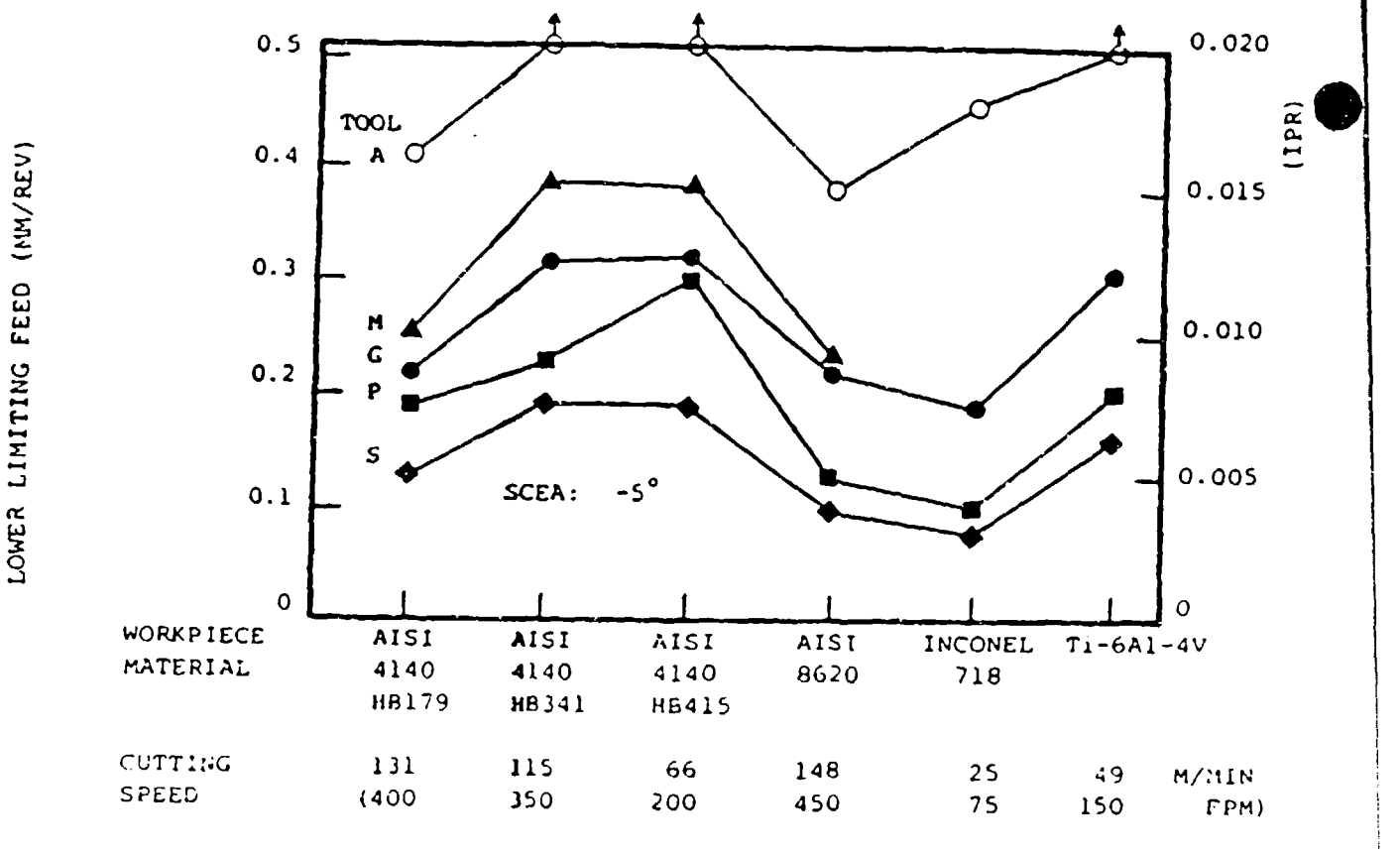

FIGURE 6. LOWER LIMITING FEED OF VARIOUS MATERIALS

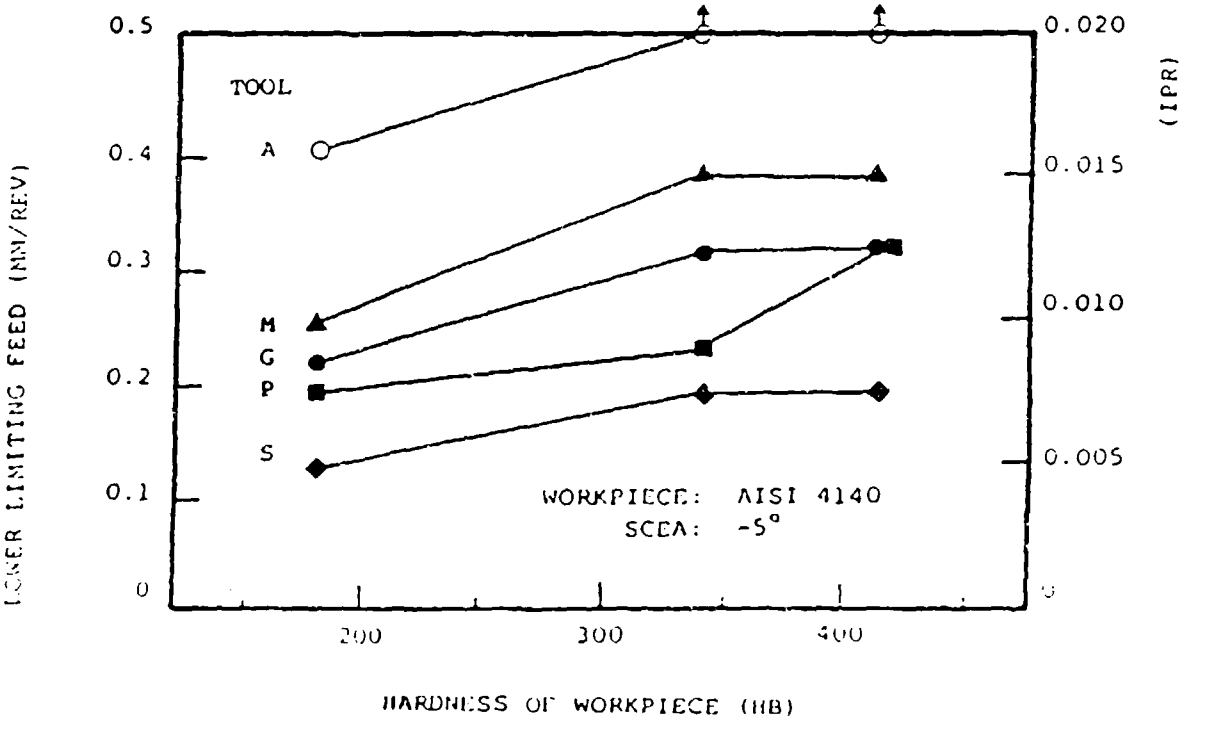

FIGURE 7. EFFECT OF WORKPIECE HARDNESS ON LOWER LIMITING FEED

LOWER LIMITING DEPTH OF CUT

When the depth of cut is smaller than the feed rate or nose radius, the direction of chip flow is perpendicular rather than parallel to the workpiece axis. The chip thickness under such conditions is strongly dependent on the value of the depth of cut. Therefore, the chip-breakage phenomena at small depths of cut and high feed rates are similar to those at low feed rates and large depths of cut. Figure 8 shows the relationship between lower limiting depth of cut and lower limiting feed. There is a good correlation between them. Because the configuration of the chip breaker at the nose region is different from that along the side cutting edge, each tool has a different correlation between the lower limiting feed and the lower limiting depth of cut. These relationships are shown as different lines in Figure 8.

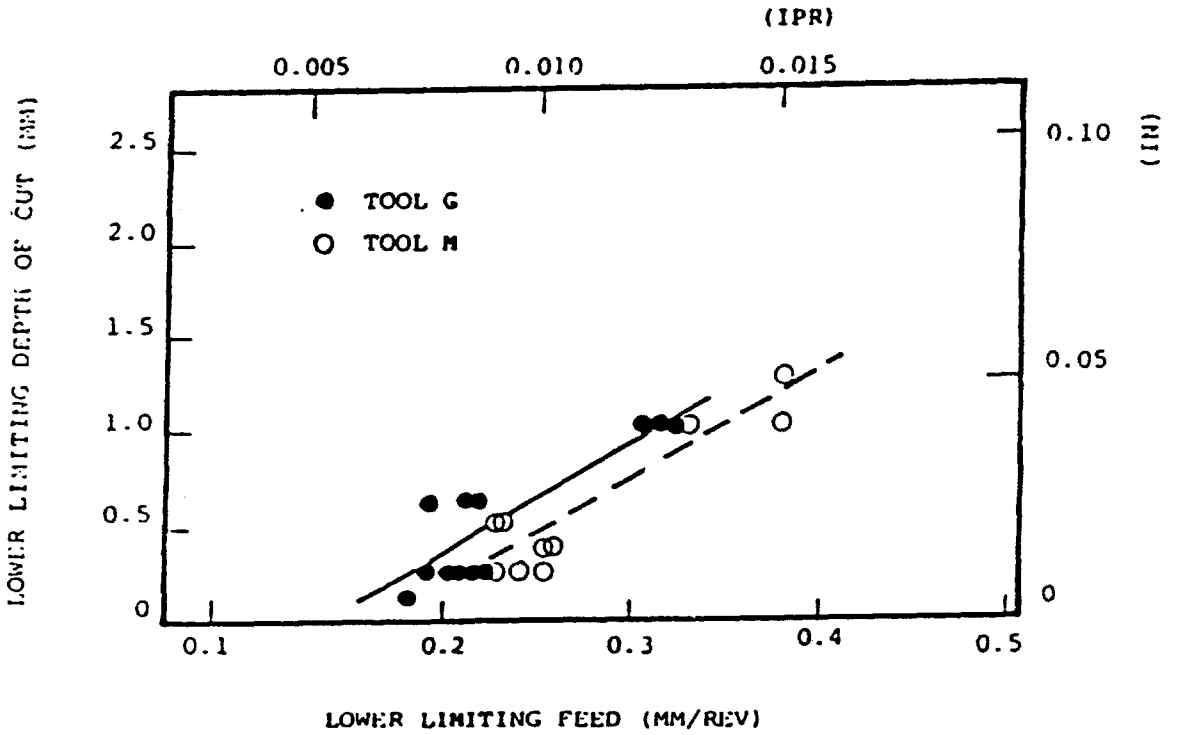

FIGURE 8. RELATIONSHIP BETWEEN LOWER LIMITING FEED AND LOWER LIMITING DEPTH OF CUT

SUMMARY OF CHIP CONTROL TESTS

From the discussion in previous sections, the following phenomena were ascertained:

1. The side cutting edge angle and the cutting speed have only a small effect on chip breakage.

2. Both workpiece material and chip-breaker shape have a significant effect on chip breakage.

3. Lower limiting feed, upper limiting feed and lower limiting depth of cut are interrelated.

In the following sections, lower limiting feed will be quantitatively discussed in terms of chip-breaker geometry and the ways to estimate the lower limiting feed for a combination of work material and cutting tool.

RELATIONSHIP BETWEEN CHIP FLOW RADIUS AND LOWER LIMITING FEED

Reference papers on chip control suggested that the chip breakage was related to both chip thickness and chip flow radius,[8] and that lower limiting feed was a function of the chip flow radius.[2] The chip flow radius can be calculated from the chip-breaker configuration. More than one equation of chip flow radius for each type of chip breaker was proposed. The following equations were used in this study:

1. Groove-type chip breaker,

$$R = \frac{H}{2} + \frac{W^2}{8H} \qquad (1)$$

Where R is chip flow radius, H is depth of groove and W is width of groove.

2. Obstruction-type chip breaker,[13]

$$R = W \cdot \cot(\theta/2) \qquad (2)$$

Where W is width of rake face and θ is the angle between rake face and obstacle face.

3. Land-angle type chip breaker

No equation has been proposed for this type of chip breaker. In this study, the land-angle-type breaker is regarded as identical to the obstruction type which has the width of rake face W + L/2, where W is the rake-face width of the land-angle-type tool, and L is its land length.

While consideration of tool-chip contact length was proposed by Trim and Boothroyd,[3] it was neglected in this study. The geometric values in the shape column used in the calculations and the calculated chip flow radii for the tools are given in Figure 2. The chip flow radius of Tool A cannot be calculated by these equations. There are some equations to estimate the natural chip flow radius for a flat tool,[8] but Tool A will be left out of the discussion for simplicity.

The chip flow radius and the lower limiting feed for some of the present tests are plotted in Figure 9. The data for each material fall on a line which goes through the origin with little scattering, which means the lower limiting feed is described by a linear equation as follows:

$$F = K \cdot R \qquad (3)$$

Where F is lower limiting feed, R is chip flow radius[3] and K is a constant. As easily understood from Figure 9 and the summary in a previous section, K is mainly dependent on the workpiece material and varies only slightly with side cutting edge angle and cutting speed. Notice that the tool chip-breaker geometry is expressed by R and it has no effect on the value of K. In other words, chip breakage or lower limiting feed is affected by tool geometry and workpiece material separately.

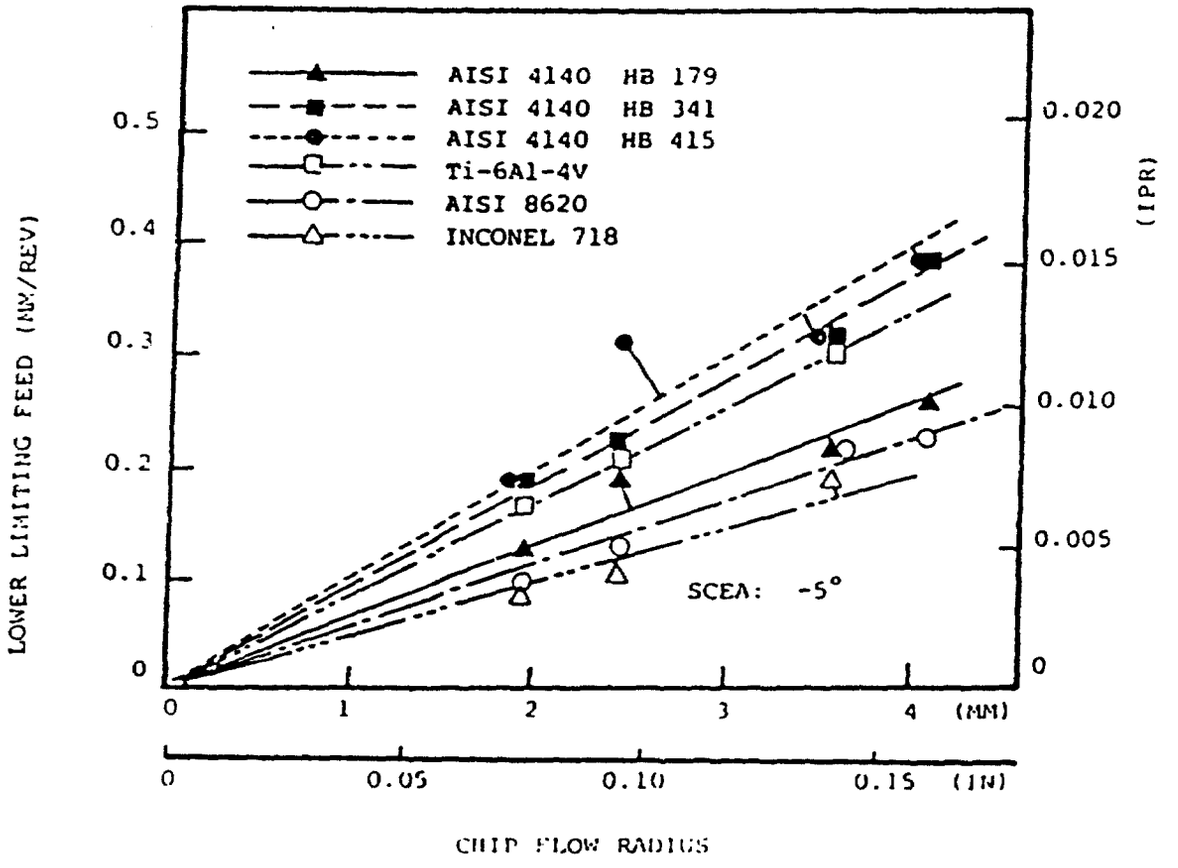

FIGURE 9. RELATIONSHIP BETWEEN CHIP FLOW RADIUS OF TOOLS AND LOWER LIMITING FEED

The values of the constant K for all the tests in this study are summarized in Table 4. Some references suggested the relationship was expressed by a square root function or $F = a \cdot \sqrt{R}$. However, within the range of the tests on this study, Equation 8 is a better fit.

TABLE 4A. CONSTANT K FOR VARIOUS MATERIALS

WORKPIECE MATERIAL:	AISI 4140 HB 179	AISI 4140 HB 341	AISI 4140 HB 415	AISI 8620	INCONEL 718	Ti-6Al-4V
CONSTANT K:	0.065	0.093	0.099	0.057	0.049	0.085

TABLE 4B. CONSTANT K FOR VARIOUS SIDE CUTTING EDGE ANGLES

Material: AISI 4140, HB 179
Cutting Speed: 131 m/min (400 fpm)

SIDE CUTTING EDGE ANGLE:	-5°	0°	15°
CONSTANT K:	0.065	0.064	0.058

TABLE 4C. CONSTANT K FOR VARIOUS CUTTING SPEEDS

Material: AISI 4140, HB 179
Side Cutting Edge Angle: -5°

CUTTING SPEED, M/MIN: (FPM):	66 (200)	98 (300)	131 (400)	164 (500)	197 (600)
CONSTANT K:	0.053	0.059	0.065	0.066	0.068

METHODS OF ESTIMATING LOWER LIMITING FEED

One of the ways to estimate lower limiting feed is to make a calculation using Equation 3 when the tool geometry and the constant K are known. Using the chip flow radius R shown in Figure 2 and the constant K in Table 3, lower limiting feeds were calculated for all the test conditions. A comparison of the values is given in Figure 10. The standard deviation of the difference (experimental value - calculated value) is 0.023 mm/rev (0.0009 ipr), which is sufficiently small compared with the normal feed rates used in machine shops.

One of the applications of this method is in building a data base. Once the values of R for each tool and the machinability value of K for each workpiece material are stored in the data file, the lower limiting feed for any combination of the tools and the workpiece materials can be calculated. To determine the value of the constant K for a material, only one chip-breakage test with the tool whose chip flow radius is known is necessary.

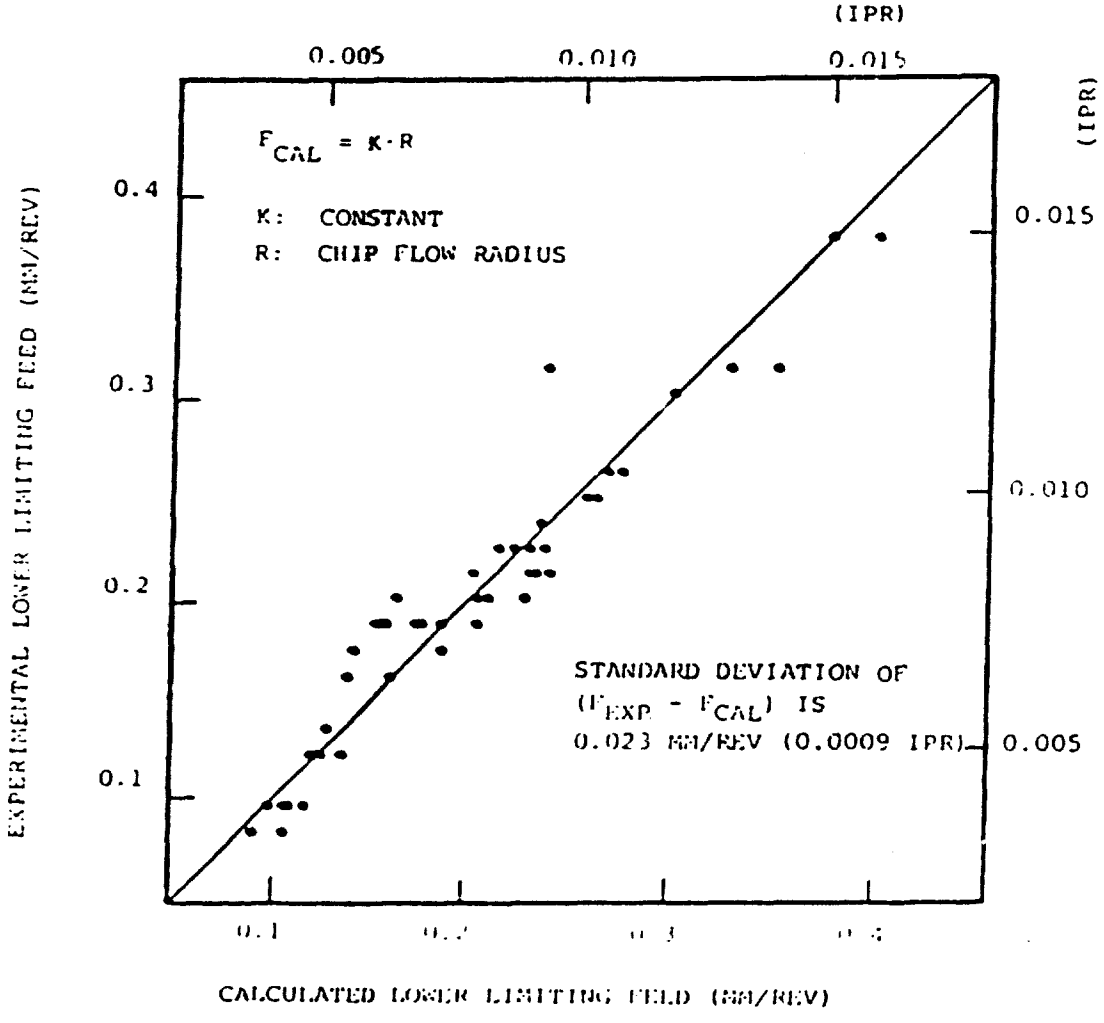

FIGURE 10. COMPARISON BETWEEN CALCULATED AND EXPERIMENTAL VALUES OF LOWER LIMITING FEED

This method cannot handle the case of flat rake face tools, like Tool A in this study, or other tools whose chip-breaker configurations are too complicated to calculate the R value mathematically.

Suppose that the lower limiting feeds for three combinations out of four composed of two types of tools and two types of materials are known. The equations are obtained from Equation 3 as follows:

$$F_{1A} = K_1 \cdot R_A \tag{4}$$

$$F_{2A} = K_2 \cdot R_A \tag{5}$$

$$F_{1B} = K_1 \cdot R_B \tag{6}$$

$$F_{2B} = K_2 \cdot R_B \tag{7}$$

In the above equations, suffixes 1 and 2 refer to material 1 and material 2 and suffixes A and B refer to Tool A and Tool B. F_{1A}, F_{1B} and F_{2A} are the known lower limiting feeds and F_{2B} is the unknown value. Substituting Equation (4) through (6) into (7) and eliminating R_A, R_B, K_1 and K_2, Equation (8) is obtained as follows:

$$F_{2B} = \frac{F_{1B}}{F_{1A}} \cdot F_{2A} \tag{8}$$

Choosing two materials out of six used in this study, and assuming the lower limiting feeds for the tools except Tool G were unknown, the unknown values were calculated by Equation (8). This process was repeated until all the combinations of tools and materials were included. Figure 11 is the comparison of such calculated limiting values to the experimental values. The standard deviation of the difference between calculated and experimental values is larger than that of the order method; however, it is still small enough to accept this method as a first estimation.

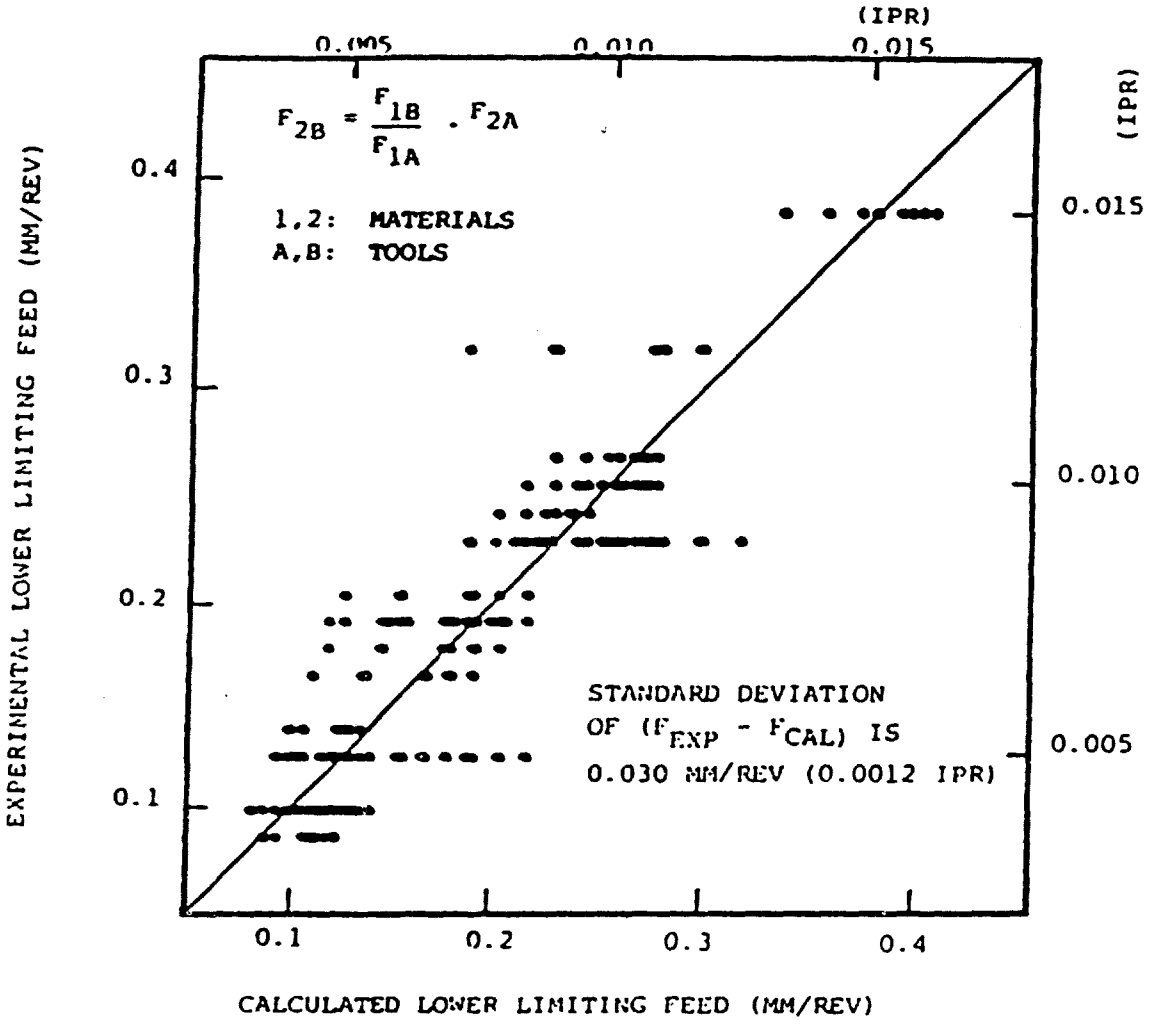

FIGURE 11. COMPARISON BETWEEN CALCULATED AND EXPERIMENTAL VALUES OF LOWER LIMITING FEED

CONCLUSIONS

From this study, the following conclusions were obtained:

1. The side cutting edge angle of the tool and the cutting speed have a small effect on chip-breakage phenomena. The increase in side cutting edge angle slightly reduces the lower limiting feed for well controlled chips. The lower limiting feed becomes a little higher when the cutting speed is raised.

2. Both workpiece material and chip-breaker shape have significant effects on the chip-breakage phenomena. The effect of these variables can be expressed by the equation:

$$F = K \cdot R \tag{9}$$

Where F is lower limiting speed, R is chip flow radius which is calculated from tool geometry, and K is a constant which is mainly related to the workpiece material.

3. The lower limiting feed, upper limiting feed, and lower limiting depth of cut are interrelated.

4. Lower limiting feeds calculated using Equation 9 coincide with experimental values. This method can be used to estimate lower limiting feeds when the tool geometry and constant K for the material are known.

5. When the chip-breaker geometry and constant K are not known, but the chip control data for three out of four combinations composed of two types of tools and two types of materials are known, unknown values can be estimated from the equation:

$$F_{2B} = \frac{F_{1B}}{F_{1A}} \cdot F_{2A} \tag{10}$$

Where 1 and 2 indicate different materials, and A and B indicate different tools.

ACKNOWLEDGEMENTS

The authors wish to express their appreciation to Kennametal Inc. for their offer of all the tools used in this study, Daido Steel Company, Ltd., who provided the workpiece materials, and to Metcut Research Associates Inc. for their support of this research.

The authors also express their gratitude to Dr. M. Field of Metcut Research Associates Inc. who offered valuable guidance from the beginning of this study and to Susan Harvey, Karen Potter and Jeanne Brotherton for their assistance in the preparation of the manuscript.

BIBLIOGRAPHY

1. Henriksen, E. K., "Chip Breakers", National Machine Tool Builders' Association, 1953.

2. Okushima, K.; Hoshi, T.; and Fujiwara, T., "On the Behavior of Chip in Steel Cutting, Part II", Bulletin of JSME, Vol. 3, No. 10, 1960, pp. 199-205.

3. Trim, A. R. and Boothroyd, G., "Action of the Obstruction Type Chip Former", International Journal of Production Research, Vol. 6, No. 3, 1968, pp. 227-240.

4. Worthington, B., "The Operation and Performance of a Groove-Type Chip Forming Device", International Journal of Production Research, Vol. 14, No. 3, 1976, pp. 529-558.

5. Spaans, C., "A Systematic Approach of Three-Dimensional Chip Curl, Chip Breaking and Chip Control", SME Technical Paper, MR70-241, 1970.

6. Spaans, C. and Goedemondt, A. A., "The Breakability. An Aspect of the Machinability -- A Computer-Simulation of Chip Formation", SME Technical Paper, MR71-154, 1971.

7. Rasch, F. O. and Tonnesen, K., "Tool Failure and Chip Form as Restrictions when Selecting Cutting Data", Annals of the CIRP, Vol. 26, No. 1, 1977, pp. 45-48.

8. Kluft, W., Konig, W., van Luttervelt, C. A., Nakayama, K., and Pekelharing, A. J., "Present Knowledge of Chip Control", Annals of the CIRP, Vol. 28, No. 2, 1979, pp. 441-455.

9. Elgamayel, J. and Pinto J. G., "Design of a Molded-in Chip Breaker in Throwaway Inserts", New Developments in Tool Materials and Applications, Illinois Institute of Technology, 1977, pp. 73-81.

10. Jones, D. G. and McCreery, J. F., "A Study of Preformed Chip Control Devices in Throwaway Carbide Inserts", SME Technical Paper MR73-215, 1973.

11. "Tool Life Testing with Single Point Turning Tools", ISO 3685-1977(E), International Organization for Standardization, 1977.

12. Machining Data Handbook, Metcut Research Associates Inc., 3rd edition, Machinability Data Center, 1980.

13. Nakayama, K., "A Study on Chip-Breaker", Bulletin of JSME, Vol. 5, No. 11, 1962, pp. 142-150.

APPENDIX B

Sketches of Machined and Honed Cylinders

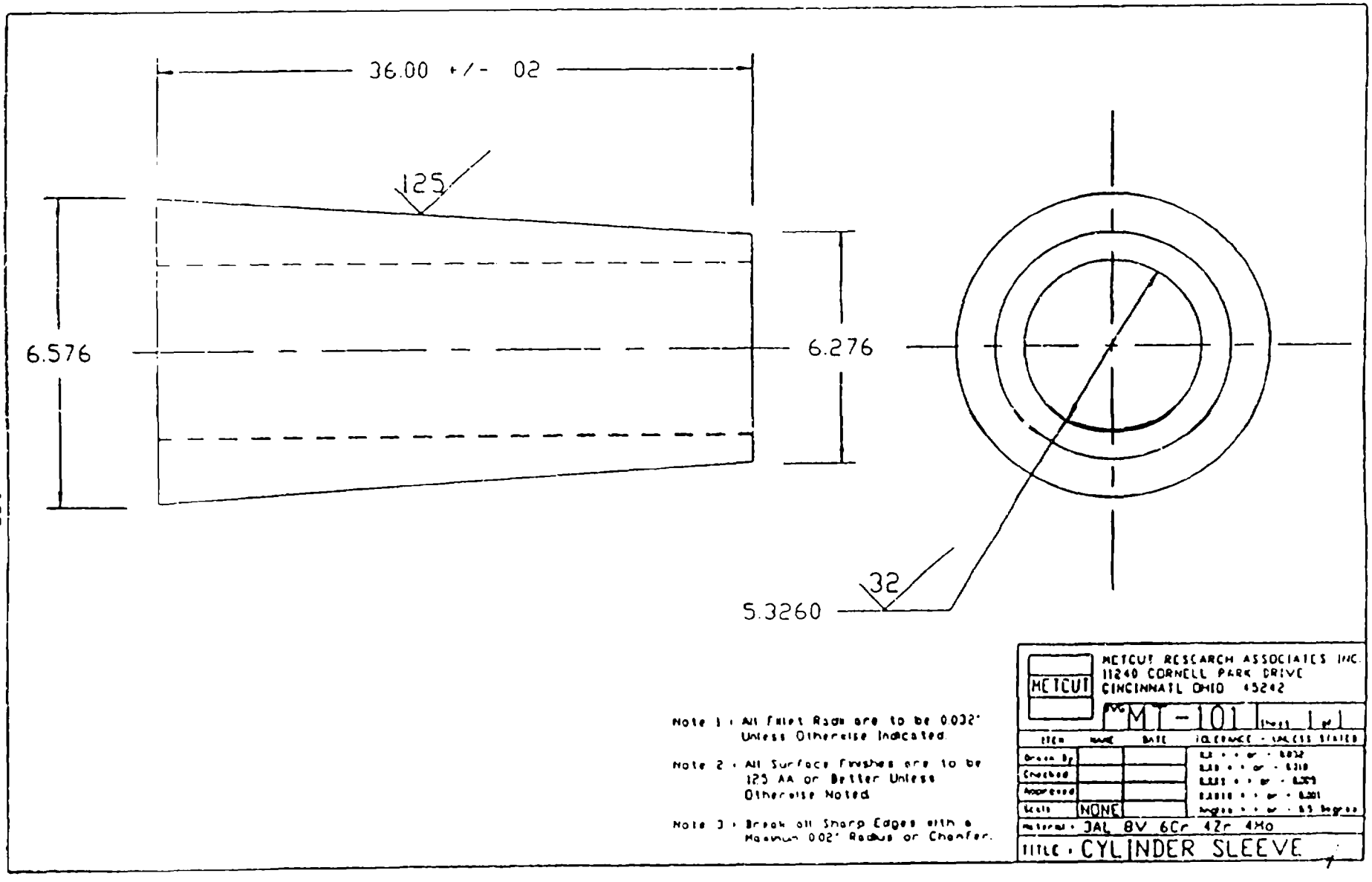
36.00 +/- 02
125
6.576
6.276
32
5.3260
Note 1 : All Fillet Rads are to be 0.032" Unless Otherwise Indicated.
Note 2 : All Surface Finishes are to be 125 AA or Better Unless Otherwise Noted.
Note 3 : Break all Sharp Edges with a Maximum 002" Radius or Chamfer.
METCUT RESEARCH ASSOCIATES INC.
11240 CORNELL PARK DRIVE
CINCINNATI OHIO 45242
METCUT
MT-101
ITEM
NAME
DATE
TOLERANCE - UNLESS STATED
Drawn By
Checked
Approved
Scale
NONE
Material : JAL 8V 6Cr 4Zr 4Mo
TITLE : CYLINDER SLEEVE

Figure A

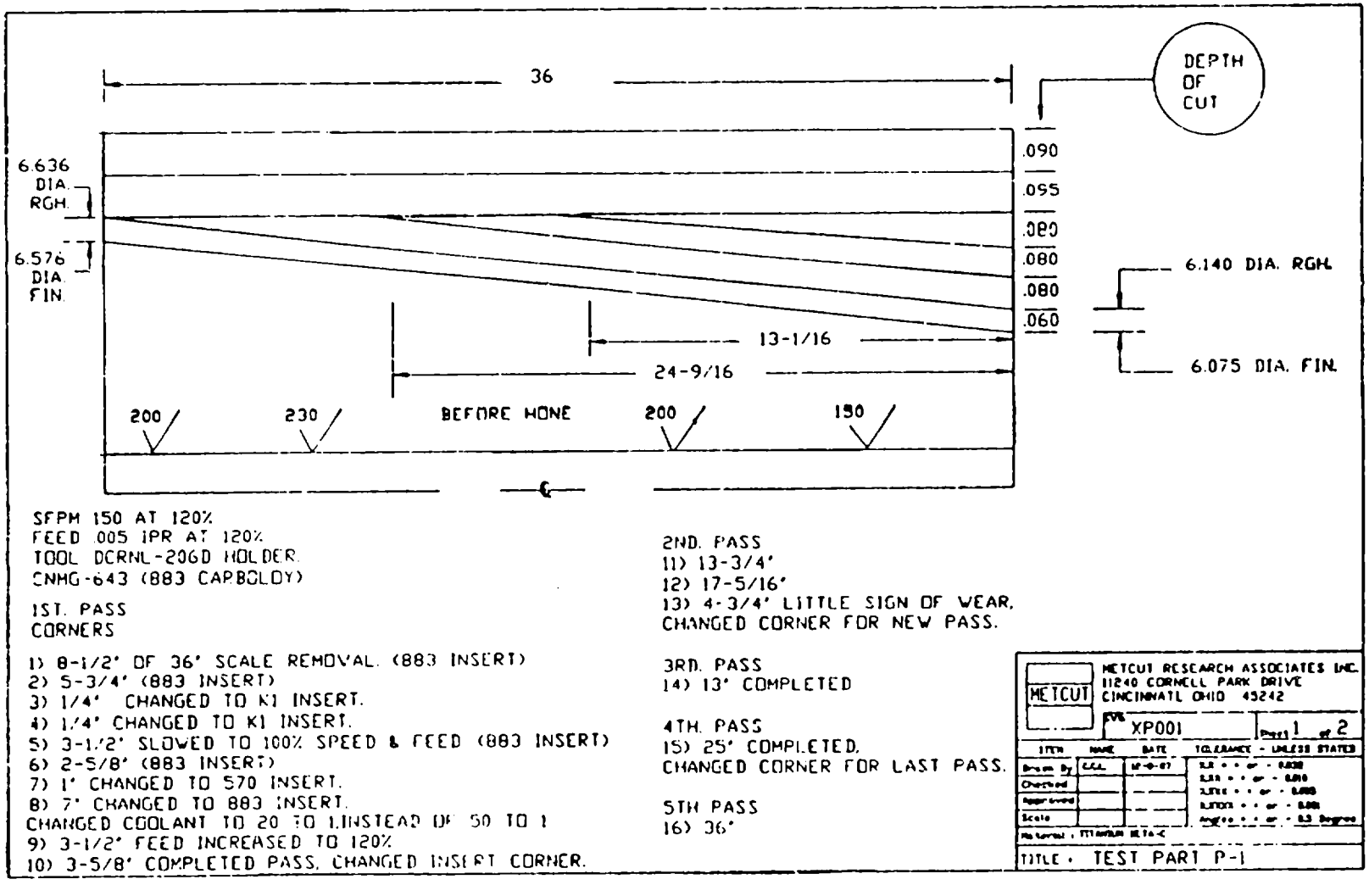
36
DEPTH OF CUT
6.636 DIA. RGH.
6.576 DIA. FIN.
.090
.095
.080
.080
.080
.060
6.140 DIA. RGH.
6.075 DIA. FIN.
13-1/16
24-9/16
200
230
BEFORE HONE
200
150
SFPM 150 AT 120%
FEED .005 IPR AT 120%
TOOL DCRNL-206D HOLDER.
CNMG-643 (883 CARBOLOY)
1ST. PASS
CORNERS
1) 8-1/2" OF 36" SCALE REMOVAL. (883 INSERT)
2) 5-3/4" (883 INSERT)
3) 1/4" CHANGED TO K1 INSERT.
4) 1/4" CHANGED TO K1 INSERT.
5) 3-1/2" SLOWED TO 100% SPEED & FEED (883 INSERT)
6) 2-5/8" (883 INSERT)
7) 1" CHANGED TO 570 INSERT.
8) 7" CHANGED TO 883 INSERT.
CHANGED COOLANT TO 20 TO 1 INSTEAD OF 50 TO 1
9) 3-1/2" FEED INCREASED TO 120%
10) 3-5/8" COMPLETED PASS. CHANGED INSERT CORNER.
2ND. PASS
11) 13-3/4"
12) 17-5/16"
13) 4-3/4" LITTLE SIGN OF WEAR, CHANGED CORNER FOR NEW PASS.
3RD. PASS
14) 13" COMPLETED
4TH. PASS
15) 25" COMPLETED, CHANGED CORNER FOR LAST PASS.
5TH PASS
16) 36"
METCUT RESEARCH ASSOCIATES INC.
11240 CORNELL PARK DRIVE
CINCINNATI OHIO 45242
METCUT
XP001
Sheet 1 of 2
ITEM NAME DATE TOLERANCE - UNLESS STATED
Drawn By C.C.L. 10-6-87
Checked
Approved
Scale
TITLE: TEST PART P-1

Figure B

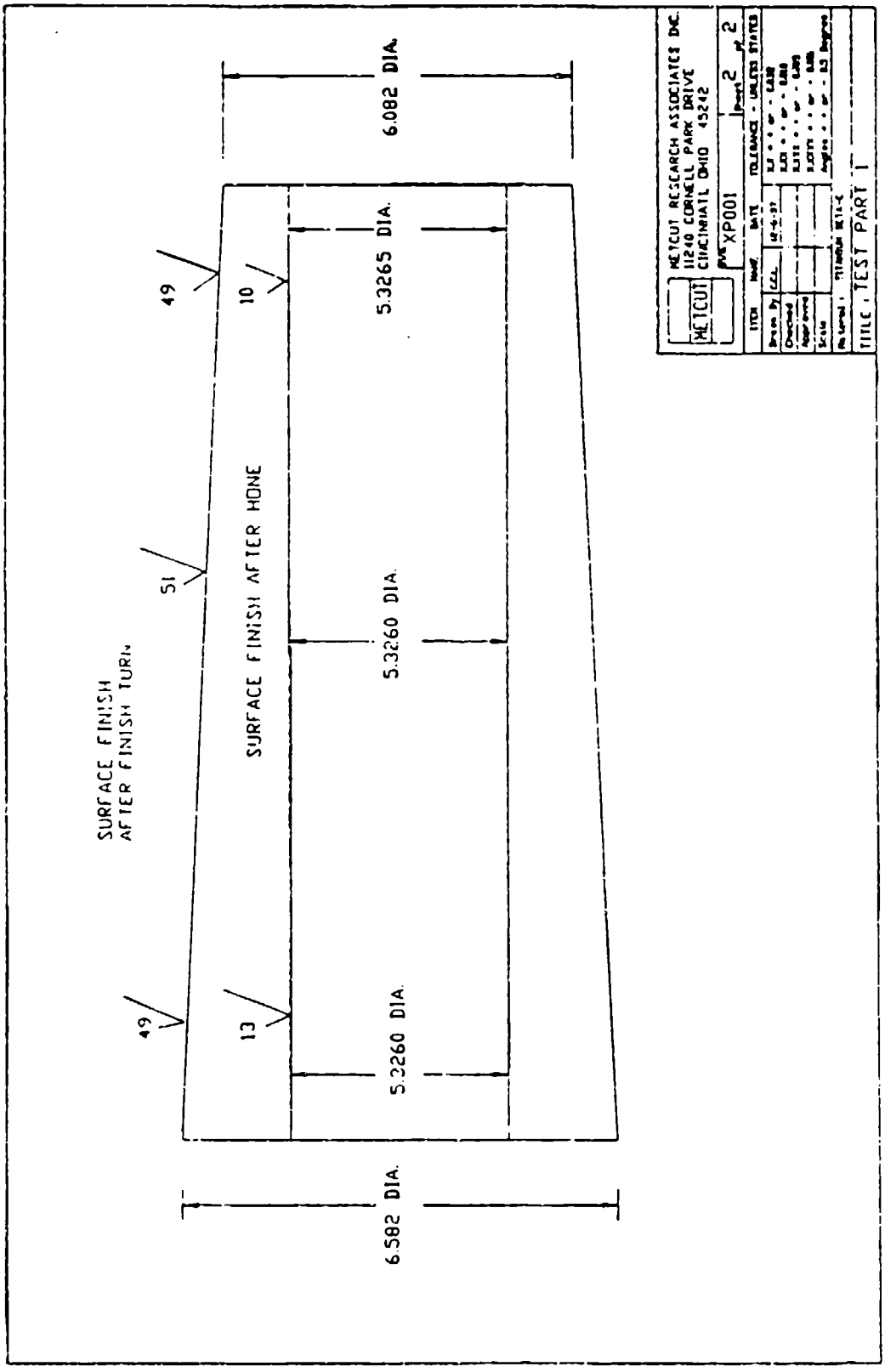
SURFACE FINISH
AFTER FINISH TURN
SURFACE FINISH AFTER HONE
49
51
49
13
10
6.582 DIA.
5.3260 DIA.
5.3260 DIA.
5.3265 DIA.
6.082 DIA.
METCUT RESEARCH ASSOCIATES INC.
11240 CORNELL PARK DRIVE
CINCINNATI OHIO 45242
METCUT
DWG XP001
TITLE, TEST PART 1

Figure C

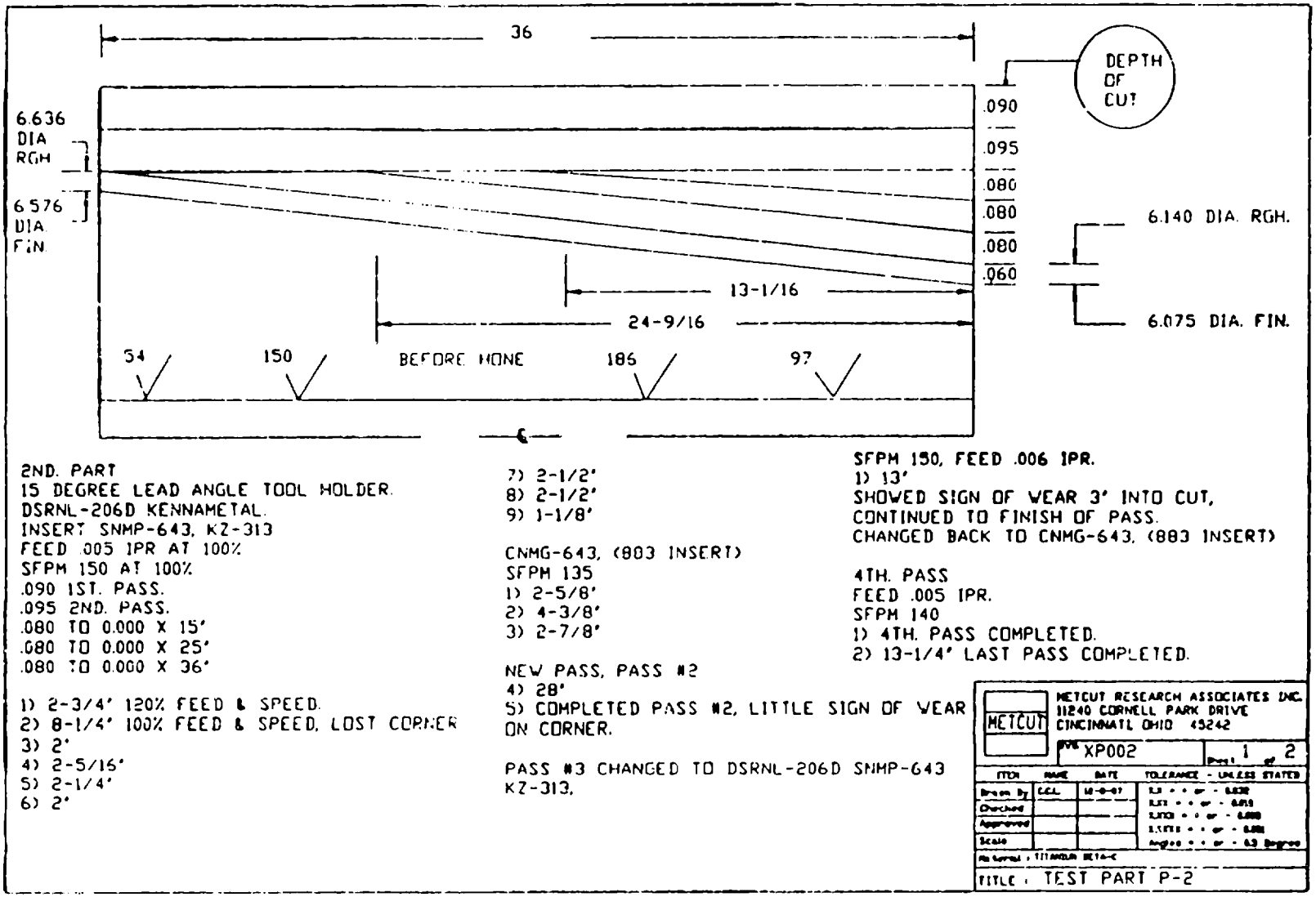
36
DEPTH OF CUT
6.636 DIA RGH
6.576 DIA FIN
.090
.095
.080
.080
.080
.060
6.140 DIA. RGH.
6.075 DIA. FIN.
13-1/16
24-9/16
54
150
BEFORE HONE
186
97
2ND. PART
15 DEGREE LEAD ANGLE TOOL HOLDER.
DSRNL-206D KENNAMETAL.
INSERT SNMP-643, KZ-313
FEED .005 IPR AT 100%
SFPM 150 AT 100%
.090 1ST. PASS.
.095 2ND. PASS.
.080 TO 0.000 X 15'
.080 TO 0.000 X 25'
.080 TO 0.000 X 36'
1) 2-3/4' 120% FEED & SPEED.
2) 8-1/4' 100% FEED & SPEED, LOST CORNER
3) 2'
4) 2-5/16'
5) 2-1/4'
6) 2'
7) 2-1/2'
8) 2-1/2'
9) 1-1/8'
CNMG-643, (883 INSERT)
SFPM 135
1) 2-5/8'
2) 4-3/8'
3) 2-7/8'
NEW PASS, PASS #2
4) 28'
5) COMPLETED PASS #2, LITTLE SIGN OF WEAR ON CORNER.
PASS #3 CHANGED TO DSRNL-206D SNMP-643 KZ-313.
SFPM 150, FEED .006 IPR.
1) 13'
SHOWED SIGN OF WEAR 3' INTO CUT, CONTINUED TO FINISH OF PASS.
CHANGED BACK TO CNMG-643, (883 INSERT)
4TH. PASS
FEED .005 IPR.
SFPM 140
1) 4TH. PASS COMPLETED.
2) 13-1/4' LAST PASS COMPLETED.
METCUT RESEARCH ASSOCIATES INC.
11240 CORNELL PARK DRIVE
CINCINNATI OHIO 45242
METCUT
XP002
Sheet 1 of 2
ITEM
NAME
DATE
TOLERANCE - UNLESS STATED
Drawn By
C.C.L.
Checked
Approved
Scale
TITLE : TEST PART P-2

Figure D

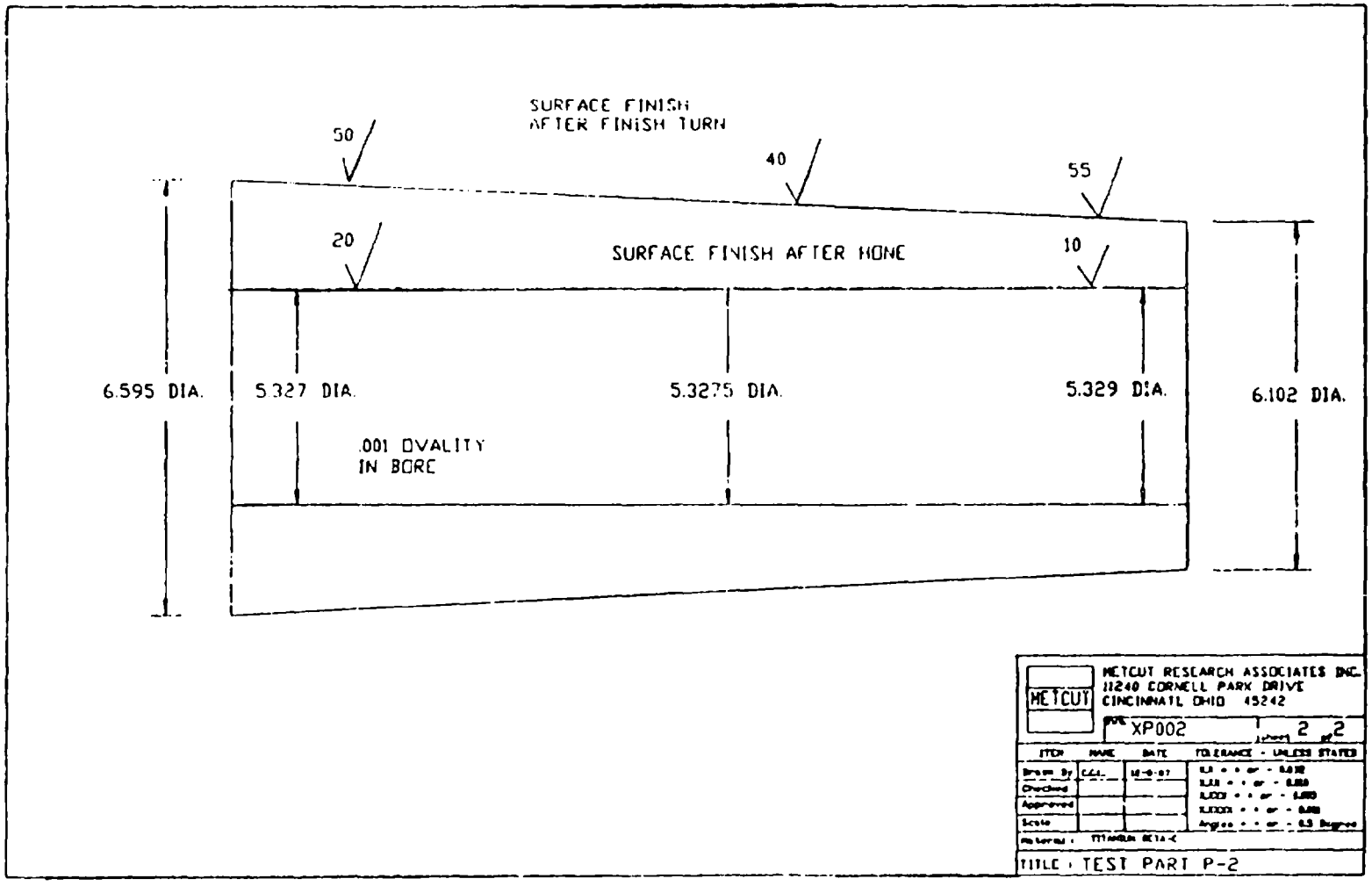
SURFACE FINISH
AFTER FINISH TURN
50
40
55
20
SURFACE FINISH AFTER HONE
10
6.595 DIA.
5.327 DIA.
5.3275 DIA.
5.329 DIA.
6.102 DIA.
.001 OVALITY
IN BORE
METCUT RESEARCH ASSOCIATES INC.
11240 CORNELL PARK DRIVE
CINCINNATI, OHIO 45242
METCUT
XP002
SHEET 2 OF 2
ITEM
NAME
DATE
TOLERANCE - UNLESS STATED
Drawn By
C.A.L.
Checked
Approved
Scale
TITLE : TEST PART P-2

Figure E

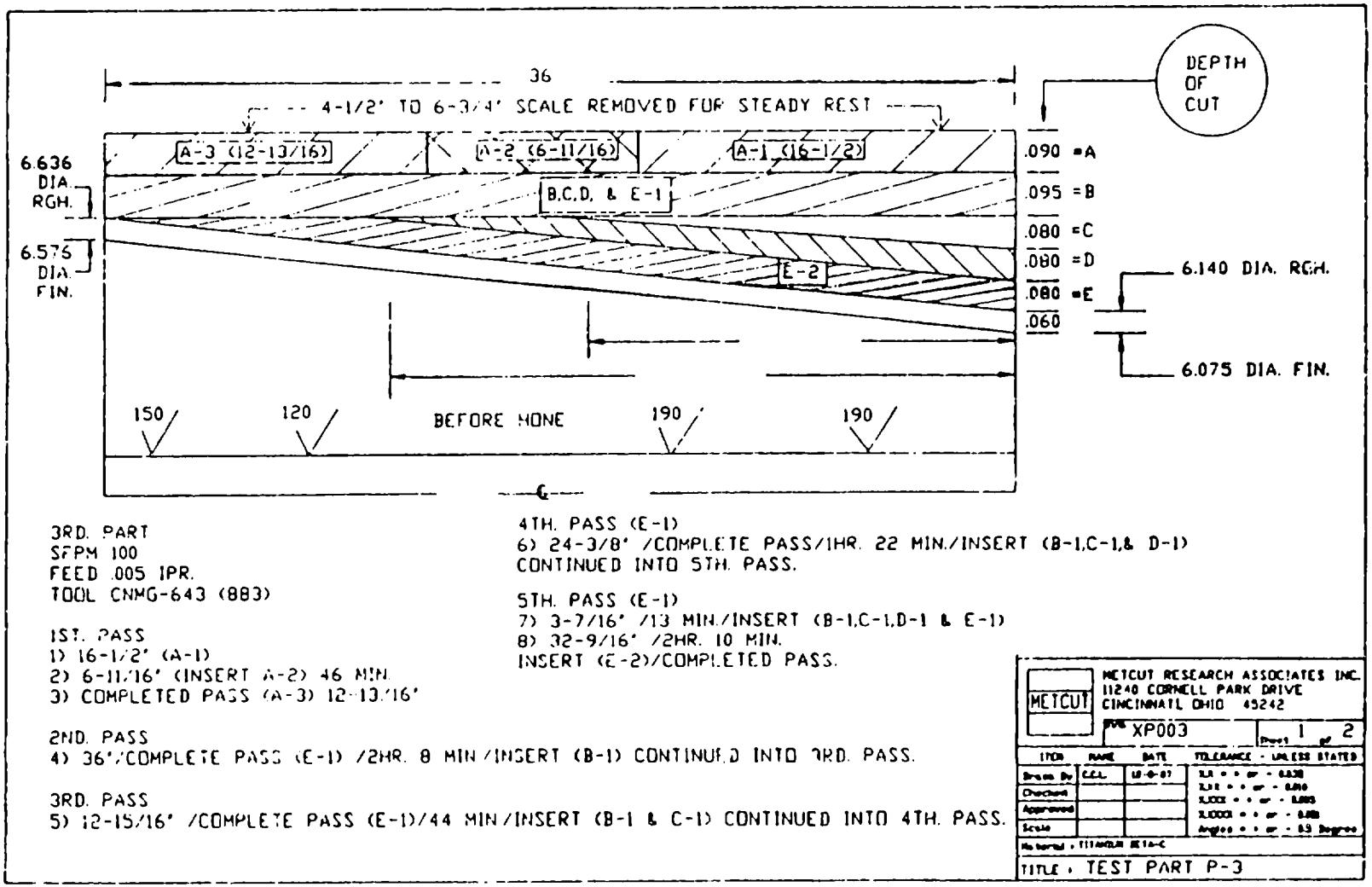
36
4-1/2" TO 6-3/4" SCALE REMOVED FOR STEADY REST
A-3 (12-13/16)
A-2 (6-11/16)
A-1 (16-1/2)
B,C,D, & E-1
E-2
6.636 DIA. RGH.
6.575 DIA. FIN.
DEPTH OF CUT
.090 =A
.095 =B
.080 =C
.080 =D
.080 =E
.060
6.140 DIA. RGH.
6.075 DIA. FIN.
150
120
BEFORE HONE
190
190
3RD. PART
SFPM 100
FEED .005 IPR.
TOOL CNMG-643 (883)
1ST. PASS
1) 16-1/2" (A-1)
2) 6-11/16" (INSERT A-2) 46 MIN.
3) COMPLETED PASS (A-3) 12-13/16"
2ND. PASS
4) 36"/COMPLETE PASS (E-1) /2HR. 8 MIN./INSERT (B-1) CONTINUED INTO 3RD. PASS.
3RD. PASS
5) 12-15/16" /COMPLETE PASS (E-1)/44 MIN./INSERT (B-1 & C-1) CONTINUED INTO 4TH. PASS.
4TH. PASS (E-1)
6) 24-3/8" /COMPLETE PASS/1HR. 22 MIN./INSERT (B-1,C-1,& D-1)
CONTINUED INTO 5TH. PASS.
5TH. PASS (E-1)
7) 3-7/16" /13 MIN./INSERT (B-1,C-1,D-1 & E-1)
8) 32-9/16" /2HR. 10 MIN.
INSERT (E-2)/COMPLETED PASS.
METCUT RESEARCH ASSOCIATES INC.
11240 CORNELL PARK DRIVE
CINCINNATI OHIO 45242
METCUT
XP003
1 2
ITEM NAME DATE TOLERANCE - UNLESS STATED
Drawn By C.E.L.
Checked
Approved
Scale
TITLE : TEST PART P-3

Figure F

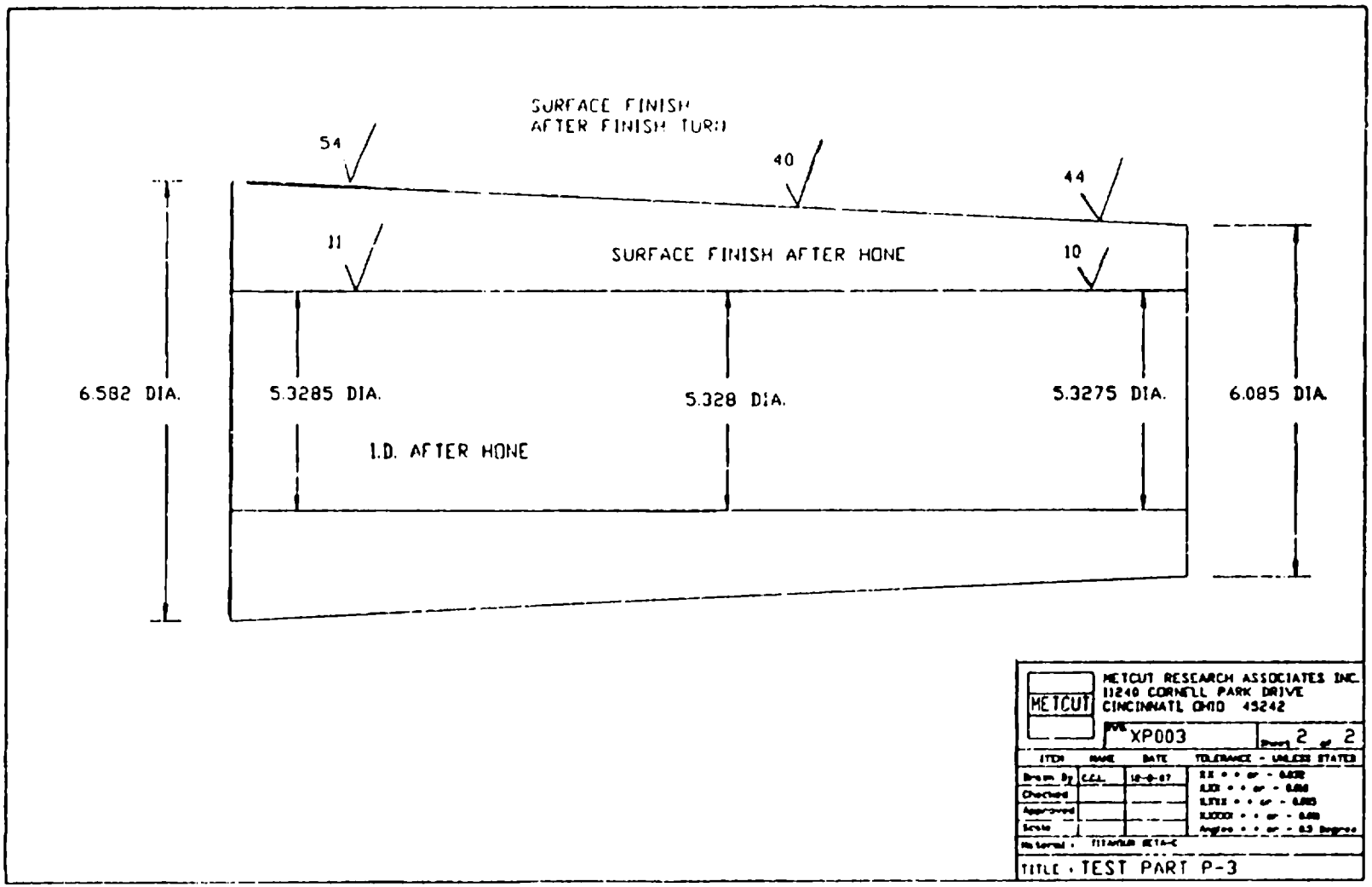
SURFACE FINISH
AFTER FINISH TURN
54
40
44
11
SURFACE FINISH AFTER HONE
10
6.582 DIA.
5.3285 DIA.
5.328 DIA.
5.3275 DIA.
6.085 DIA.
I.D. AFTER HONE
METCUT RESEARCH ASSOCIATES INC.
11240 CORNELL PARK DRIVE
CINCINNATI OHIO 45242
METCUT
XP003
2 of 2
ITEM
NAME
DATE
TOLERANCE - UNLESS STATED
Drawn By
C.C.L.
Checked
Approved
Scale
TITLE : TEST PART P-3

Figure G

TECHNICAL REPORT INTERNAL DISTRIBUTION LIST

	NO. OF COPIES
CHIEF, DEVELOPMENT ENGINEERING DIVISION	
ATTN: SMCAR-CCB-D	1
-DA	1
-DC	1
-DI	1
-DP	1
-DR	1
-DS (SYSTEMS)	1
CHIEF, ENGINEERING SUPPORT DIVISION	
ATTN: SMCAR-CCB-S	1
-SE	1
CHIEF, RESEARCH DIVISION	
ATTN: SMCAR-CCB-R	2
-RA	1
-RE	1
-RM	1
-RP	1
-RT	1
TECHNICAL LIBRARY ATTN: SMCAR-CCB-TL	5
TECHNICAL PUBLICATIONS & EDITING SECTION ATTN: SMCAR-CCB-TL	3
DIRECTOR, OPERATIONS DIRECTORATE ATTN: SMCWV-OD	1
DIRECTOR, PROCUREMENT DIRECTORATE ATTN: SMCWV-PP	1
DIRECTOR, PRODUCT ASSURANCE DIRECTORATE ATTN: SMCWV-QA	1

NOTE: PLEASE NOTIFY DIRECTOR, BENET LABORATORIES, ATTN: SMCAR-CCB-TL, OF ANY ADDRESS CHANGES.

TECHNICAL REPORT EXTERNAL DISTRIBUTION LIST

	NO. OF COPIES
ASST SEC OF THE ARMY RESEARCH AND DEVELOPMENT ATTN: DEPT FOR SCI AND TECH THE PENTAGON WASHINGTON, D.C. 20310-0103	1
ADMINISTRATOR DEFENSE TECHNICAL INFO CENTER ATTN: DTIC-FDAC CAMERON STATION ALEXANDRIA, VA 22304-6145	12
COMMANDER US ARMY ARDEC ATTN: SMCAR-AEE	1
SMCAR-AES, BLDG. 321	1
SMCAR-AET-O, BLDG. 351N	1
SMCAR-CC	1
SMCAR-CCP-A	1
SMCAR-FSA	1
SMCAR-FSM-E	1
SMCAR-FSS-D, BLDG. 94	1
SMCAR-IMI-I (STINFO) BLDG. 59 PICATINNY ARSENAL, NJ 07806-5000	2
DIRECTOR US ARMY BALLISTIC RESEARCH LABORATORY ATTN: SLCBR-DD-T, BLDG. 305 ABERDEEN PROVING GROUND, MD 21005-5066	1
DIRECTOR US ARMY MATERIEL SYSTEMS ANALYSIS ACTV ATTN: AMXSY-MP ABERDEEN PROVING GROUND, MD 21005-5071	1
COMMANDER HQ, AMCCOM ATTN: AMSMC-IMP-L ROCK ISLAND, IL 61299-6000	1
COMMANDER ROCK ISLAND ARSENAL ATTN: SMCRI-ENM ROCK ISLAND, IL 61299-5000	1
DIRECTOR US ARMY INDUSTRIAL BASE ENGR ACTV ATTN: AMXIB-P ROCK ISLAND, IL 61299-7260	1
COMMANDER US ARMY TANK-AUTMV R&D COMMAND ATTN: AMSTA-DDL (TECH LIB) WARREN, MI 48397-5000	1
COMMANDER US MILITARY ACADEMY ATTN: DEPARTMENT OF MECHANICS WEST POINT, NY 10996-1792	1
US ARMY MISSILE COMMAND REDSTONE SCIENTIFIC INFO CTR ATTN: DOCUMENTS SECT, BLDG. 4484 REDSTONE ARSENAL, AL 35898-5241	2
COMMANDER US ARMY FGN SCIENCE AND TECH CTR ATTN: DRXST-SD 220 7TH STREET, N.E. CHARLOTTESVILLE, VA 22901	1
COMMANDER US ARMY LABCOM MATERIALS TECHNOLOGY LAB ATTN: SLCMT-IML (TECH LIB) WATERTOWN, MA 02172-0001	2

NOTE: PLEASE NOTIFY COMMANDER, ARMAMENT RESEARCH, DEVELOPMENT, AND ENGINEERING CENTER, US ARMY AMCCOM, ATTN: BENET LABORATORIES, SMCAR-CCB-TL, WATERVLIET, NY 12189-4050, OF ANY ADDRESS CHANGES.

TECHNICAL REPORT EXTERNAL DISTRIBUTION LIST (CONT'D)

	NO. OF COPIES
COMMANDER US ARMY LABCOM, ISA ATTN: SLCIS-IM-TL 2800 POWDER MILL ROAD ADELPHI, MD 20783-1145	1
COMMANDER US ARMY RESEARCH OFFICE ATTN: CHIEF, IPO P.O. BOX 12211 RESEARCH TRIANGLE PARK, NC 27709-2211	1
DIRECTOR US NAVAL RESEARCH LAB ATTN: MATERIALS SCI & TECH DIVISION CODE 26-27 (DOC LIB) WASHINGTON, D.C. 20375	1 1
COMMANDER AIR FORCE ARMAMENT LABORATORY ATTN: AFATL/MN EGLIN AFB, FL 32542-5434	1
COMMANDER AIR FORCE ARMAMENT LABORATORY ATTN: AFATL/MNF EGLIN AFB, FL 32542-5434	1
METALS AND CERAMICS INFO CTR BATTELLE COLUMBUS DIVISION 505 KING AVENUE COLUMBUS, OH 43201-2693	1

NOTE: PLEASE NOTIFY COMMANDER, ARMAMENT RESEARCH, DEVELOPMENT, AND ENGINEERING CENTER, US ARMY AMCCOM, ATTN: BENET LABORATORIES, SMCAR-CCB-TL, WATERVLIET, NY 12189-4050, OF ANY ADDRESS CHANGES.